Role of astrocytes in the development of synaptic plasticity induced by chronic treatment with drugs of abuse

2006

Mayumi Miyatake

A dissertation submitted in partial fulfillment of the requirements leading to the degree of Doctor (Pharmacy) presented to the Department of Toxicology, Hoshi University School of Pharmacy and Pharmaceutical Sciences, Tokyo, Japan

This dissertation is dedicated to my parents, my brother and my friends.

Table of Contents

Abbreviations

Chemical substances and Drugs

AG490: α-Cyano-(3,4-dihydroxy)-N-benzylcinnamide

AMPA: α-Amino-3-hydroxy-5-methylisoxazole-4-propionic acid

CHE: 1,2-Dimethoxy-12-methyl[1,3]benzodioxolo[5,6-c] phenanthridinuim cloride (chelerythrine chloride)

DNQX: 6,7-Dinitroquinoxaline-2,3-dione

Ifenprodil: 2-(4-Benzylpiperidino)-1-(4-hydroxyphenyl)-1-propanol hemitartrate

KN-93:2-[N-(2-Hydroxythyl)-N-(4-methoxy-benzenesulfonyl)]amino-N-(4-chlorocinnamyl)-N-methylbensylamine

METH: Methamphetamine hydrochloride

MPEP: 2-Methyl-6-(phenylethynyl)-pyridine hydrochloride

MRP: Morphine hydrochloride

NMDA: *N*-Methyl-*D*-aspartate acid

NPC-15437:S-2,6-Diamino-N-[(1-[1-oxotridecyl]-2-piperidinyl)methyl]hexamide dihydorochloride

PDBu: Phorbol 12, 13-dibutyrate

PPF: 3-methyl-1-(5-oxohexyl)-7-propylxanthine (propentofylline)

U73122:1-(6-[([17β]-3-methoxyestra-1,3,5[10]-trien-17-yl)-1H-pyrrole-2,-dione

Buffers

BSS: Balanced salt saline

PBS: Phosphate-buffered saline

Brain regions

CG: Cingulate cortex

CPu: Corpus striatum

N.Acc.: Nucleus accumbens

VTA: Ventral tegmental area

Endogenous substances

EGF: Erythropoietic growth factors

GFAP: Glial fibrillary acidic protein

G-CSF: Granulocyte-colony stimulating factor

GM-CSF: Granulocyte-macrophage colony-stimulating factor

IFN: Interferon

IP-10: Interferon-γ-inducible protein-10

IL: Interleukin

M-CSF: Macrophage-colony stimulating factor

MCP: Monocyte chemoattractant protein

NeuN: Neuronal nuclei

RANTES: Regulated upon activation normal T cell expressed and secreted

sTNFR-1: Soluble tumor necrosis factor receptor-1

TGF: Transforming growth factor

Receptors

mGluR: Metabotropic glutamate receptor

Enzymes and intracellular messengers

CaMKII: Calcium/calmodulin-dependent protein kinase II

Jak/STAT: Janus kinase/signal transducer and activator of transcription

PKC: Protein kinase C

PLC: Phospholipase C

Serum

FBS: Fetal bovin serum

HS: Horse serum

Injection routes

i.c.v.: Intracerebroventricular

i.p.: Intraperitoneal

s.c.: Subcutaneous

Others

ACM: Astrocyte-conditioned medium

ANOVA: Analysis of variance

CNS: Central nervous system

DMEM: Dulbecco's modified Eagle's medium

IgG: Immunoglobulin G

$[Ca^{2+}]i$: Intracellular Ca^{2+} concentration

LTP: Long-term potentiation

MCM: Microglia-conditioned medium

METH-ACM: Astrocyte-conditioned medium collected from methamphetamine-treated astrocytes

MRP-ACM: Astrocyte-conditioned medium collected from morphine-treated astrocytes

NSC: Neural stem cell

p-PKC: Phosphorylated-protein kinase C

Structures of drugs using in the present study

AG490: α-cyano-(3,4-dihydroxy)-N-benzylcinnamide

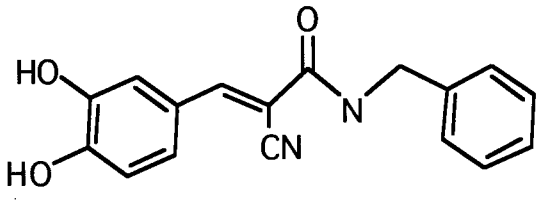

Chelerythrine chloride: 1,2-Dimethoxy-12-methyl[1,3]benzodioxolo[5,6-c] phenanthridinuim cloride

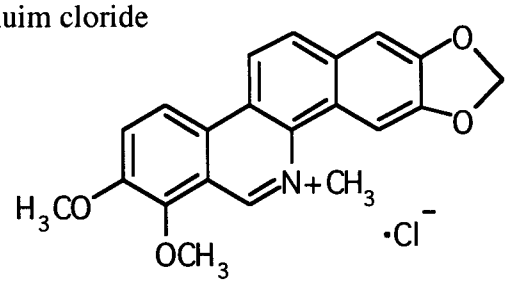

DNQX: 6,7-Dinitroquinoxaline-2,3-dione

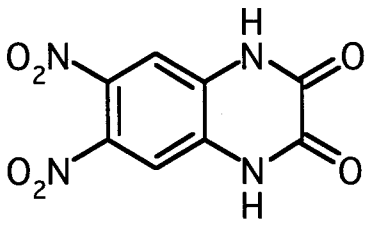

Fluo-3 acetoxymethyl ester

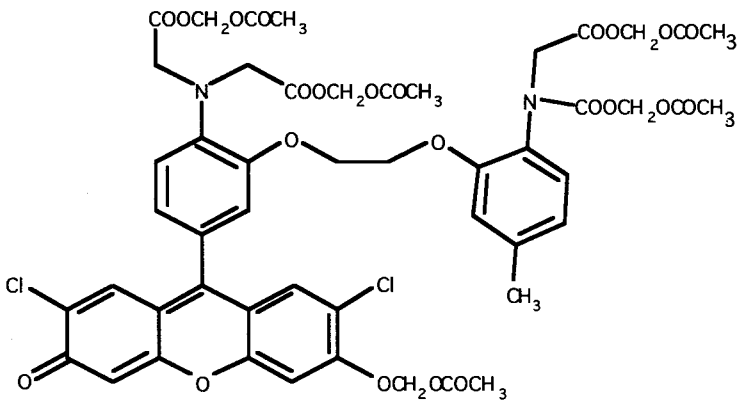

Ifenprodil hemitartrate: 2-(4-Benzylpiperidino)-1-(4-hydroxyphenyl)-1-propanol hemitartrate

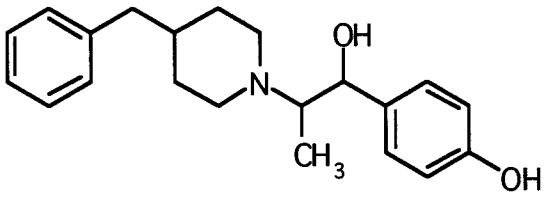

· 1/2 $C_4H_6O_6$

KN-93: 2-[N-(2-Hydroxythyl)-N-(4-methoxy-benzenesulfonyl)]amino-N-(4-chlorocinnamyl)-N-methylbensylamine

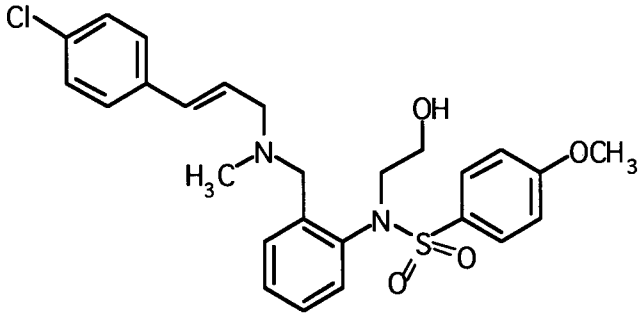

Methamphetamine hydrochloride

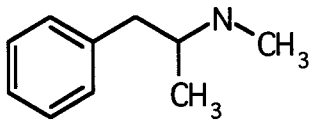

· HCl

Morphine hydrochloride

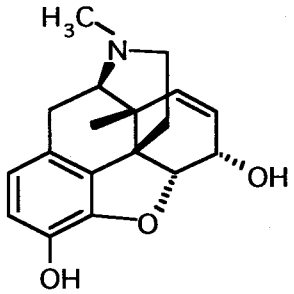

· HCl

MPEP: 2-Methyl-6-(phenylethynyl)-pyridine hydrochloride

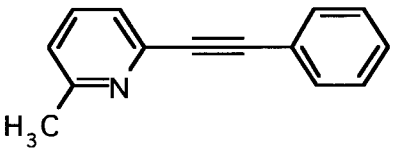

NPC-15437: S-2,6-Diamino-N-[(1-[1-oxotridecyl]-2-piperidinyl)methyl]hexamide dihydorochloride

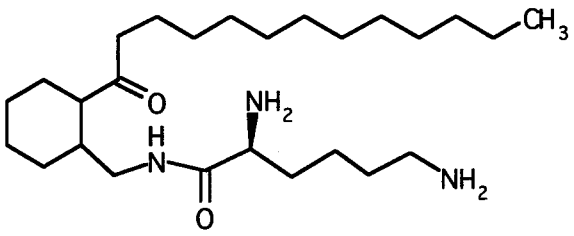

· 2HCl

PDBu: Phorbol 12, 13-dibutyrate

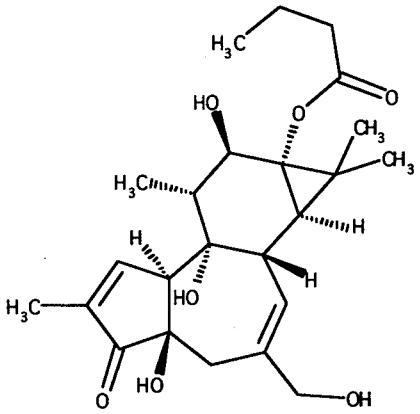

Propentofylline: 3-Methyl-1-(5-oxohexyl)-7-propylxanthine

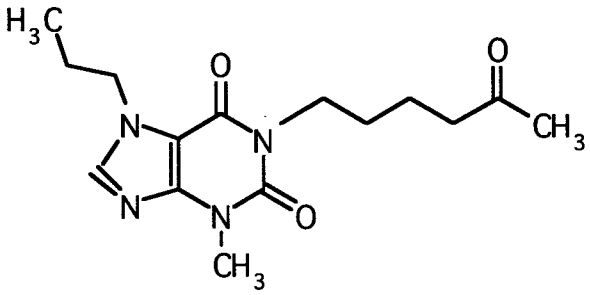

U73122:1-(6-[([17β]-3-Methoxyestra-1,3,5[10]-trien-17-yl)-1H-pyrrole-2,-dione

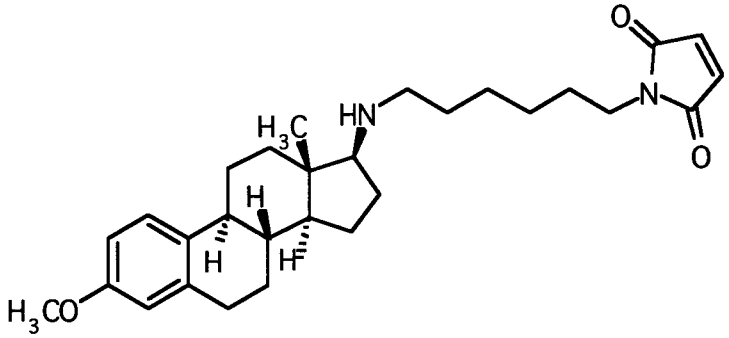

General Introduction

Astrocytes

There are two categories of cells in the central nervous system (CNS); neurons and adjacent glial cells including astrocytes, microglia and oligodendrocytes. Throughout the last century, most neurophysiologists believed that synaptic transmission in the brain was mediated by neurons. Ironically, glial cells were considered to be minor players in the mammalian CNS, even though they outnumber neurons 10-fold. Glial cells were simply thought to function as passive support cells, bringing nutrients to and removing waste from neurons.

Over the past decade, however, an increasing number of observations have progressively challenged this classical view. Glial cells have important physiological properties as they relate to CNS homeostasis[1]. Moreover, glial cells affect neuronal function through the release of neurotransmitters, neurotrophic factors, cytokines, chemokines and extracellular matrix, guide neuronal development, contribute to the metabolism of neurotransmitters, and regulate extracellular pH and ion levels[2-5].

Astrocytes are a subpopulation of glial cells in the CNS. Astrocytes have traditionally been considered to be structural elements within the CNS with the main function of maintaining nerve tissue. Astrocytes come in close contact with several cellular components of the brain parenchyma including blood vessels, pial surfaces, neurons and other glial cells. Astrocytes have a large variety of receptors for neurotransmitters and hormones, including glutamate receptors[6-8], ATP receptors[9, 10] and

dopamine receptors[11, 12], which are coupled to various intracellular signaling cascades[4, 13, 14]. Astrocytes are known to exhibit a form of excitability and communication based on changes in the intracellular Ca^{2+} concentration ($[Ca^{2+}]i$), which can be stimulated by neuronal synaptic activity, and release glutamate, ATP and nitric oxide that signal back to adjacent neurons and other astrocytes[14-18]. More recently, astrocytes have been reported to promote axonal extension and neuronal migration, whereas astrocyte-derived cues also play a critical role in the pathological process by forming boundaries and retarding axonal outgrowth[19-22].

Astrocytes are immunocompetent cells in the CNS[23-25]. Both *in vitro* and *in vivo* studies have documented the ability of astrocytes to produce interleukin (IL)-1, -6 and -10; interferon (IFN)-α, and -β; granulocyte-macrophage colony-stimulating factor (GM-CSF), macrophage-colony stimulating factor (M-CSF), and granulocyte-colony stimulating factor (G-CSF); and tumor necrosis factor-α (TNF-α) and transforming growth factor-β (TGF-β). Astrocytes also produce chemokines including regulated on activation normal T-cell expressed and secreted (RANTES), IL-8, monocyte chemoattractant protein-1 (MCP-1) and IFN-γ-inducible protein-10 (IP-10).

Activation of astrocytes

Astrocytes undergo a process of proliferation, morphological changes, and enhancement of glial fibrillary acidic protein (GFAP) expression, which has been referred to as the activation of astrocytes or astrogliosis[26-28]. Astrocytes become activated in response to many CNS pathologies[29, 30], such as stroke, trauma, growth of a

tumor or neurodegenerative disease, such as Alzheimer' disease and Parkinson's disease.

Although the activation of astrocytes has been considered to be the major impediment to axonal regrowth after an injury, the formation of a glial barrier around a lesion site is also an advantage, because it isolates the still-intact CNS tissue from secondary lesions[27, 28]. In fact, the role of GFAP in neurite outgrowth has been assessed *in vitro*[28, 31-33]. Collectively, the activation of astrocytes and astrogliosis are very complex phenomena, involving interactions of several cell types with neurons, leading eventually to neuron survival or death and axonal regeneration.

Role of astrocytes in central synaptic plasticity

It has been estimated that individual astrocytes in the adult rodent brain may ensheathe and interact with as many as 10,000 synapses. Accumulating evidence suggests that astrocytes may actively participate in synaptic plasticity[34-37]. *In vitro* studies have found that astrocytes exert powerful control over the number of CNS synapses[34-38]. Astrocytes are also essential for postsynaptic function, and are required for synaptic stability and maintenance[34-38]. In fact, astrocytes and other perisynaptic glia, such as Schwann cells, release soluble proteinaceous signals that profoundly enhance synaptic activity by nearly 100-fold[34, 37]. Moreover, astrocytes induce an increase in the number of synapses in these cells[35, 37]. In addition, these new synapses are ultrastructurally normal and functional[35, 37]. Taken together, these findings indicate that astrocytes profoundly increase the number of synapses that form between CNS

neurons *in vitro*. These reports also provide evidence that the number of synapses is not solely determined by the intrinsic properties of neurons but can be powerfully controlled by extracellular signals from adjacent astrocytes. Recent studies increasingly implicate astrocytes *in vivo* as participants in activity-dependent structural and functional synaptic changes throughout the mammalian CNS[37, 38].

Dopaminergic and glutamatergic neurotransmission in the development of synaptic plasticity induced by drugs of abuse

Studies of human addicts and behavioral studies in rodent models of addiction indicate that key behavioral abnormalities associated with addiction are extremely long-lived. Drugs of abuse are chemically divergent molecules with very different initial activities. However, many pharmacological and biochemical findings support the idea that long-term exposure to psychostimulants induces neuronal plasticity[39-41].

Among brain neurotransmitters, dopamine has been more extensively implicated in the mechanism of drug addiction, not only as a substrate of psychostimulant reward but, more generally, also as a substrate of drug-related learning and neuroadaptation. A prominent amount of psychostimulant-related actions is thought to depend on the activation of the mesolimbic dopamine system[42-44]; this activation involves increased firing of dopamine neurons in the ventral tegmental area (VTA) of the midbrain and a subsequent increase of dopamine released into the nucleus accumbens (N.Acc.).

On the other hand, several lines of evidence suggest that glutamatergic projection to the N.Acc. originating from the prefrontal cortex and amygdala[45] regulates emotional

and behavioral processing. Glutamate is a major fast excitatory neurotransmitter in the CNS, and glutamate receptors have been shown to play important roles in synaptic plasticity such as long-term potentiation (LTP), which is thought to underlie physiopathological phenomena, neuronal development, synaptic plasticity and synaptogenesis[46-48]. Therefore, it is likely that the long-lasting synaptic adaptations in dopaminergic and/or glutamatergic neurotransmission provide a neuronal framework for altered behavioral processing underlying the development of psychological dependence on drugs of abuse.

Protein kinase C

Protein kinase C (PKC) plays a major role in cellular regulatory and signaling processes involving the phosphorylation of proteins, modulation of neuronal function, synthesis and release of neurotransmitters and regulation of receptors[49, 50].

PKC is activated by diacylglycerol, which can be generated by phospholipase C (PLC). There are three mammalian PLC form families: PLCβ, PLCγ and PLCδ[51]. All known forms of PLCβ isoforms are stimulated to various extents by α subunits of the $G_{q/11}$ family. PLCβ2 and β3 are also activated by βγ subunits of the G-protein. In contrast, PLCγ isoforms are stimulated mainly through receptor tyrosine kinases.

Several lines of evidence have demonstrated that activated PKC plays a key role in the modulation of synaptic plasticity[19, 21, 52]. Considerable evidence suggests that the activation of PKC in the brain modulates the development of sensitization to drugs of abuse, such as methamphetamine (METH)[53], cocaine[54] and morphine (MRP)[55].

Moreover, PKC also plays a positive regulatory role in the development and/or expression of rewarding effects induced by METH[53], amphetamine[56] and MRP[57]. These findings strongly suggest that activated PKC in the brain may play a substantial role during the development of dependence and sensitization induced by chronic treatment with drugs of abuse.

Astrocytic responses to drugs of abuse

Many studies have documented that astrocytes show hypertrophy and proliferation upon treatment with drugs of abuse at neurotoxic doses. For example, Pu and Vorhees[58] have shown that repeated *in vivo* treatment with METH (4 injections of 10 mg/kg, i.p. at 2 hr intervals) induced depletion of tyrosine hydroxylase-positive neurons and proliferation of astrocytes in rat striatum. More recently, Guilarte et al.[59] reported that repeated administration of METH (4 injections of 15 mg/kg, i.p. at 2 hr intervals) induced the loss of dopamine transporters, serotonin transporters and vesicular monoamine transporter type-2 with the activation of astrocytes and microglia in rat striatum. Fattore et al.[60] also demonstrated that repeated daily administration of cocaine (20 mg/kg, i.p.) caused the enhancement of GFAP expression in the mouse dentrate gyrus. These observations raise the possibility that astrocytes may play an important role in psychostimulant-induced neurodegeneration. However, relatively little is known about the mechanism that underlies psychostimulant-induced astrocytic responses during the development of dependence, even if astrocytes are considered to play a critical role in long-term synaptic plasticity in the CNS.

Aim and Scope

The aim of the present study was to investigate the role of astrocytes in the development of central synaptic plasticity induced by chronic treatment with drugs of abuse. Behavioral, neurochemical and biochemical experiments were conducted.

The specific aims of the proposed research were:

In Chapter 1:

To ascertain the influence of *in vitro* treatment with drugs of abuse on astrocytes, I investigated whether *in vitro* treatment with METH and MRP could affect the morphology of astrocytes in mouse purified cortical astrocytes and neuron/glia co-cultures. Furthermore, I also explored the difference between METH and MPR in the PKC-dependent expression and maintenance of the activation of astrocytes. In addition, I examined the *in vivo* astrocytic response during the development of sensitization to hyperlocomotion induced by chronic treatment with METH.

In Chapter 2:

To clarify the role of glutamatergic neurotransmission and its association with PKC in neuron-astrocyte communication, *in vitro* studies were undertaken to investigate the mechanism underlying glutamate-induced Ca^{2+} response in both neurons and astrocytes.

Moreover, I have demonstrated functional and morphological changes in glutamatergic neurotransmission induced by METH.

In Chapter 3:

To clarify the substantial role of astrocytes in the development of rewarding effects induced by drugs of abuse, behavioral studies were undertaken to investigate whether astrocyte-related soluble factors affect the expression of rewarding effects induced by METH and MRP. I also explored the implication of Janus kinase/signal transducer and activator of transcription (Jak/STAT) pathway-dependent astrogliosis and astrogliogenesis during the development of rewarding effects induced by METH and MRP.

Ethics

The present study was conducted in accordance with the Guiding Principles for the Care and Use of Laboratory Animals, as adopted by the Committee on Animal Research of Hoshi University, which is accredited by the Ministry of Education, Culture, Sports, Science and Technology of Japan. Every effort was made to minimize the numbers and any suffering of animals used in the following experiments. Animals were used only once in the present study.

Chapter 1

Long-lasting change in brain dynamics by methamphetamine: Enhancement of protein kinase C-dependent astrocytic response and behavioral sensitization

Introduction

METH and cocaine are strongly addictive psychostimulants that dramatically affect the CNS, and are highly abused drugs worldwide. Abuse of psychostimulants leads to the development of psychotic symptoms that resemble those of paranoid schizophrenia[61]. In rodents, it has been shown consistently that repeated exposure to psychostimulants results in a progressive and enduring enhancement in the motor stimulant effect elicited by a subsequent drug challenge, which termed behavioral sensitization[53, 55, 62]. Accumulating evidence suggests that the behavioral sensitization induced by psychostimulants may be accompanied by long-lasting neural plasticity[63-65], which may involve structural modifications in the dopaminergic and/or glutamatergic systems.

The present study was undertaken to investigate the mechanism of METH- and MRP-induced astrocytic activation in purified cortical astrocytes and cortical neuron/glia co-cultures. I also explored the difference between METH and MRP in the maintenance of astrocytic activation in cultured cells and behavioral sensitization in mice.

Materials and Methods

Tissue Processing

Purified cortical astrocytes were grown as follows; cerebral cortices were obtained from newborn ICR mice (Tokyo Laboratory Animals Science Co., Ltd., Tokyo, Japan), minced, and treated with trypsin (0.025 %, Invitrogen Co., Carsbad, CA, USA) dissolved in phosphate-buffered saline (PBS) solution containing 0.02 % L-cysteine monohydrate (Sigma-Aldrich Co., St. Louis, MO, USA), 0.5 % glucose (Wako Pure Chemicals Ind., Ltd., Osaka, Japan) and 0.02 % bovine serum albumin (Wako Pure Chemicals Ind., Ltd.). After enzyme treatment at 37 °C for 15 min, cells were dispersed by gentle agitation through a pipette and plated on a flask. One week after seeding in Dulbecco's modified Eagle's medium (DMEM, Invitrogen Co.) supplemented with 5 % fetal bovine serum (FBS, Invitrogen Co.), 5 % heat-inactivated (56 °C, 30 min) horse serum (HS, Invitrogen Co.), 10 U/mL penicillin and 10 μg/ml streptomycin in a humidified atmosphere of 95 % air and 5 % CO_2 at 37 °C, the flask was shaken for 12 hr at 37 °C to remove non-astrocytic cells. The cells were seeded at a density of 1 x 10^5 cells/cm^3. The cells were maintained for 3 to 10 days in DMEM supplemented with 5 % FBS, 5 % HS, 10 U/mL penicillin and 10 μg/mL streptomycin in a humidified atmosphere of 95 % air and 5 % CO_2 at 37 °C.

Cortical neuron/glia co-cultures were grown as follows; cerebral cortex was obtained from newborn ICR mice (Tokyo Laboratory Animals Science Co.), minced, and treated with papain (9 U/mL, Worthington Biochemical, Lakewood, NJ, USA) dissolved in

PBS solution containing 0.02 % L-cysteine monohydrate, 0.5 % glucose and 0.02 % bovine serum albumin. After enzyme treatment at 37 °C for 15 min, cells were seeded at a density of 2 x 10^6 cells/cm^3. The cells were maintained for 7 days in DMEM supplemented with 10 % FBS, 10 U/mL penicillin and 10 μg/mL streptomycin. On day 8, the cells were treated with drugs.

Drug treatment and immunohistochemistry

At day 3-7 *in vitro*, the cells were treated with either normal medium, methamphetamine hydrochloride (METH, 0.01-1000 μM, Dainippon Pharmaceutical Co. Ltd., Osaka, Japan), a selective protein kinas C (PKC) inhibitor chelerythrine chloride (CHE, 10 nM, Sigma-Aldrich Co.) + METH (1-100 μM), morphine hydrochloride (MRP, 0.1-1000 μM, Sankyo Co., Ltd., Tokyo, Japan), MRP (10-100 μM) + CHE (10 nM) or CHE (10-100 nM). The treatments lasted for 1-3 days. The cells were then identified by immunofluorescence using a rabbit polyclonal antibody to GFAP (1:1000; Chemicon International, Inc., Temecula, CA, USA), a mouse polyclonal antibody to GFAP (1:1000, Chemicon, International, Inc.), a rabbit polyclonal antibody to phosphorylated-protein kinas C (p-PKC, 1:400; Cell Signaling Technology Inc., Beverly, MA, USA), or a rabbit polyclonal antibody to cleaved caspase-3 (1:100, Cell Signaling Technology Inc., Beverly, MA, USA), followed by incubation with Alexa 488-conjugated goat anti-rabbit IgG (1:4000) or Alexa 546-conjugated goat anti-rabbit IgG (1:4000) for GFAP, Alexa 488-conjugated goat anti-rabbit IgG (1:4000) for p-PKC, and Alexa 488-conjugated goat anti-rabbit IgG (1:10000) for cleaved caspase-3.

Images were collected using a Radiance 2000 laser-scanning microscope (BioRad, Richmond, CA, USA). The experiments were repeatedly performed by, at least, 3 independent culture preparations.

The intensity of GFAP-like immunoreactivity was measured with a computer-assisted system (NIH Image). The upper and lower threshold intensity ranges were adjusted to encompass and match the immunoreactivity to provide an image with immunoreactive material appearing in black pixels, and non-immunoreactive material as white pixels. The area and intensity of pixels within the threshold value representing immunoreactivity were calculated. I randomly chose 10 areas (80 x 80 pixels) for calculation of GFAP-like immunoreactivity in each image (512 x 512 pixels). The intensity of GFAP-like immunoreactivity was expressed as a percent increase (mean ± SEM) with respect to that in control cells.

Evaluation of astrocytic stellation

In order to evaluate the astrocytic stellation, purified cortical astrocytes were cultured on 24 well plates and treated with METH (0.01-100 μM) or METH (1-100 μM) + CHE (10 nM) for 1-3 days. The cells were fixed in 4 % paraformaldehyde and stained with cresyl violet (0.1 %, ICN Biomedicals, Aurora, OH, USA) to determine the percentage of stellate cells in cultures. Cells with processes longer than their perinuclear diameters were defined as stellate cells. Stained cells were mounted on glass slides and viewed under transmitted light using a microscope with a 10 x objective lens (IX 70, Olympus Optical, Tokyo, Japan). For each coverslips, four randomly chosen fields

were counted (about 170 cells in each field), and the percentage of stellate cells was determined. Each experimental condition was repeated from 4 independent culture preparations. The percentage of stellate cells was expressed as mean ± SEM.

Confocal Ca^{2+} imaging

Cells were loaded with 10 μM fluo-3 acetoxymethyl ester (Dojindo molecular Technologies, Inc., Kumamoto, Japan) for 90 min at room temperature. After a further 20-30 min of de-esterification with the acetoxymethyl ester, the coverslips were mounted on a microscope equipped with a confocal Ca^{2+} imaging system (Radiance 2000, BioRad). Fluo-3 was excited with the 488 nm line of an argon-ion laser and the emitted fluorescence was collected at wavelengths > 515 nm, and average baseline fluorescence (F_0) of each cells was calculated. To compensate for the uneven distribution of fluo-3, self-ratios were calculated (Ratio = F/F_0).

Dopamine hydrochloride (1-100 μM, Sigma-Aldrich Co.) or glutamate (1-100 μM, Wako Pure Chemicals Ind., Ltd.) was perfused for 30 sec at 5 mL/min at room temperature in cells followed by superfusion of balanced salt saline (BSS, pH 7.4) containing 150 mM NaCl, 5.0 mM KCl, 1.8 mM $CaCl_2$, 1.2 mM $MgCl_2$, 25 mM N-2-hydroxyethylpiperazine-N'-2-ethaneslufonic acid and 10 mM D-glucose.

Locomotor assay for METH and MRP

Male ICR mice (20-25 g) were housed at a room temperature of 23 ± 1 °C with a 12-hr light-dark cycle (lights on 8:00 to 20:00). Food and water were available *ad*

libitum.

The locomotor activity of mice was measured by an ambulometer (ANB-M20, O'Hara, Tokyo, Japan) as described previously[66]. Briefly, a mouse was placed in a tilting-type round activity cage of 20 cm in diameter and 19 cm in height. Any slight tilt of the activity cage caused by horizontal movement of the animal was detected by microswitches. Total activity counts in each 10-min segment were automatically recorded for 30 min prior to the injections and for 180 min following METH administration.

According to previous reports[55, 67], a repeated injection paradigm was used in which animals were treated with an injection of METH (2 mg/kg, s.c.) or MPR (10 mg/kg, s.c.) every 96 hr to induce sensitization to METH- or MRP-induced hyperlocomotion. Total activity was counted for 3 hr after each treatment.

To investigate the implication of PKC in the development of sensitization to METH-induced hyperlocomotion, mice were pretreated with saline or a selective PKC inhibitor S-2,6-diamino-N-[(1-[1-oxotridecyl]-2-piperidinyl)methyl]hexamide dihydorochloride (NPC-15437: 1 mg/kg, s.c., Sigma-Aldrich Co.) 30 min prior to METH (2 mg/kg, s.c.) treatment.

Immunohistochemistry using brain-slice sections

Twenty four hr after the last METH treatment, animals were deeply anesthetized with sodium pentobarbital (50 mg/kg, i.p.) and perfused transcardially with 4 % paraformaldehyde in 0.1 M PBS. Then, the brains were removed quickly after

perfusion and thick coronal section of the forebrain including the N.Acc. and cingulate cortex (CG) region was initially dissected using brain blocker. The coronal section of the midbrain was post-fixed in 4 % paraformaldehyde for 2 hr. After the brains were permeated with 20 % sucrose for 2 days and 30 % sucrose for 2 days, they were frozen in an embedding compound (Sakura Finetechnical, Tokyo, Japan) on isopentane using liquid nitrogen and stored at -30 °C until used. Frozen coronal sections (8 μm) were cut in a cryostat, and thaw-mounted on poly-L-lysine-coated glass slides.

Each primary antibody was diluted in 0.01 M PBS containing 10 % normal horse serum [1:10 GFAP (Nichirei Co., Tokyo, Japan)] and was incubated twice overnight at 4 °C. The antibodies were then rinsed and incubated with each secondary antibody for 2 hr at room temperature. For each labeling, Alexa 488-conjugated goat anti-rabbit IgG for GFAP was diluted 1:1200 in PBS containing 10 % normal horse serum.

Statistical analysis

The data of GFAP-like immunoreactivity, astrocytic stellation and confocal Ca^{2+} imaging are presented as the mean ± SEM. The statistical significance of differences between the groups were assessed by one-way analysis of variance (ANOVA) with Student's t-test. The statistical significance of differences between the groups were assessed by two-way ANOVA followed by the Bonferroni/Dunn multiple-comparison test.

Results

METH-induced astrocytic activation

Treatment with METH (10 μM) for 3 days caused a robust activation of purified cortical astrocytes, as detected by a stellate morphology and an increase in the level of GFAP-like immunoreactivity compared to that in normal medium-treated cells (Figure 1-1A). As shown in Figure 1-1B, treatment with METH (1-100 μM) for 1-3 days significantly increased the number of stellate astrocytes in purified cortical astrocytes. Although 1 day treatment with METH even caused a significant stellation in purified cortical astrocytes, 3 days treatment with METH (10-100 μM) showed a drastic stellation. In addition, this activation of astrocytes was partially reversed by treatment with the specific PKC inhibitor CHE (Figure 1-1A, B), indicating the possible implication of PKC in this event. Immunohistochmical staining with an antibody to p-PKC confirmed that treatment with METH increased the immunoreactiviy of p-PKC in astrocytes (Figure 1-1C). These results suggest that astrocytic PKC is involved in MEHT-induced astrocytic activation. Treatment with METH (10-100 μM) for 3 days also caused a robust atrocytic activation in cortical neuron/glia co-cultures, and this activation was reversed by co-treatment with CHE (Figure 1-2A, B).

I next investigated whether treatment with METH could induce any functional changes in astrocytes. Either dopamine (1-100 μM) or glutamate (1-100 μM) produced a transient increase in $[Ca^{2+}]i$ in purified cortical astrocytes (Figure 1-3A, B, C). The Ca^{2+} responses to dopamine and glutamate in astrocytes were significantly

enhanced by 3 days of treatment with METH (10 μM, 3 days, Figure 1-3A, B, C).

Morphine-induced astrocytic activation

To compare its effects with those of METH, I investigated the effect of MRP in astrocytes. Unlike METH, treatment with MRP (1-1000 μM) for 1-3 days did not produce morphological changes in the activation of purified cortical astrocytes (Figure 1-4A, B). In contrast to MRP treatment in purified cortical astrocytes, treatment with MRP (10-100 μM) for 3 days activated GFAP-positive astrocytes in cortical neuron/glia co-cultures (Figure 1-4C, D), and this activation was partially attenuated by CHE (10 nM).

Different maintenance of METH- and MRP-induced astrocytic activation

I next explored the difference between METH and MRP in the maintenance of astrocytic activation. Treatment with METH (10 μM) for 1 day caused the activation of GFAP-positive astrocytes in cortical neuron/glia co-cultures (Figure 1-5A). The METH-contained medium was then switched to normal medium, and the cells were cultured for additional 2 days. It is of interest to note that the METH-induced increase in the level of GFAP-immunoreactivity still remained after an additional 2 days of cultured with normal medium (Figure 1-5A). Treatment with MRP (10 μM) for 1 day also caused the activation of GFAP-positive astrocytes in cortical neuron/glia co-cultures (Figure 1-5B). The MRP-containing medium was then switched to normal medium, and the cells were cultured for additional 2 days. Unlike METH, the MRP-

induced increase in the level of GFAP-immunoreactivity was reversed after an additional 2 days of cultured with normal medium (Figure 1-5B).

Long-lasting maintenance of behavioral sensitization to METH, but not MRP

The repeated administration of psychostimulant drugs results in a progressive and enduring elevation in the motor response elicited, which may be accompanied by a long-lasting neural plasticity. Therefore, I hypothesized that the psychostimulant-induced astrocytic activation may be related to behavioral sensitization. Based on the data presented above and the hypothesis, I next investigated whether repeated *in vivo* treatment with METH could cause a long-lasting maintenance of behavioral sensitization to METH-induced hyperlocomotion.

To clarify the development of sensitization to METH- or MRP-induced hyperlocomotion, mice were given five times with METH (2 mg/kg, s.c.) or MRP (10 mg/kg, s.c.) every 96 hr. Repeated injection of either METH or MRP produced a progressive elevation of the METH- or MRP-induced locomotor-enhancing effect, indicating the development of sensitization to METH- or MRP-induced hyperlocomotion ($P < 0.01$, first session versus fifth session, Figure 1-6A, B). Intriguingly, the METH-induced sensitization to hyperlocomotion was maintained even after 2 months withdrawal following intermitted METH administration (Figure 1-6A). However, the MRP-induced sensitization was reversed by 2 months withdrawal following intermitted MRP administration (Figure 1-6B).

METH-induces neuronal cell death

METH has been recognized as a drug of abuse that induces nerve terminal degeneration and neuronal apoptosis in the mammalian brain[59, 68]. I therefore confirmed whether *in vitro* treatment with high concentration of METH or MRP could induce neuronal cell death. Treatment with METH (100μM, 1 mM) for 3 days in cortical neuron/glia co-cultures caused the robust activation of cleaved caspase-3, which is a marker of neuronal death (Figure 1-7A). However, unlike METH, high concentration of MRP failed to produce the caspase-3 activation (Figure 1-7B).

***In vivo* Astrocytic Responses by METH**

Finally, I investigated *in vivo* astrocytic responses during the development of METH-induced sensitization. In order to investigate the direct involvement of PKC in the development of sensitization to METH-induced hyperlocomotion, mice were given intermittently METH (2 mg/kg, s.c.) in combination with a specific PKC inhibitor NPC-15437 (1 mg/kg, s.c.). Intermittent co-administration of NPC-15437 abolished the development of sensitization to METH-induced hyperlocomotion (Figure 1-8).

I also confirmed that repeated *in vivo* treatment with METH under the present schedule failed to cause the neuronal cell death; the present schedule of treatment with METH had no effect on the caspase-3 activity in the caudate putamen (data not shown). Immunohistochemical studies were also performed in order to investigate the change in GFAP-IR levels in the CG (Figure 1-9A) and N.Acc. (Figure 1-9B) following intermittent treatment with METH. The GFAP-immunoreactivity level was clearly

increased in METH-sensitized mice compared to those in mice that had been repeatedly treated with saline (Figure 1-9A, B). This increase in GFAP-IR level in METH-sensitized mice was completely abolished by intermittent co-administration of NPC-15437 (Figure 1-9A, B).

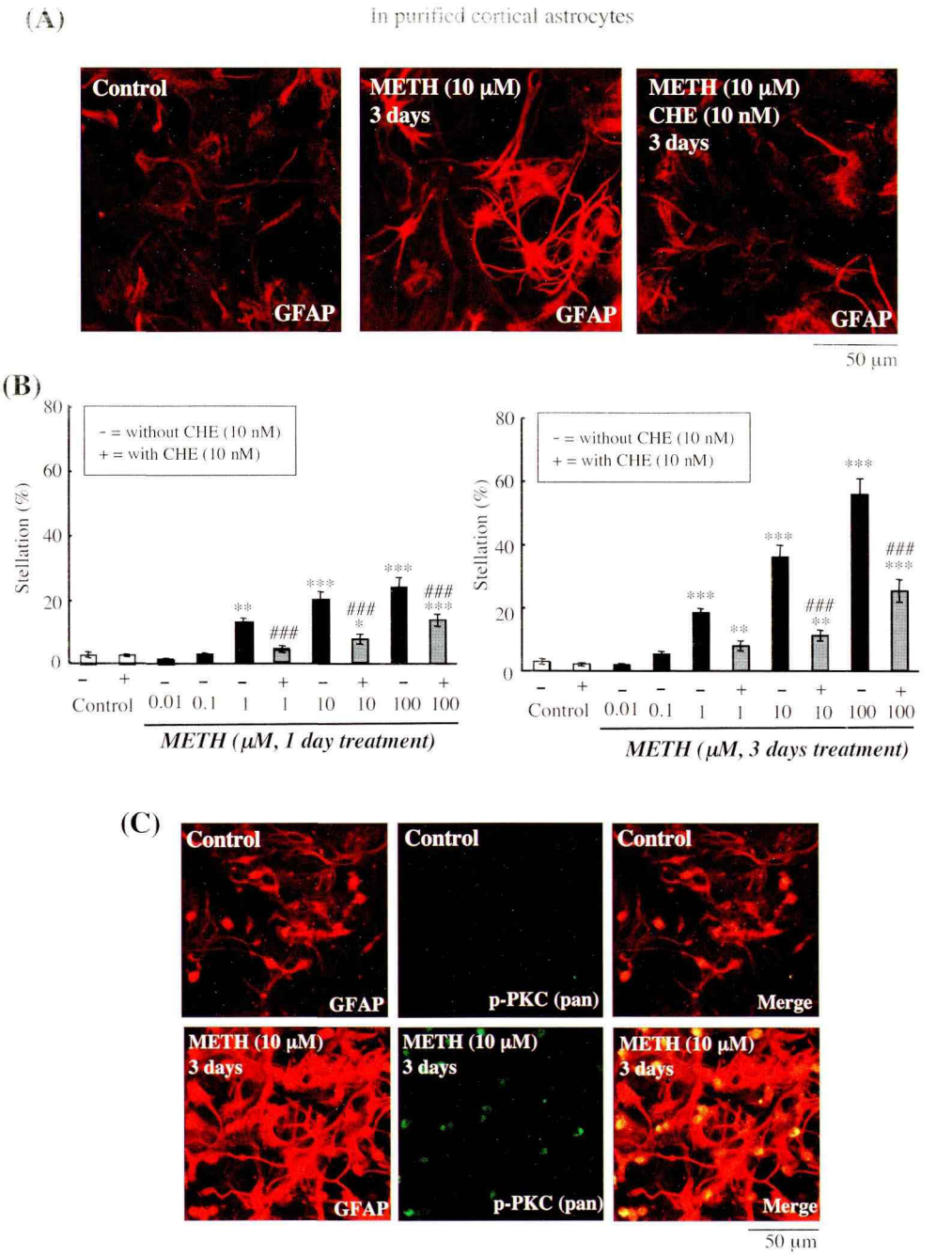

Figure 1-1 Treatment with methamphetamine (METH) causes astrocytic activation in purified cortical astrocytes. (A) Purified cortical astrocytes were incubated with normal medium, METH (10 μM) or METH + chelerythrine (CHE, 10 nM) for 3 days. The cells were stained with a rabbit polyclonal antibody to GFAP. (B) Purified cortical astrocytes were incubated with normal medium, METH (0.01-100 μM) or METH (1-100 μM) + CHE (10 nM) for 1-3 days. Astrocytic activation as shown by a stellate morphology with processes longer than their perinuclear diameters was evaluated. Data represent the mean ± SEM of 139-250 cells from 4 separate observations. $^{**}p < 0.01$, $^{***}p < 0.001$; control , $^{###}p < 0.001$; vs. cells without CHE. (C) The green labeled for p-PKC (pan) stained with a rabbit polyclonal antibody and the red labeled for GFAP stained with a mouse polyclonal antibody are mostly overlapped as yellow in METH-treated astrocytes.

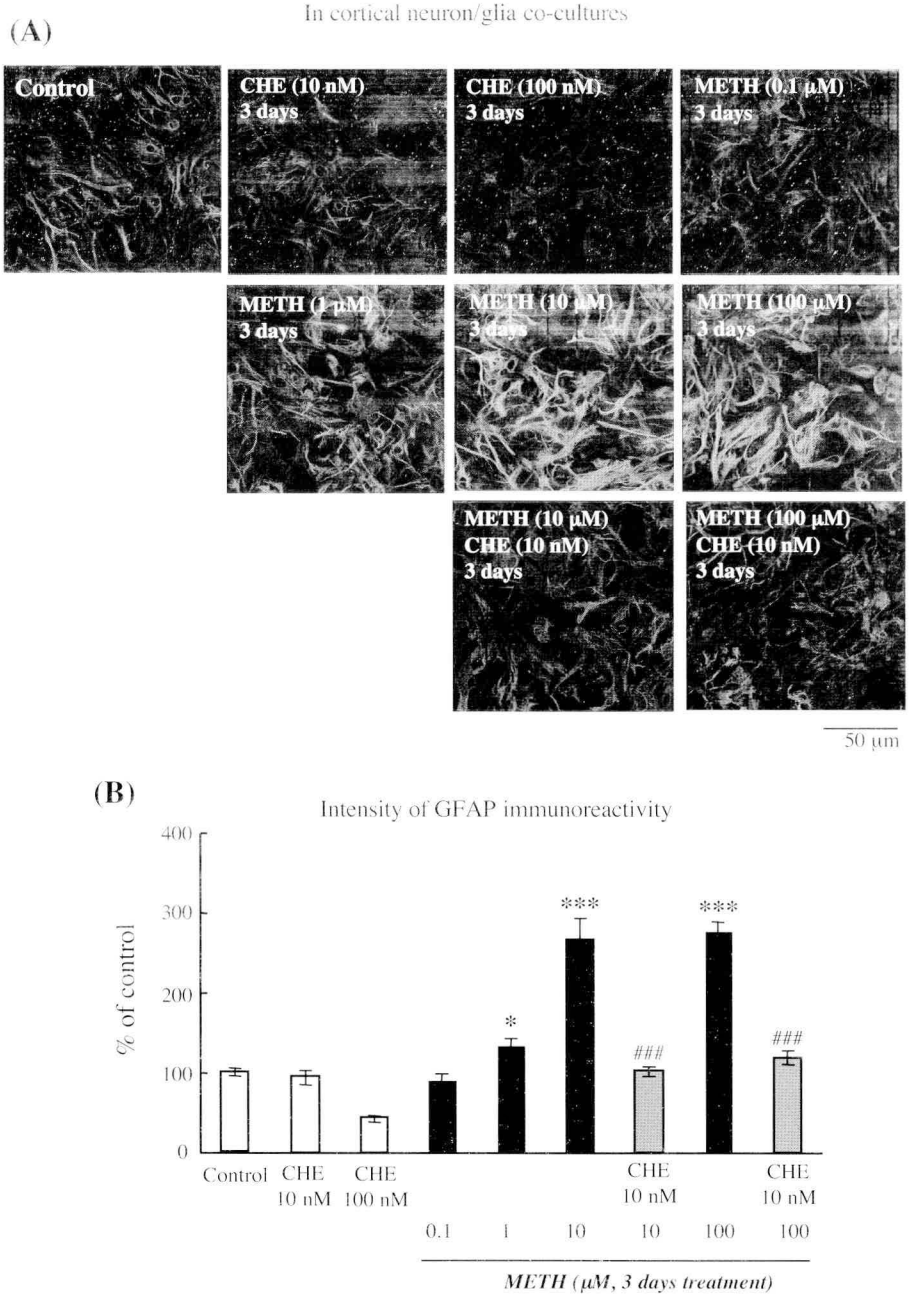

Figure 1-2 Treatment with methamphetamine (METH) for 3 days causes astrocytic activation in cortical neuron/glia co-cultures. (A) Cortical neuron/glia co-cultures were with normal medium, METH (0.1-100 μM) or METH (1-100 μM) + CHE (10 nM) for 3 days. The cells were stained with a rabbit polyclonal antibody to GFAP. (B) The intensity of GFAP-like immunoreactivity of each image was measured using an NIH image. The level of GFAP like immunoreactivity on MEHT- and METH + CHE-treated cells is expressed as a percent increase (mean ± SEM) with respect to that on control cells. * $p < 0.05$, ***$p < 0.001$; vs. control cells. ###$p < 0.001$; vs. METH-treated cells.

In purified cortical astrocytes

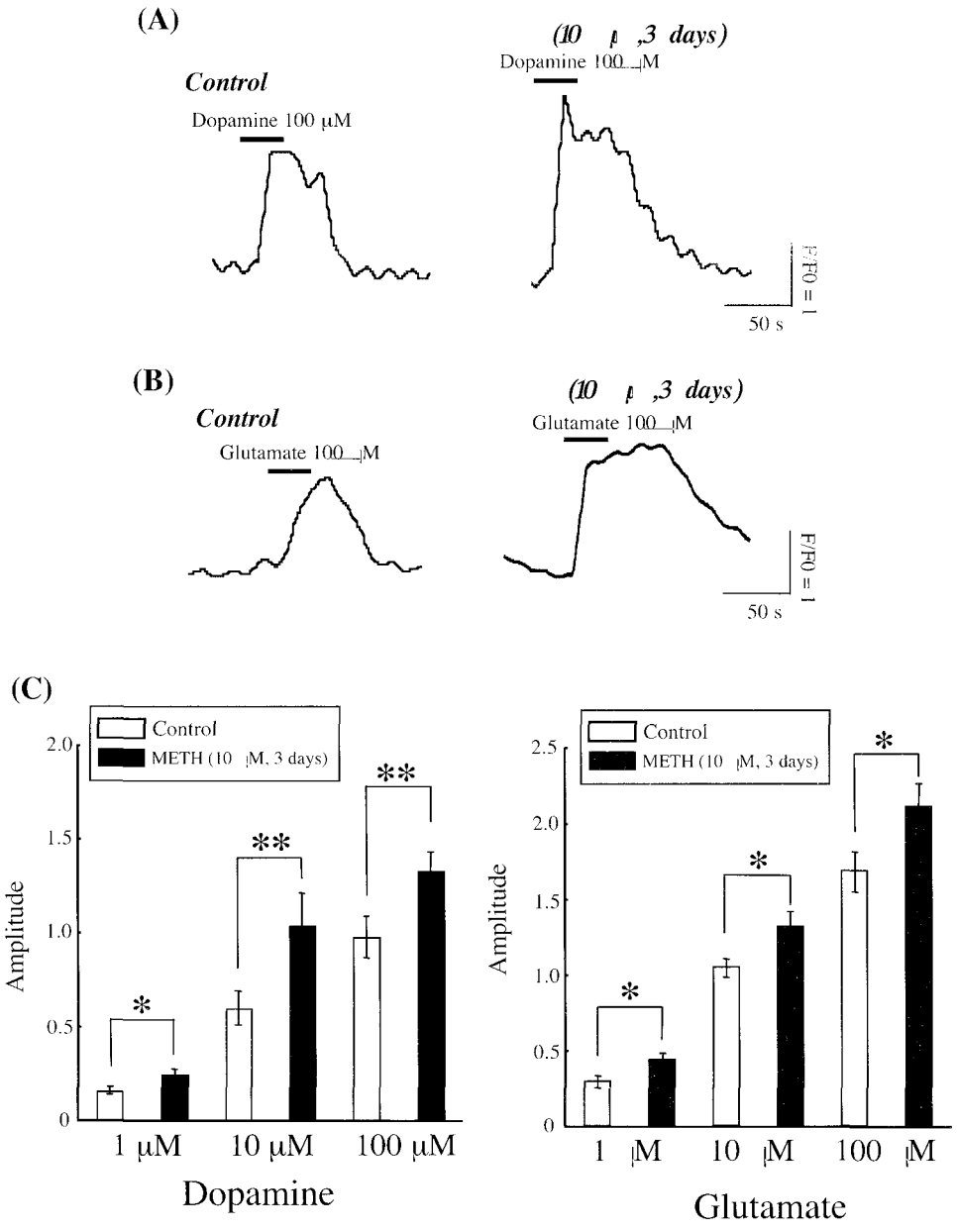

Figure 1-3 The Ca^{2+} responses to dopamine and glutamate in astrocytes were significantly enhanced by 3 days of treatment with METH. (A) Traces show the dopamine (100 μM)-evoked increase in the intracellular Ca^{2+} concentration in control and METH-treated astrocytes. (B) Traces show the glutamate (100 μM)-evoked increase in the intracellular Ca^{2+} concentration in control and METH-treated astrocytes. (C) The Ca^{2+} responses to dopamine and glutamate in control and METH-treated astrocytes are summarized. Data represent the mean ± SEM of 54-72 cells. *$p < 0.05$, **$p < 0.01$ vs. control astrocytes.

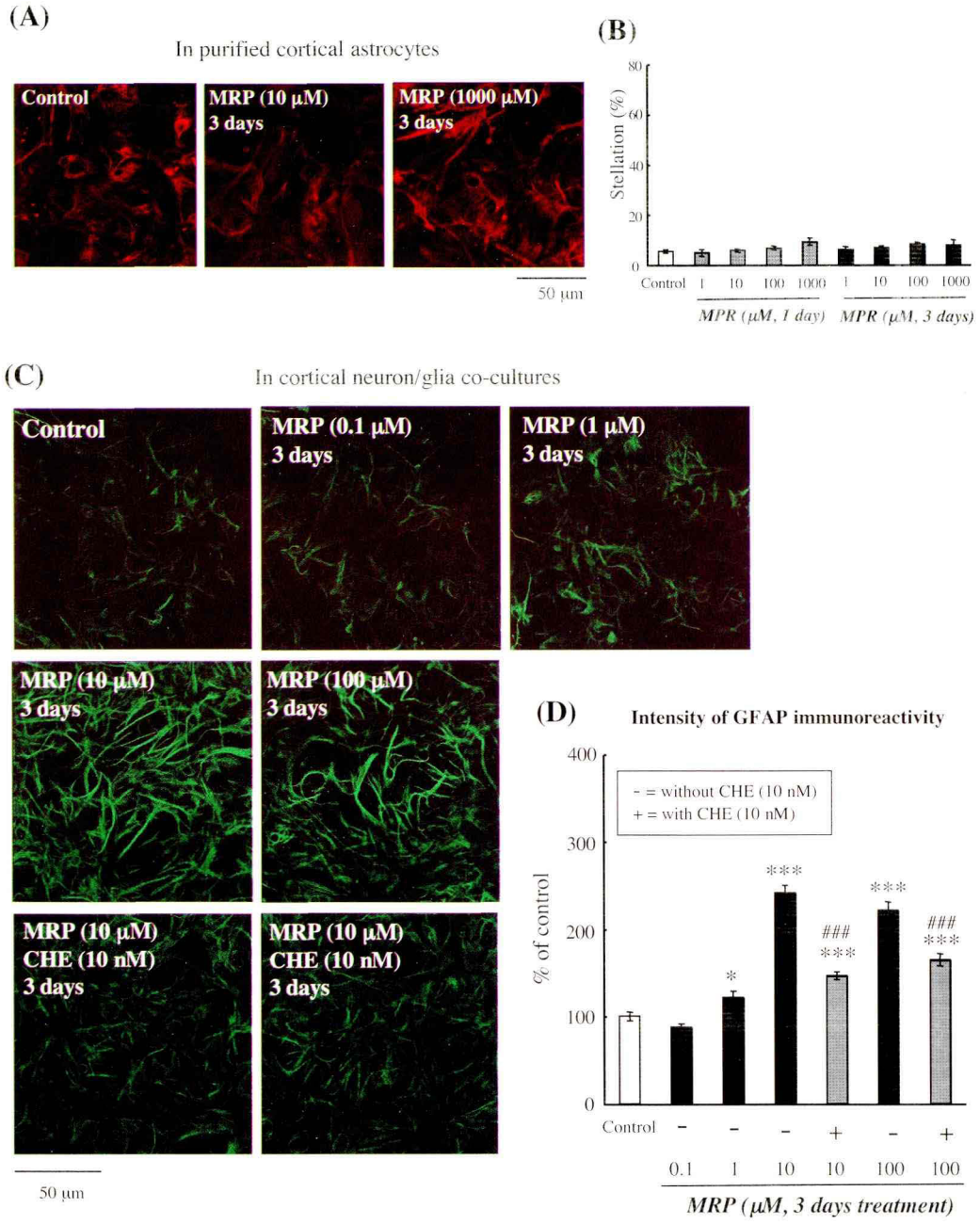

Figure 1-4 Morphine (MRP) causes astrocytic activation in cortical neuron/glia co-cultures, but not in cortical purified astrocytes. (A) Purified cortical astrocytes were incubated with normal medium or MRP (1-1000 μM) for 3 days. The cells were stained with a rabbit polyclonal antibody to GFAP. (B) Purified cortical astrocytes were incubated with normal medium and MRP (1-1000 μM) for 1-3 days. Astrocytic activation as shown by a stellate morphology with processes longer than their perinuclear diameters was evaluated. Data represent the mean ± SEM of 175-230 cells from 4 separate observations. (C) Cortical neuron/glia co-cultures were incubated with normal medium, MRP (0.1-100 μM) or MRP (10-100 μM) + CHE (10 nM) for 3 days. The cells were stained with a rabbit polyclonal antibody to GFAP. (D) The intensity of GFAP-like immunoreactivity of each image was measured using an NIH image. The level of GFAP like immunoreactivity on MRP- or MRP + CHE-treated cells is expressed as a percent increase (mean ± SEM) with respect to that on control cells. * $p < 0.05$, *** $p < 0.001$; vs. control cells. ### $p < 0.001$; vs. MRP-treated cells.

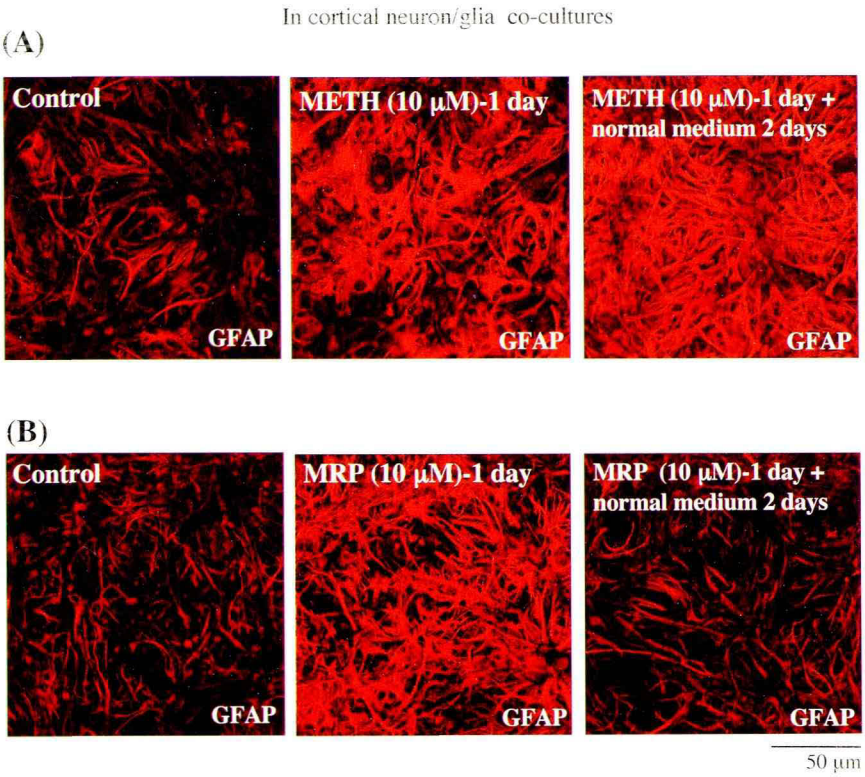

Figure 1-5 METH, but not MRP, causes a long-lasting astrocytic activation in cortical neuron/glia co-cultures. (A) Cortical neuron/glia co-cultures were incubated with normal medium or METH (10 μM) for 1 day or 3 days, and cells were cultured with normal medium for additional 2 days. (B) Cortical neuron/glia co-cultures were incubated with MRP (10 μM) for 1 day or 3 day, and then, cells were cultured with normal medium for additional 2 days. All cells were stained with a rabbit polyclonal antibody to GFAP.

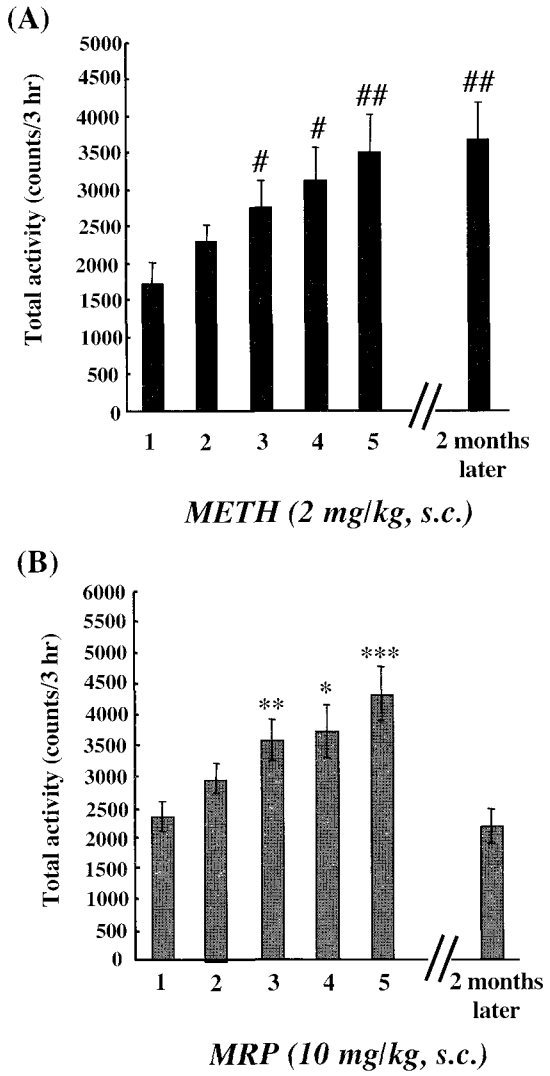

Figure 1-6 The difference between METH and MRP in the maintenance of behavioral sensitization in mice. (A) Mice were treated with METH (2 mg/kg, s.c.) every 96 hr for five sessions. Mice were then administered with METH (2 mg/kg, s.c.) after 2 months withdrawal. Total activity was counted for 3 hr after each treatment (1, 5, 9, 13, 17 days and after 2 months withdrawal). #$p < 0.05$, ##$p < 0.01$, vs. the 1st administration. (B) Another group of mice were given five intermittent treatments morphine (10 mg/kg, s.c.) every 96 hr. Mice were then administered with morphine (10 mg/kg, s.c.) after 2 months withdrawal. Total activity was counted for 3 hr after the treatment (1, 5, 9, 13, 17 days and after 2 months withdrawal). *$p < 0.05$, ** < 0.01, ***$p<0.001$ vs. the 1st administration.

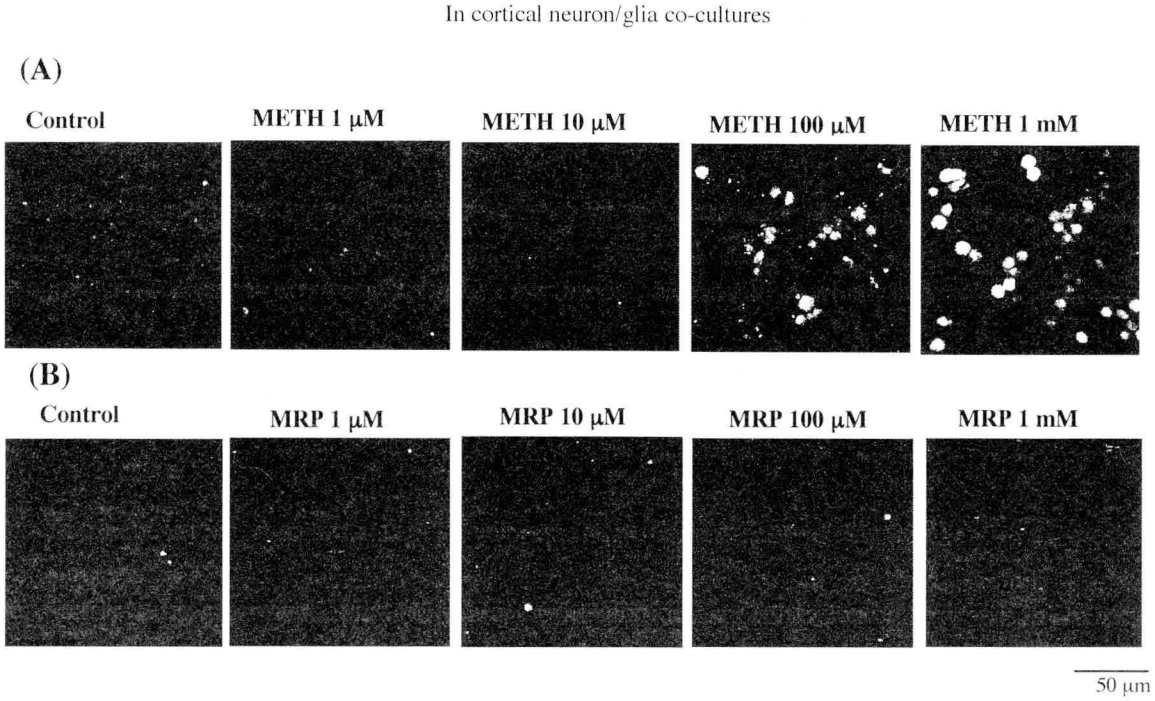

Figure 1-7 High concentration of METH, but not MRP, causes a neuronal cell death in cortical neuron/glia cocultures. (A) Cortical neuron/glia co-cultures were incubated with normal medium or METH (1, 10, 100 μM, 1 mM) for 3 days. (B) Cortical neuron/glia co-cultures were incubated with MRP (1, 10, 100 μM, 1 mM) for 3 days. All cells were stained with a rabbit polyclonal antibody to cleaved caspase-3.

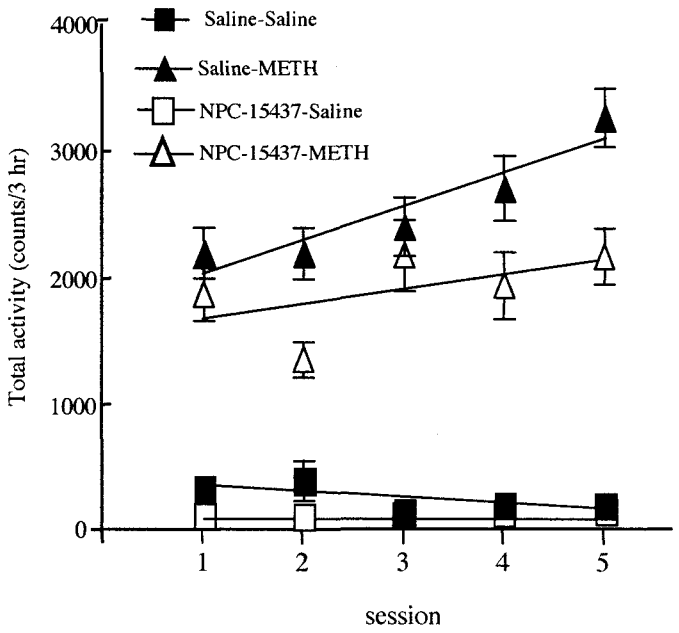

Figure 1-8 Blockade of the development of sensitization to METH (2 mg/kg, s.c.)-induced hyperlocomotion by co-treatment with a PKC inhibitor NPC-15437 (1 mg/kg, s.c.) in mice. METH (2 mg/kg, s.c.) or saline was repeatedly given to mice every 96 hr, and the total activity was counted for 3 hr after each treatment. Repeated injection of METH produced a progressive elevation of the METH-induced locomotor-enhancing effect, indicating the development of sensitization to METH-induced hyperlocomotion ($F_{1, 190}$=430.20, $p < 0.001$ vs. Saline-Saline). Another groups of mice were given intermittently with METH in combination with NPC (1 mg/kg, s.c.) every 96 hr. NPC or saline was pretreated at 30 min before METH administration (2 mg/kg, s.c.). Intermittent co-administration of NPC-15437 significantly suppressed the development of sensitization to METH-induced hyperlocomotion ($F_{1,90}$=20.54, $p < 0.001$ vs. Saline-METH). There were no significant differences between the 1st and 5th administration in NPC-15437-treated mice.

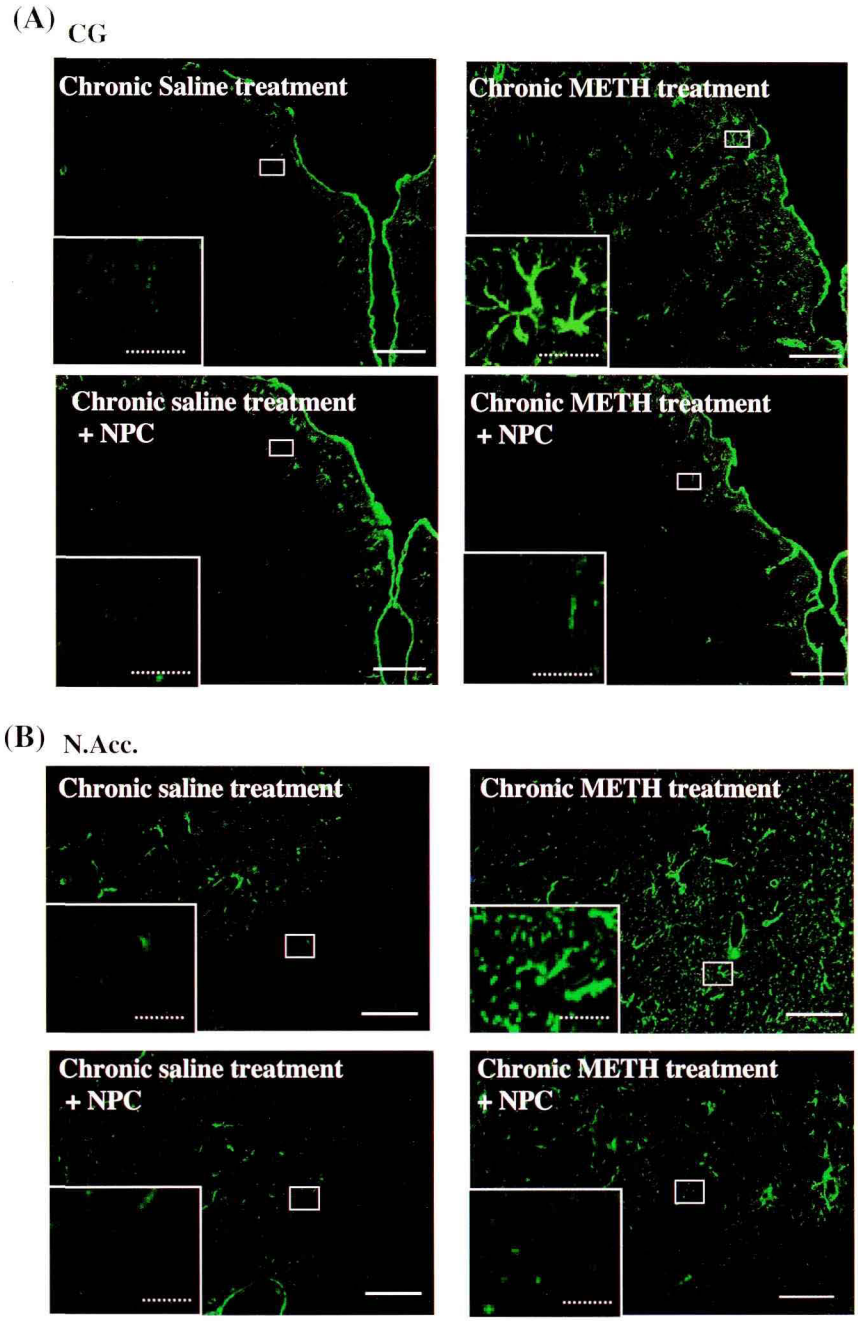

Figure 1-9 GFAP-like immunoreactivity (IR) in the cingulate cortex and nucleus accumbens of mice by repeated *in vivo* treatment with METH with or without co-treatment with a specific PKC inhibitor NPC-15437. The density of GFAP-IR was increased in the cingulate cortex (CG, A) and nucleus accumbens (N.Acc., B) of mice during the development of sensitization to METH. There were no changes in the density of GFAP-IR in the CG (A) and N.Acc. (B) of mice treated with METH in combination with NPC-15437 as compared to saline treatment. Scale bar (unbroken line): 100 μm, Scale bar (broken line): 20 μm (A) or 50 μm (B).

Discussion

In the present study, I observed morphological changes in astrocytes by treatment with either METH or MRP in cortical neuron/glia co-cultures. A difference was noted between the effects of METH and MRP in purified cortical astrocytes: while METH markedly activated astrocytes with phosphorylation of PKC, MRP had no such effect.

I also found that treatment with METH (10 μM) for 3 days increased the sensitivity of cortical astrocytes to dopamine and glutamate, which can be responsible for rewarding effects of psychostimulants and opioids[69, 70]. Many lines of evidence support the idea that the enhanced Ca^{2+} signaling in astrocytes is not only restricted to single cells, but also can cross cell borders via gap junctions, resulting in intracellular Ca^{2+} waves traveling from one astrocyte to another, and the induction of Ca^{2+} responses in neurons[13, 71]. Taken together, these findings suggest that treatment with METH may cause the functional up-regulation of neuroactive substances in astrocytes. It is also likely that the increase in astrocytic Ca^{2+} signaling induced by dopamine and glutamate following chronic exposure to METH may result from an enhancement of astrocytic dopamine and glutamate receptor functions induced by METH.

A study of cultures of newborn rodent CNS cells has shown that heterogeneous subpopulations of astrocytes can express one or more types of opioid receptor[72, 73]. It has been reported that preferential μ-opioid receptor agonists can interfere with neuronal cell division[74]. In the present study, I found that the μ-opioid receptor agonist MRP had no effect on astrocytic activation in purified cortical astrocytes,

whereas it caused astrocytic activation in cortical neuron/glia co-cultures. These findings constitute evidence that MRP might activate astrocytes via neurons. Furthermore, the present results raise the possibility that METH and MRP may differentially regulate long-term changes in neuron-glia communication.

Here I demonstrated that the astrocytic activation in cortical neuron/glia co-cultures induced by either METH or MRP was blocked by treatment with a specific PKC inhibitor. Several lines of evidence have suggested that neurite outgrowth on several cell adhesion and matrix molecules[19, 52], including fibronectin[75], laminin and collagen[76], are reduced by the specific inhibition of PKC, suggesting that PKC plays an important role in regulating the direction of neurite growth. These findings, along with those in the present study, suggest that PKC is likely to be one of the most important factors in modulating the synaptic plasticity induced by METH and MRP.

I also found the difference between METH and MRP in the maintenance of astrocytic activation: METH produced prolonged astrocytic activation, whereas MRP caused a reversible activation of astrocytes in cortical neuron/glia co-cultures. Astrocytic activation has been considered for a long time as the major impediment to axonal regrowth after an injury in the CNS[26, 27]. However, there are increasing evidences that astrocytes play a dynamic role in regulating synaptic strength, synaptogenesis and neurogenesis[20-22]. Although the exact function of METH- and MRP-induced astrocytic activation remains unclear at this time, it may positively modulate synaptic activity by directly controlling synaptic strength, leading to synaptic plasticity in the CNS.

Cultured cells used in the present *in vitro* study represents a simplified relative to the state of neuron-glia communication in the CNS. Thus, additional interactions with these cells and matrix components in *in vivo* system are likely to reflect the behavioral change such as behavioral sensitization. In fact, one of the most important aspects of the present study was that the METH-induced behavioral sensitization was maintained even after a long period of abstinence, while the MRP-induced sensitization was reversible. This may be consistent with the evidence that METH, but not MRP, produced long-lasting astrocytic activation in cortical neuron/glia co-cultures. It is, therefore, worthwhile in future studies to identify the precise molecular steps associated with astrocyte-to-neuron signaling on a long-lasting maintenance of METH-induced behavioral sensitization.

Another key finding of the present study was that the levels of GFAP in the mouse CG and N.Acc. were clearly increased by repeated *in vivo* administration of METH, which was related to behavioral sensitization. These results suggest the repeated *in vivo* treatment of METH could produce the activation of astrocytes in the CG and N.Acc. Central dopamine systems have been implicated in mediating reward-related behaviors[41-43]. In particular, the N.Acc. of the mesolimbic dopamine pathway plays an important role in regulating the rewarding effects of many stimuli including drugs of abuse[41-43]. It has been also recognized that the CG is responsible for stimulus-reward learning[77]. Taken together, these studies suggest the possibility that METH-induced astrocytic activation in these areas modulates the development of METH-induced behavioral sensitization.

The development of behavioral sensitization to METH with astrocytic activation was abolished by co-treatment with the PKC inhibitor NPC-15437. Although further experiment is still required, these findings indicate that activated PKC-dependent astrocytic response in the CG and N.Acc. by intermittent METH treatment may be implicated in the development of sensitization to the METH-induced hyperlocomotion.

Finally, I investigated the neurotoxic effects of METH and MRP: METH markedly induced neuronal cell death in cortical neuron/glia co-cultures, while MRP had no such effect. Glial activation is thought to be neuroprotective[26-28], however, excess activation can be deleterious in the brain[28, 78]. In fact, overexpression of astrocyte-derived neurotrophic protein S100β has been shown to induce neuronal cell death through nitric oxide released from astrocytes[79]. Taken together, the present findings support the idea that the direct effect induced by high concentration of METH on astrocytes may lead to a dynamic change in neuron-glia network, resulting in the neurotoxicity.

In conclusion, the present data clearly provide direct evidence for the distinct mechanisms between METH and MRP on the astrocytic and neuronal responses. Nevertheless opioids, such as MRP, have been used worldwide to control chronic pain, the appearance of opioid addiction following chronic administration of opioids seriously limits their use for the relief of moderate to severe pain. The information of the reversibility of astrocytic response and behavioral sensitization with no neuronal cell death induced by MRP could break through the definition of "opioid addiction" and the misleading of concept that MRP is dangerous. Furthermore, the long-lasting maintenance of behavioral sensitization to METH and neuronal cell death by high

concentration of METH observed in this study strongly support the idea for the high risk of the psychostimulant use in humans.

Chapter 2

Glutamatergic neurotransmission and protein kinase C play a role in neuron-glia communication during the development of the rewarding effect induced by methamphetamine

Introduction

It has been established that astrocytes respond to the synaptic release of various neurotransmitters[6-10], such as glutamate and ATP, which often leads to the transient elevation of $[Ca^{2+}]i$[4, 13, 14]. The Ca^{2+} response, and the subsequent activation of various signaling pathway, regulate the release of various signaling molecules from astrocytes[4]. Therefore, both neuron-to-astrocyte and astrocyte-to-neuron signaling pathways are integral units which serve multiple and diverse roles in the CNS.

On the other hand, long-lasting synaptic adaptations in dopaminergic and/or glutamatergic neurotransmission provide a neuronal framework for altered behavioral processing which underlies the development of psychological dependence on drugs of abuse[39-41]. As described in Chapter 1, I found that *in vitro* treatment of mouse cortical neuron/glia co-cultures with drugs of abuse, such as METH and MRP, caused morphological changes in astrocytes via PKC. I also found that treatment with METH increased the sensitivity of astrocytes to glutamate and dopamine. These findings indicate that astrocytes play an important role in the dependence producing of drugs of abuse. However, the exact function of astrocytic changes induced by drugs of abuse remains unclear.

The purpose of the present study was to clarify the role of glutamatergic neurotransmission and its association with PKC in METH-induced functional and/or morphological changes in astrocytes using cortical neuron/glia co-cultures. I also examined the effects of glutamate receptor antagonists on the activation of astrocytes

and the development of the rewarding effect induced by METH.

Materials and methods

Tissue Processing

Tissue processing was conducted as previously described in Chapter 1.

Drug treatment and immunohistochemistry

At day 7 *in vitro*, the cells were treated with either normal medium, METH (10 μM), a selective NR2B subunit-containing *N*-methyl-*D*-aspartate (NMDA) receptor antagonist 2-(4-benzylpiperidino)-1-(4-hydroxyphenyl)-1-propanol hamitartrate (ifenprodil hemitartrate: 1-10 μM, Grelan Pharmacol. Co. Ltd., Tokyo, Japan) + METH, an α-amino-3-hydroxy-5-methylisoxazole-4-propionic acid (AMPA) receptor antagonist 6,7-dinitroquinoxaline-2,3-dione (DNQX, 1-10 μM, Acros Organics One Reagent Lane, Fairlawn, NJ, USA) + METH or a metabotropic glutamate receptor 5 (mGluR5) antagonist 2-methyl-6-(phenylethynyl)-pyridine hydrochloride (MPEP, 1-10 μM, Sigma-Aldrich Co.) + METH for 1 day. Other cells were treated with glutamate (1-100 nM, Wako Pure Chemicals Ind., Ltd.), a selective PKC inhibitor CHE (10 nM,) + glutamate, a PKC activator phorbol 12, 13-dibutyrate (PDBu: 1-100 nM, Sigma-Aldrich Co.) or PDBu + CHE for 1 day. The cells were then identified by immunofluorescence using a mouse polyclonal antibody to neuronal nuclei (NeuN, 1:1000: Chemicon International Inc.), a mouse polyclonal antibody to GFAP (1:1000) or a rabbit polyclonal antibody to p-PKC (1:400) followed by incubation with Alexa 488-conjugated goat anti-mouse IgG (1:4000; for GFAP and NeuN) or Alexa 546-conjugated

goat anti-rabbit IgG (1:4000; for p-PKC). Images were collected using a Radiance 2000 laser-scanning microscope (Radiance 2000). The experiments were repeatedly performed by, at least, 3 independent culture preparations

The measurement of GFAP-like immunoreactivity was conducted as previously described in Chapter 1.

Confocal Ca^{2+} imaging

The experiment involving confocal Ca^{2+} imaging was performed following the method described in Chapter 1.

Glutamate (10 μM) or PDBu (100 nM) was perfused for 30 sec at 5 mL/min at room temperature in cultured cortical neurons or astrocytes, followed by superfusion of BSS. Either CHE (1 μM), a calcium/calmodulin-dependent protein kinase II (CaMKII) inhibitor 2-[N-(2-hydroxythyl)-N-(4-methoxy-benzenesulfonyl)]amino-N-(4-chlorocinnamyl)-N-methylbensylamine (KN-93, 10 μM, Calbiochem-Novabichem Co., CA, USA) or a PLC inhibitor 1-(6-[([17β]-3-methoxyestra-1,3,5[10]-trien-17-yl)-1H-pyrrole-2,-dione (U73122, 5 μM, Sigma-Ardrich Co.) was incubated 10 min before glutamate (10 μM) or PDBu (100 nM) treatment.

Place conditioning

Male ICR mice weighting 25-30 g were obtained from Tokyo Laboratory Animals Science Co. (Tokyo, Japan). Animals were housed in a room maintained at 23 ± 1 °C with a 12 hr light-dark cycle. Food and water were available *ad libitum*.

Place conditioning studies[57, 80] were conducted using apparatus consisting of a shuttle box (15 x 30 x 15 cm, w x l x h), which was made of acrylic resin board and divided into two equal-sized compartments. One compartment was white with a textured floor and the other was black with a smooth floor to create equally inviting compartments. The conditioned place preference schedule consisted of the three phases (pre-conditioning test, conditioning and post-conditioning test). The pre-conditioning test was performed as follows: the partition separating the two compartments was raised to 7 cm above the floor, a natural platform was inserted along the seam separating the compartments, and mice that had not been treated with either drugs or saline were then placed on the platform. The time spent in each compartment during 900-sec session was then recorded automatically using an infrared beam sensor (KN-80, Natsume Seisakusyo Co. Ltd., Tokyo, Japan).

Conditioning sessions were started after s.c. injection of either METH (1 mg/kg) or saline; these animals were placed in the compartment opposite that, in which they had spent the most time in the pre-conditioning test, for 1 hr. On alternate days, these animals received with saline and were placed in the other compartment for 1 hr. Intracerebroventricular (i.c.v.) administration of either vehicle, ifenprodil (10 nmol/mouse), DNQX (30 nmol/mouse) or MPEP (100 nmol/mouse) was performed 30 min before s.c. treatment with METH (1 mg/kg, s.c.) or saline. On the day after the final conditioning session, these animals were placed in the test apparatus without any confinements, and then the relative amount of time spent in these compartments was measured (post-conditioning). The preference for drug-paired place was shown as

mean difference between time spent during the post-conditioning and pre-conditioning tests.

Statistical analysis

The data of confocal Ca^{2+} imaging and GFAP-like immunoreactivity are presented as the mean ± SEM. The statistical significance of differences between the groups were assessed by one-way ANOVA with Student's t-test.

Conditioning scores for each mouse are obtained by subtracting the cumulative time (sec) spent in the saline-paired side from that in the METH-paired side, are expressed as means ± SEM. A statistical analysis for place conditioning study was performed using one-way ANOVA followed by Bonferroni/Dunnett's test.

Results

Treatment with METH induced the phosphorylation of both neuronal and astrocytic PKC in cortical neuron/glia co-cultures

Immunohistochemical staining with an antibody to p-PKC confirmed that treatment with METH (10 μM, 3 days) increased the immunoreactivity of p-PKC in both neurons and astrocytes (Figure 2-1A, B), indicating that PKC may be involved in this event.

To ascertain whether the direct activation of PKC could induce any morphological changes, the selective PKC activator PDBu was applied to cortical neuron/glia co-cultures. Treatment with PDBu (10, 100 nM) for 24 hr induced a robust activation of astrocytes, as detected by a stellated morphology and an increase in the level of GFAP-like immunoreactivity in cortical neuron/glia co-cultures ($p < 0.001$ vs. control cells, Figure 2-2A, B). This astrocytic activation was abolished by co-treatment with CHE (10 nM, $p < 0.01$ vs. PDBu-treated cells, Figure 2-2A,B). Treatment with glutamate (10, 100 nM) for 24 hr also induced a robust activation of astrocytes in mouse cortical neuron/glia co-cultures ($p < 0.05$, $p < 0.001$ vs. control cells, Figure 2-2A, C), and this activation of astrocytes was reversed by treatment with the PKC inhibitor CHE (10 nM, $p < 0.001$ vs. glutamate-treated cells, Figure 2-2A, C).

Role of PKC in glutamate-induced Ca^{2+} response in neurons

To study the PKC-dependent glutamate response in mouse cortical neuron/glia co-cultures, I performed Ca^{2+} imaging experiments. Glutamate (10 μM, 30 sec) produced

a transient increase in $[Ca^{2+}]i$ in cultured cortical neurons (Figure 2-3A, B). The Ca^{2+} response to glutamate was dramatically and significantly abolished by pretreatment with CHE (1 μM: $p < 0.001$ vs. glutamate 10 μM, Figure 2-3A, B). In addition, this Ca^{2+} response was also significantly abolished by pretreatment with the CaMKII inhibitor NK-93 (10 μM: $p < 0.001$ vs. glutamate 10 μM, Figure 2-3A, B) and the PLC inhibitor U73122 (5 μM: $p < 0.001$ vs. glutamate 10 μM, Figure 2-3A, B). The direct activation of PKC induced by PDBu (100 nM, 30 sec) also produced a transient increase in $[Ca^{2+}]i$ in cultured cortical neurons, and this Ca^{2+} response was significantly prevented by pretreatment with either CHE (1 μM: $p < 0.001$ vs. PDBu 100 nM, Figure 2-3C, D) or KN-93 (10 μM: $p < 0.01$ vs. PDBu 100 nM, Figure 2-3C, D). However, unlike glutamate-induced Ca^{2+} responses, pretreatment with U73122 (5 μM) failed to attenuate the PDBu-induced Ca^{2+} responses in cultured cortical neurons (Figure 2-3C, D).

I next tried to investigate the role of PKC in glutamate-induced Ca^{2+} responses in purified cortical astrocytes. Glutamate (10 μM, 30 sec) produced a transient increase in $[Ca^{2+}]i$ in purified cortical astrocytes (Figure 2-4A, B). Similar to the glutamate-induced Ca^{2+} response in neurons, pretreatment with both CHE (1 μM) and U73122 (5 μM) significantly abolished the glutamate-induced Ca^{2+} responses in purified cortical astrocytes ($p < 0.001$ vs. glutamate 10 μM, Figure 2-4A, B). However, KN-93 (10 μM) failed to block the glutamate-induced increase in Ca^{2+} in purified cortical astrocytes (Figure 2-4A, B). PDBu (100 nM, 30 sec) also produced a transient increase in $[Ca^{2+}]i$ in purified cortical astrocytes (Figure 2-4C, D). This event was completely blocked by CHE (1 μM: $p < 0.001$ vs. PDBu 100 nM, Figure 2-4C, D).

Unlike PDBu-induced Ca^{2+} responses in neurons, both KN-93 (10 μM) and U73122 (5 μM) failed to affect the PDBu-induced Ca^{2+} responses in purified cortical astrocytes (Figure 2-4C, D).

Enhancement of the glutamate-induced Ca^{2+} response by PDBu

I next investigated whether the activation of PKC could induce any functional changes in neurons or astrocytes. PDBu (10 nM, 30 sec) itself failed to induce Ca^{2+} responses in both cortical neurons (Figure 2-5A) and astrocytes (Figure 2-5A, B). Since a long-term treatment with PDBu has been known to induce the down-regulation of PKC, I applied a low concentration of PDBu (10 nM) to cells and then treated them with glutamate or dopamine to estimate the effect of PKC activation. The Ca^{2+} response to glutamate (1 μM) was significantly enhanced by co-treatment with PDBu (10 nM) in both cultured mouse cortical neurons and astrocytes ($p < 0.001$ vs. control cells, Figure 2-5A, B). The Ca^{2+} response to glutamate (1-10 μM) was also enhanced by co-treatment with PDBu (10 μM) in purified cortical astrocytes ($p < 0.001$, Figure 2-5B). On the other hand, co-treatment with PDBu (10 nM) failed to affect the dopamine (1-10 μM)-induced Ca^{2+} responses in both neurons and astrocytes.

Enhancement of the glutamate-induced Ca^{2+} response by METH

METH (10-100 μM, 30 sec) itself failed to induce Ca^{2+} responses in cultured cortical neurons (Figure 2-6A). However, the glutamate (1-100 μM, 30 sec)-induced Ca^{2+} responses in neurons were significantly enhanced by treatment with METH (10 μM, 3

days, $p < 0.001$ vs. control cells for 1-10 μM glutamate, $p < 0.01$ vs. control cells for 100 μM glutamate, Figure 2-6B, C). Unlike glutamate-induced Ca^{2+} responses in neurons, treatment with METH (10 μM, 3 days) failed to enhance the dopamine (1, 100 μM, 30 sec)-induced Ca^{2+} responses in neurons (Figure 2-6D). Although the dopamine (10 μM, 30 sec)-induced Ca^{2+} responses in neurons were significantly enhanced by treatment with METH (10 μM, 3 days, $p < 0.05$ vs. control cells, Figure 2-6D), the potency of enhancement was weaker than that of glutamate-induced Ca^{2+} responses.

Role of glutamatergic transmission in the activation of astrocytes induced by METH.

The activation of astrocytes induced by METH (10 μM, 3 days) was completely reversed by co-treatment with the specific NMDA receptor NR2B subunit antagonist ifenprodil (1-10 μM, $p < 0.001$ vs. METH treated cells, Figure 2-7A, B) and the mGluR5 antagonist MPEP (1-10 μM, $p < 0.001$ vs. METH treated cells, Figure 2-7A, B) in cortical neuron/glia co-cultures. This activation of astrocytes was partially reversed by co-treatment with the specific AMPA receptor antagonist DNQX (1-10 μM, $p < 0.01$, $p < 0.001$ vs. control cells, $p < 0.001$ vs. METH-treated cells, Figure 2-7A, B) in cortical neuron/glia co-cultures. Under these conditions, each of the glutamate receptor antagonists (1-10 μM, 3 days) failed to affect the GFAP-like immunoreactivity in cortical neuron/glia co-cultures (data not shown).

Role of glutamatergic transmission in the rewarding effect induced by METH.

Finally, I ascertained the effects of glutamate receptor antagonists on the rewarding effect of METH in mice. It was previously reported that chronic *in vivo* treatment with METH produced a significant dose-dependent preference for the drug-associated place in the conditioned place preference paradigm[53]. In the present study, I found that the place preference produced by chronic administration of METH (1 mg/kg, s.c.) was significantly suppressed by i.c.v. pretreatment with either ifenprodil (10 nmol/mouse, 174.9 ± 33.4 sec for vehicle-METH group, 63.9 ± 27.2 sec for ifenprodil-MEHT group; $^{\#\#}p < 0.01$ vs. vehicle-METH group, Figure 2-8A), DNQX (30 nmol/mouse, 142.7 ± 11.7 sec for vehicle-METH group, 25.6 ± 25.9 sec for DNQX-METH group; $^{\#\#\#}p < 0.001$ vs. vehicle-METH group, Figure 2-8B) or MPEP (100 nmol/mouse, 156.9 ± 11.9 sec for vehicle-METH group, 72.1 ± 33.0 sec for MPEP-METH group; $^{\#\#}p < 0.01$ vs. vehicle-METH group, Figure 2-8C).

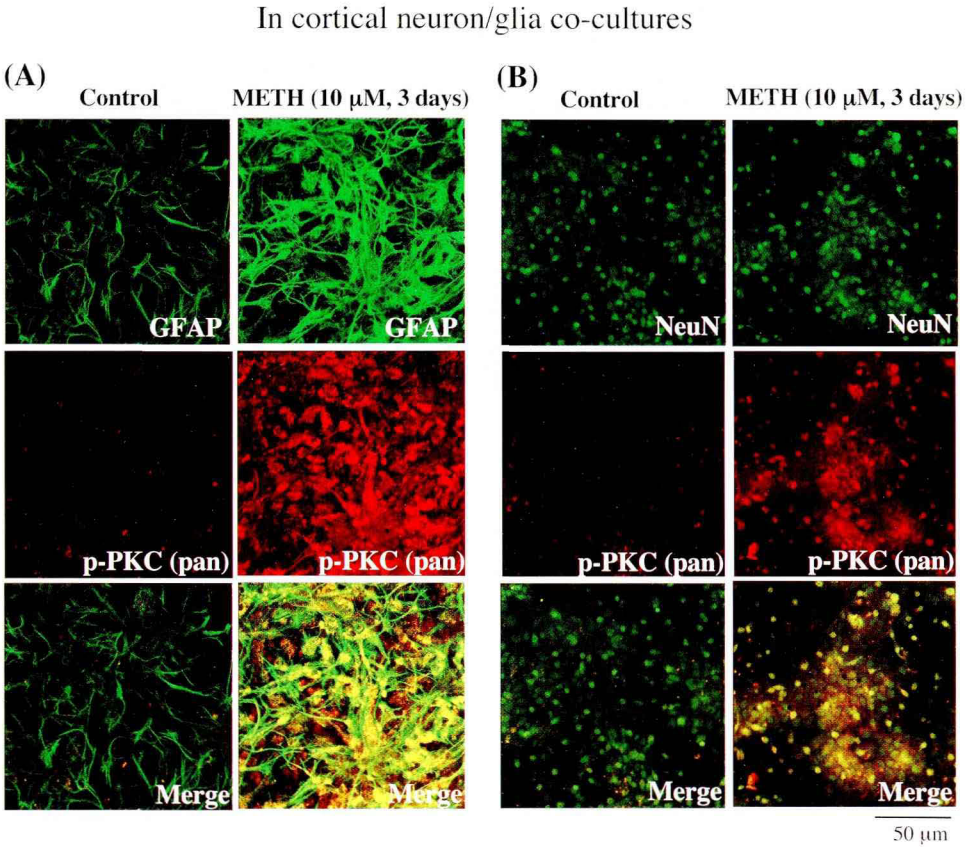

Figure 2-1 Treatment with METH (10 μM) for 3 days caused astrocytic activation associated with phosphorylation of protein kinase C (PKC) in cortical neuron/glia co-cultures. (A) The red label for p-PKC stained with a rabbit polyclonal antibody and the green label for GFAP stained with mouse polyclonal antibody are colocalized in cortical neuron/glia co-cultures. (B) The green label for Neu-N stained with a mouse polyclonal antibody and the red label for p-PKC stained with a rabbit polyclonal antibody show colocalization in cortical neuron/glia co-cultures.

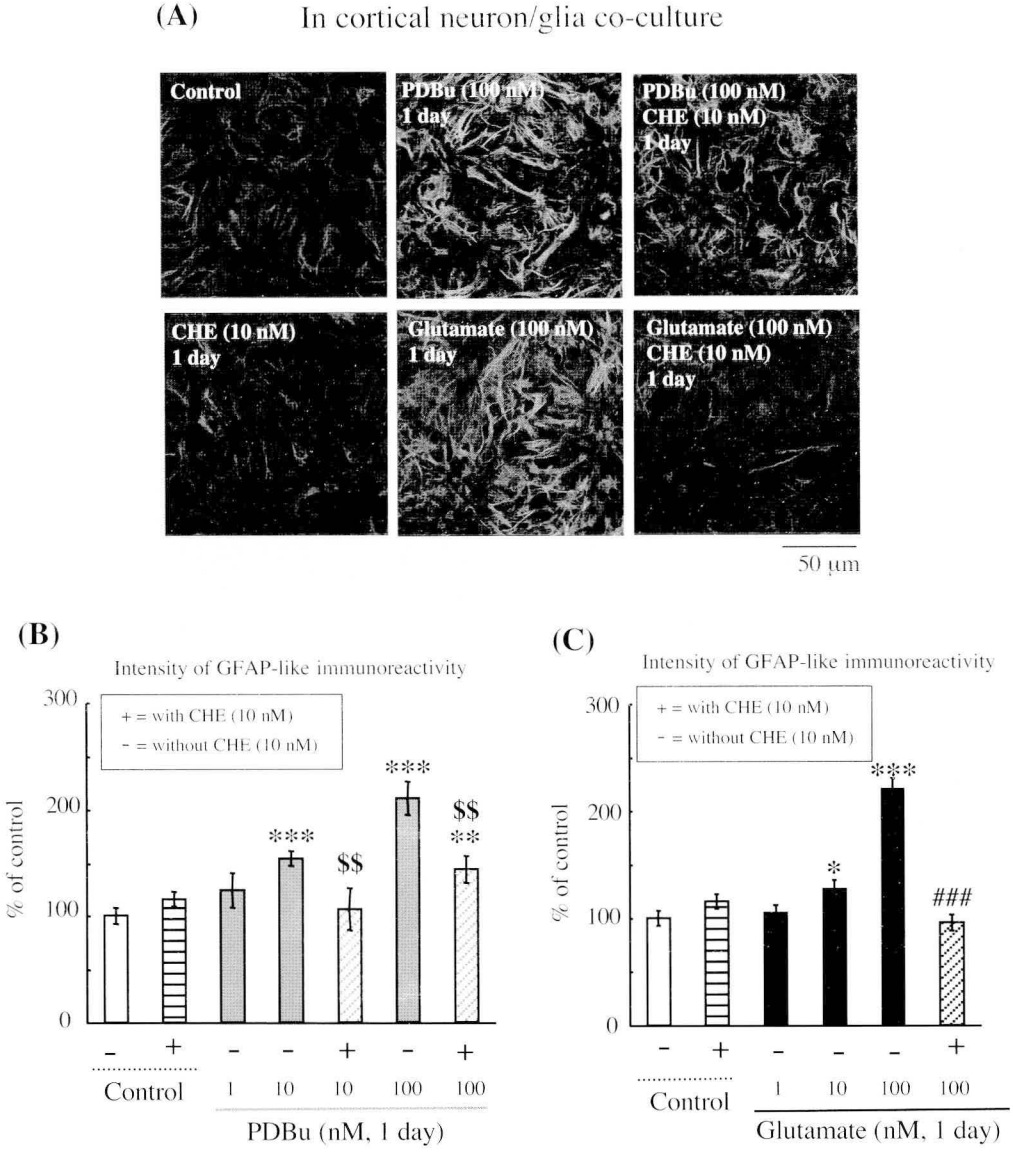

Figure 2-2 PKC-dependent astrocytic activation induced by treatment with glutamate or PDBu for 1 day in cortical neuron/glia co-cultures. (A) Cortical neuron/glia co-cultures were treated with normal medium, CHE (10 nM), PDBu (100 nM), PDBu + CHE (100 nM), glutamate (100 nM) or glutamate + CHE (10 nM). The cells were stained with a rabbit polyclonal antibody to GFAP. (B) Cortical neuron/glia co-cultures were treated with normal medium or PDBu (1-100 nM) with or without chelerythrine (10 nM). (C) Mouse cortical neuron/glia co-cultures were treated with normal medium or glutamate (1-100 nM) with or without CHE (10 nM). In panels B and C, the intensity of GFAP-like immunoreactivity in each image was measured using NIH image. The level of GFAP-like immunoreactivity on PDBu- or glutamate-treated cells is expressed as a percent increase (mean ± SEM) with respect to that on control cells. $^{*}p < 0.05$, $^{***}p < 0.001$ vs. control cells. $^{\$\$}p < 0.01$ vs. PDBu-treated cells. $^{\#\#\#}p < 0.001$ vs. glutamate-treated cells.

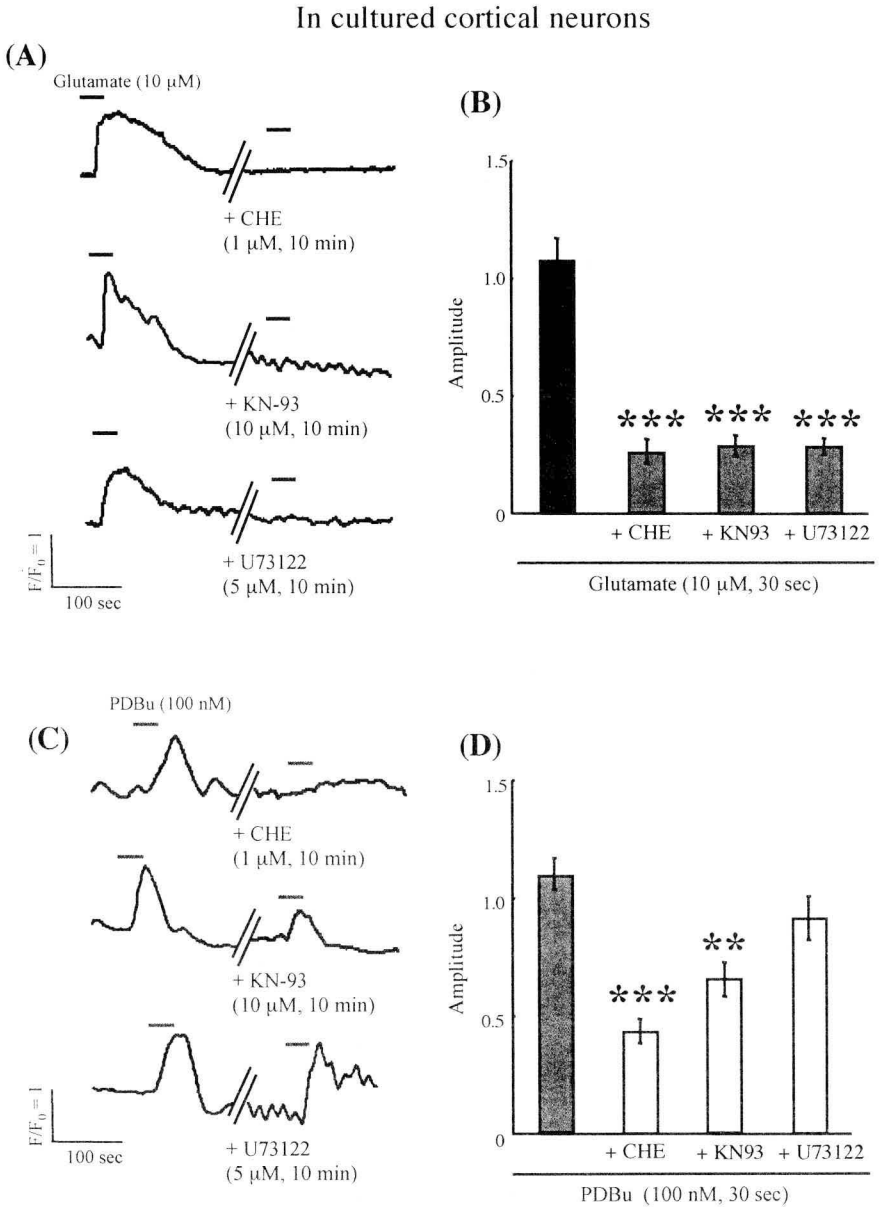

Figure 2-3 Characterization of the glutamate- and PDBu-induced increase in intracellular Ca^{2+} concentration $[Ca^{2+}]i$ in cultured cortical neurons. (A) Traces show the glutamate (10 μM, 30 sec)-evoked increase in $[Ca^{2+}]i$ in mouse cortical neurons with or without the PKC inhibitor CHE (1 μM), the CaMKII inhibitor KN93 (10 μM) or the PLC inhibitor U73122 (5 μM). Cells were pretreated with these inhibitors for 10 min prior to glutamate (10 μM) application. (B) The Ca^{2+} responses to glutamate in neurons are summarized. Data represent the mean ± SEM of 54-72 cells. $^{**}p < 0.01$, $^{***}p < 0.001$ vs. glutamate (10 μM)-treated cells. (C) Traces show the PDBu (100 nM, 30 sec)-evoked increase in $[Ca^{2+}]i$ in neurons with or without CHE (1 μM), KN93 (10 μM) or U73122 (5 μM). Cells were then pretreated with these inhibitors for 10 min prior to PDBu (100 nM) application. (D) The Ca^{2+} responses to PDBu in neurons are summarized. Data represent the mean ± SEM of 63-72 cells. $^{**}p < 0.01$, $^{***}p < 0.001$ vs. PDBu (100 nM)-treated cells.

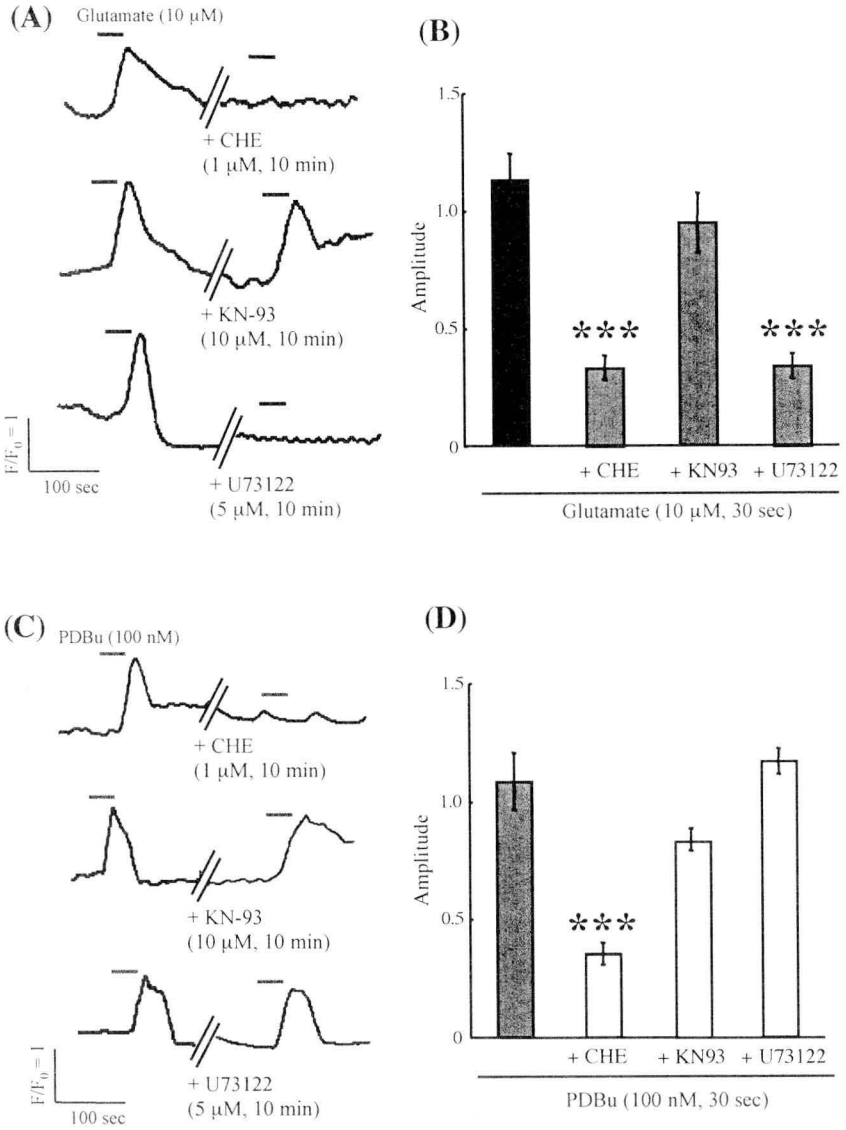

Figure. 2-4 Characterization of the glutamate- and PDBu-induced increase in intracellular Ca^{2+} concentration ($[Ca^{2+}]i$) in purified cortical astrocytes. Traces show the glutamate (10 μM, 30 sec)-evoked increase in $[Ca^{2+}]i$ in cortical astrocytes with or without CHE (1 μM), KN93 (10 μM) or U73122 (5 μM). Cells were then pretreated with these inhibitors for 10 min prior to the application of glutamate (10 μM). (B) The Ca^{2+} responses to glutamate in astrocytes are summarized. Data represent the mean ± SEM of 63-72. ***$p < 0.001$ vs. glutamate (10 μM)-treated cells. (C) Traces show the PDBu (100 nM, 30 sec)-evoked increase in $[Ca^{2+}]i$ in cortical astrocytes with or without CHE (1 μM), KN93 (10 μM) or U73122 (5 μM). Cells were then pretreated with these inhibitors for 10 min prior to PDBu (100 nM) application. (D) The Ca^{2+} responses to PDBu are summarized. Data represent the mean ± SEM of 63-72 cells. ***$p < 0.001$ vs. PDBu (100 nM)-treated cells.

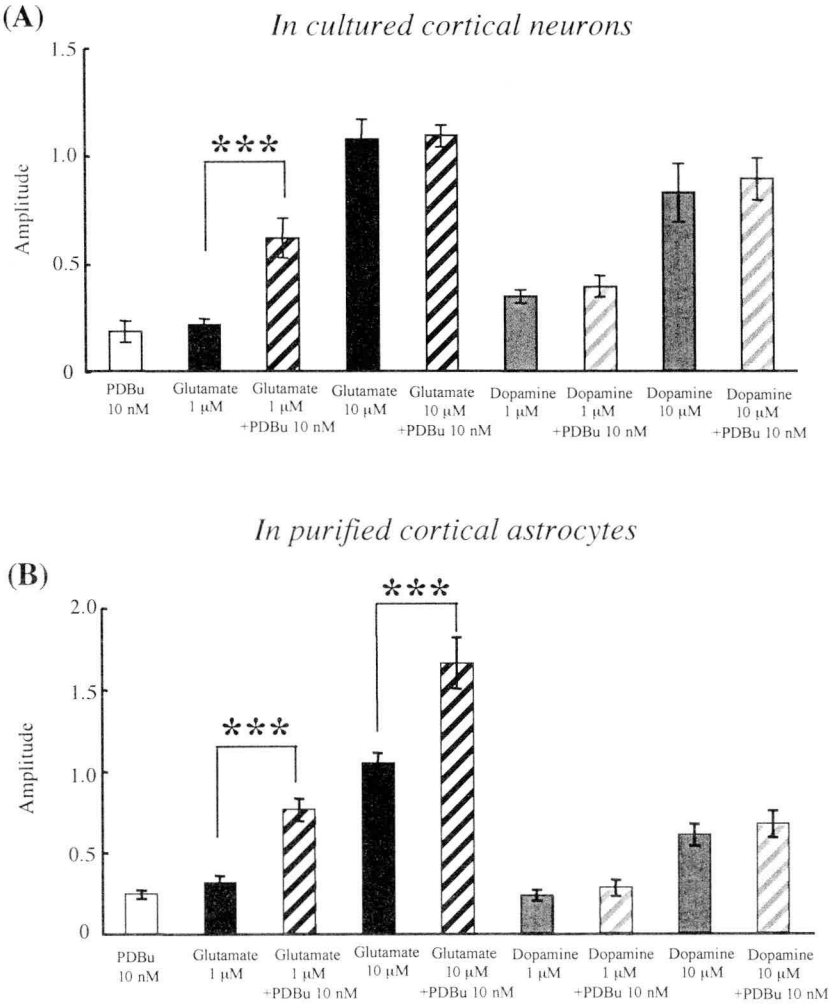

Figure 2-5 Enhancement of Ca^{2+} responses to glutamate by the PKC activator PDBu in both mouse cortical neurons and astrocytes. PDBu (10 nM, 30 sec, open columns) itself failed to induce Ca^{2+} responses in cortical neurons (A) and astrocytes (B). Co-treatment with PDBu (10 nM) significantly enhanced glutamate (1 μM, 30 sec)-induced Ca^{2+} responses in neurons (A). Co-treatment with PDBu (10 nM) significantly enhanced glutamate (1-10 μM, 30 sec)-induced Ca^{2+} responses in astrocytes (B). Co-treatment with PDBu (10 nM) failed to affect dopamine (1-10 μM, 30 sec)-induced Ca^{2+} responses in both neurons (A) and astrocytes (B). Data represent the mean ± SEM of 54-81 cells. ***$p < 0.001$ vs. glutamate (10 or 100 μM, 30 sec)-treated cells.

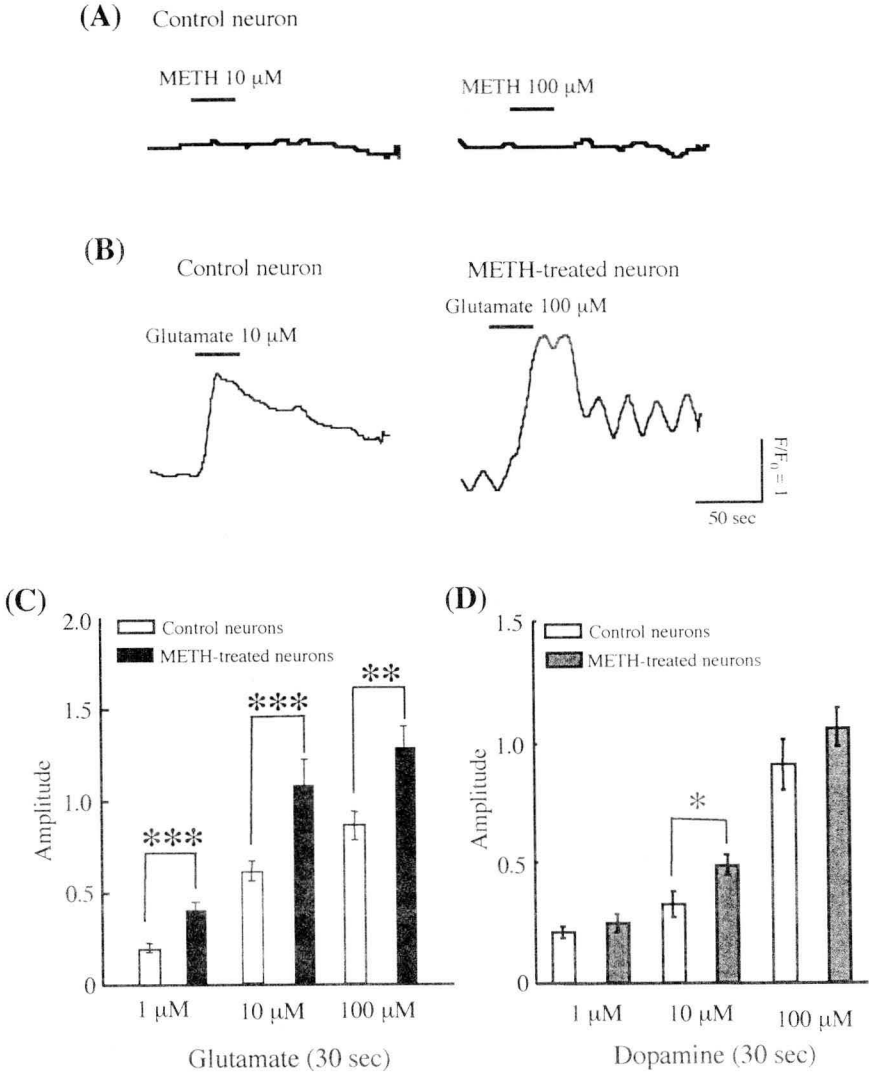

Figure 2-6 Ca^{2+} responses to glutamate in neurons were potently enhanced by 3 days treatment with METH (10 μM). (A) METH (10-100 μM, 30 sec) itself failed to induce Ca^{2+} responses in cultured cortical neurons. (B) Traces show the glutamate (100 μM, 30 sec)-evoked Ca^{2+} responses in control or METH (10 μM, 3 days)-treated neurons. (C) The Ca^{2+} responses to glutamate (1-100 μM) in neurons are summarized. Data represent the mean ± SEM of 54-72 cells. $^{**}p < 0.01$, $^{***}p < 0.001$ vs. control neurons. (D) The Ca^{2+} responses to dopamine (1-100 μM, 30 sec) in neurons are summarized. Data represent the mean ± SEM of 63-72 cells. $^{*}p < 0.05$ vs. control neurons.

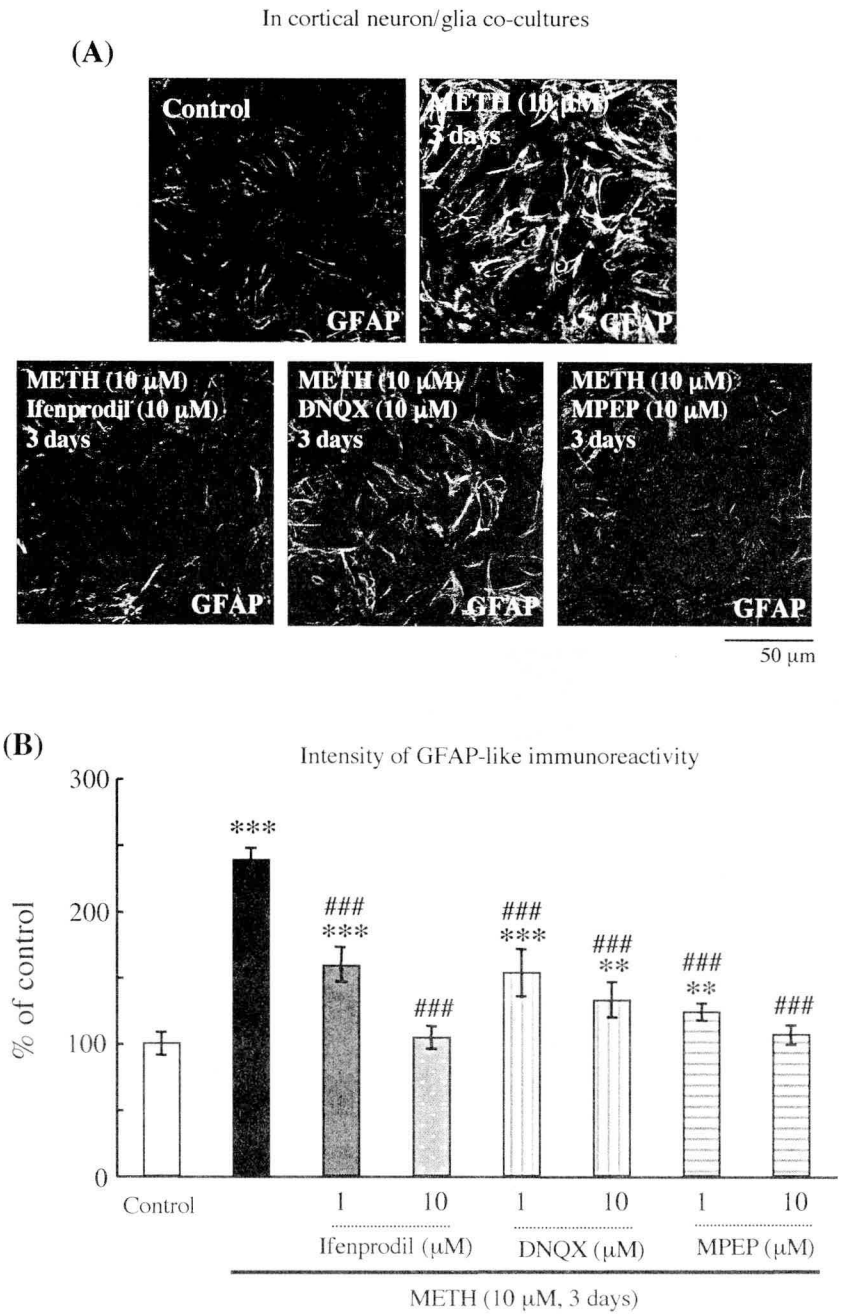

Figure 2-7 METH (10 μM, 3 days)-induced astrocytic was blocked by co-treatment with glutamate receptor antagonists. (A) Cortical neuron/glia co-cultures were treated with normal medium, METH (10 μM), METH + the NMDA receptor antagonist ifenprodil (10 μM), METH + the AMPA receptor antagonist DNQX (10 μM) or the mGluR5 antagonist MPEP (10 μM) for 3 days. The cells were stained with a rabbit polyclonal antibody to GFAP. (B) The intensity of GFAP-like immunoreactivity of each image was measured using NIH image. The level of GFAP-like immunoreactivity is expressed as a percent increase (mean ± SEM) with respect to that in control cells. $^{**}p < 0.01$, $^{***}p < 0.001$ vs. control cells. $^{###}p < 0.001$ vs. METH (10 μM, 3 days)-treated cells.

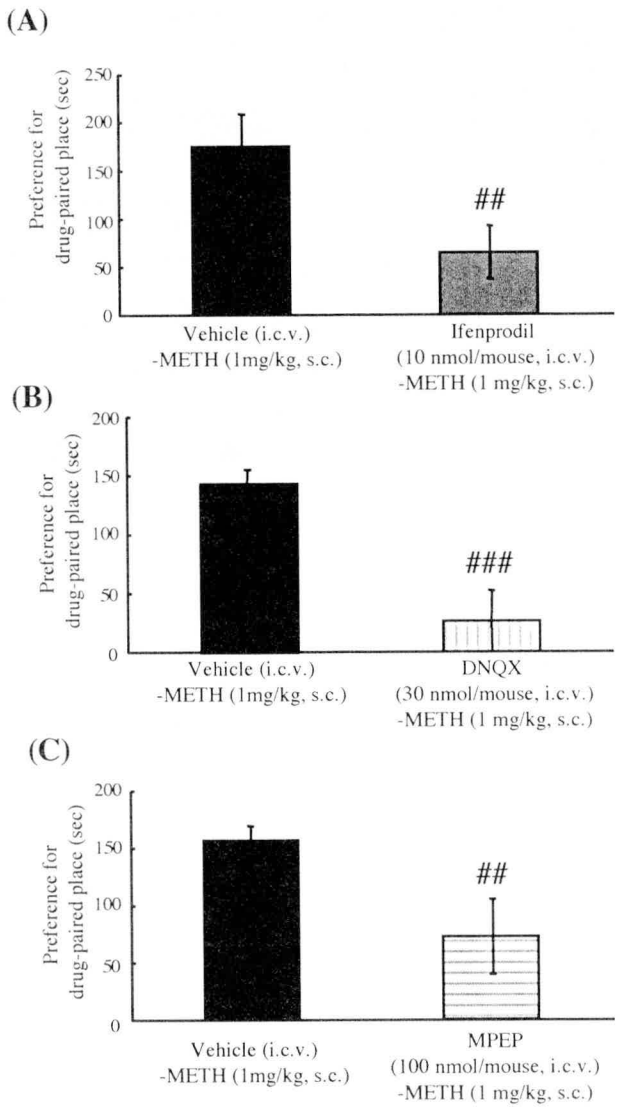

Figure 2-8 Effects of glutamate receptor antagonists on METH-induced rewarding effect in mice. Pretreatment i.c.v. with vehicle, ifenprodil (10 nmol/mouse, i.c.v., A), DNQX (10 nmol/mouse, i.c.v., B) or MPEP (100 nmol/mouse, i.c.v., C) was performed 30 min before METH (1 mg/kg, s.c.) injection. Chronic administration of METH (1 mg/kg, s.c.) produced a clear place preference in mice. This place preference was significantly suppressed by pretreatment with either ifenprodil (10 nmol/mouse, i.c.v., A), DNQX (30 nmol/mouse, i.c.v., B) or MPEP (100 nmol/mouse, i.c.v., C). Each column represents the mean ± SEM of 8 mice. $^{\#\#}p < 0.01$, $^{\#\#\#}p < 0.001$ vs. vehicle-METH (1 mg/kg, s.c.) group.

Discussion

It has been reported that PKC contributes to the direction of neurite growth in cell adhesion[19, 52]. PKC could also regulate the morphology of astrocytes[78, 81]. I confirmed here that the direct activation of PKC by PDBu caused a robust activation of astrocytes. *In vitro* treatment with glutamate also caused PKC-dependent astrocytic activation. The key finding of the present study was that *in vitro* treatment with METH enhanced the glutamate-induced Ca^{2+} response in neurons. Furthermore, *in vitro* treatment of cortical neuron/glia co-cultures with METH caused the phosphorylation of PKC in both neurons and astrocytes. It should be noted that treatment with METH caused morphological stellation and an increase in the levels of GFAP in astrocytes.

Activated astrocytes are thought to differ from non-activated astrocytes with respect to their ability to adjacent neurons from excitotoxicity[24]. Several studies have shown that neuronal excitotoxicity is associated with excess activation of astrocytes[26, 82]. Astrocytic activation could contribute to deterioration in conditions of chronic neurodegeneration, hence activated astrocytes secrete nitric oxide and inflammatory cytokines, and exert strong neurotoxic effects[26]. On the other hand, astrocytic activation could counteract the neuroprotective effect of astrocyte-derived growth factors[83, 84]. Thus, activation of astrocytes may affect the neuronal environment, resulting in synaptic plasticity in the CNS. Taken together, the present findings suggest that the changes induced by METH may regulate neural circuits during the

development of psychological dependence on METH.

Neurons and astrocytes respond to various electrical and chemical stimuli, including neurotransmitters, neuromodulators and hormones, with an increase in $[Ca^{2+}]i$. These Ca^{2+} responses result from the coordinated activity of several molecular cascades responsible for Ca^{2+} movement into or out to the cytoplasm by way of either the extracellular space or intracellular stores. On the other hand, PKC activity is stimulated by a rise in $[Ca^{2+}]i$. In the present study, the specific PKC inhibitor CHE produced a dramatic suppression of the glutamate-induced Ca^{2+} responses in both neurons and astrocytes. Direct activation of PKC by PDBu also produced transient Ca^{2+} responses in both neurons and astrocytes. Conversely, co-treatment with a low concentration of the PKC activator PDBu clearly enhanced the glutamate-induced Ca^{2+} responses in both neurons and astrocytes. Thus, the present data suggest that PKC is involved in glutamatergic neurotransmission in the CNS.

CaMKII is a ubiquitously expressed protein kinase that transduces the elevated Ca^{2+} signals in cells to several target proteins ranging from ion channels to transcriptional activators. It has been reported that the activation of CaMKII induces phosphorylation of the carboxy-terminal region of the NR2B subunit of NMDA receptors[85]. In my preliminary study, I found that a nonselective NMDA receptor antagonist MK-801 (disocylpine) and the selective NR2B subunit-containing NMDA receptor antagonist ifenprodil abolished the glutamate-induced Ca^{2+} responses in cultured cortical neurons[86]. In the present study, the CaMKII inhibitor KN93 also produced a dramatic suppression of the glutamate-induced Ca^{2+} response in neurons. Thus, the present findings suggest

that the activity of CaMKII, as well as PKC, may contribute to the positive regulation of glutamatergic signaling presumably through the NR2B subunit of NMDA receptors in neurons.

CaMKII-dependent glutamatergic Ca^{2+} signaling may be responsible for the development and/or expression of rewarding effects induced by drugs of abuse. In fact, it has been already reported that the MRP-induced rewarding effect was significantly suppressed by treatment with KN-93[87], suggesting that activated CaMKII plays a substantial role in the development of MRP-induced rewarding effects.

Recent reports have stated that there are three mammalian PI-PLC isoform families: PLCβ, PLCγ and PLCδ[51]. All known forms of PKCβ (β1-β4) are stimulated to various extents by the $G_{q/11\alpha}$ family. On the other hand, mGlu5 receptor is physically linked to the NR2B subunit of NMDA receptors[88]. mGluR5 receptors coupling to $G_{q/11\alpha}$[89, 90] could stimulate PLCβ-isozyme, which generate diacylglycerol and inositol triphosphate, leading to the activation of PKC and Ca^{2+} mobilization, respectively. In the present study, I found that the PLC inhibitor U73122 completely blocked the glutamate-induced Ca^{2+} response in neurons. Therefore, it seems likely that U73122 could affect metabotropic receptor-coupled $G_{q/11\alpha}$ /PLCβ signaling. The present data suggest that the functional interaction between mGluRs and NMDA receptors could involve the expression of PKC/CaMKII-dependent glutamate-induced intracellular signaling in neurons.

mGluRs, but not NMDA receptors, are ordinarily expressed in astrocytes[4, 6-8, 78]. In fact, I previously confirmed that the selective mGluR5 receptor antagonist MPEP

clearly blocked the glutamate-induced Ca^{2+} responses in astrocytes, whereas either MK-801 or ifenprodil failed to block this phenomenon[86]. In the present study, I found that CHE and U73122, but not KN93, completely blocked the glutamate-induced Ca^{2+} responses in astrocytes. Considering these observations, it seems likely that glutamate affects the coupling of mGluR receptors to $G_{q/11\alpha}$, stimulate PLCβ-isozyme, and thus leads to Ca^{2+} responses in astrocytes.

In contrast, a low concentration of PDBu failed to affect the dopamine-induced Ca^{2+} responses in neurons and astrocytes. Although the various actions of dopamine are mediated by five different receptor subtypes, which are members of the large G-protein–coupled family, none of these dopamine receptors are coupled with $G_{q/11}$ or any ion channels. Thus, these results seem to indicate that PKC may not be critical for dopaminergic neurotransmission in cortical cultures.

Notably, treatment with METH (10 μM) for 3 days increased the sensitivity of cortical neurons to glutamate, indicating that treatment with METH may cause the functional up-regulation of glutamatergic neurotransmission. As mentioned above, treatment with METH caused a robust phosphorylation of PKC, which could regulate the glutamate-induced Ca^{2+} responses in neurons and astrocytes. Collectively, the enhancement of PKC-dependent Ca^{2+} responses to glutamate induced by METH could lead to an increase in the excitability of the CNS, resulting in the development of synaptic changes induced by METH.

Moreover, the activation of astrocytes induced by METH (10 μM) for 3 days was dramatically diminished by treatment with either ifenprodil, the AMPA receptor

antagonist DNQX or MPEP. These findings raise the possibility that METH activates astrocytes through glutamatergic transmission. Activated astrocytes may regulate synaptic transmission by the release of glutamate or the uptake of glutamate from the synaptic cleft via membrane transporters. In Chapter 1, I demonstrated that the glutamate-induced Ca^{2+} responses in astrocytes were significantly enhanced by 3 days of treatment with METH (10 μM). Activated astrocytes may, at least in part, potentiate glutamatergic neurotransmission, leading to the development and/or expression of the rewarding effects by METH.

Several lines of evidence suggest that glutamatergic projections to the N.Acc. originating from the prefrontal cortex, hippocampus and amygdala regulate emotional and behavioral processing[45]. Therefore, I confirmed the role of glutamatergic neurotransmission during the development of the rewarding effect induced by METH. The place preference produced by repeated *in vivo* administration of METH was significantly suppressed by i.c.v. treatment with either ifenprodil, DNQX or MPEP. These findings suggest that the activation of glutamatergic neurotransmission is necessary for the development and/or expression of the rewarding effects induced by METH. The activation of NMDA receptor, AMPA receptor and mGluR5 may regulate each other in the development of the rewarding effect induced by METH.

In summary, I demonstrated here that PKC plays a positive regulatory role in the availability of Ca^{2+} signaling in response to glutamate in both neurons and astrocytes. On the other hand, CaMKII, which modulates the development and/or expression of the rewarding effects induced by psychostimulants, also has the ability to modulate

glutamatergic transmission in neurons, but not in astrocytes. METH could induce PKC-dependent astrocytic activation through glutamatergic transmission. PKC-dependent glutamatergic transmission in both neurons and astrocytes may, at least in part, modulate the expression of the rewarding effect of METH. These findings raise the fascinating possibility that METH-induced dynamic changes in PKC-dependent communication between neurons and astrocytes may be associated with glutamatergic synaptic plasticity.

Chapter 3

Direct evidence of astrocytic modulation in the development of rewarding effects induced by drugs of abuse

Introduction

As described in chapter 1 and 2, two-way communication between neurons and glial cells is essential for axonal conduction and synaptic transmission. It has been widely accepted that long-term exposure to psychostimulants induces neuronal plasticity[34-38]. Accumulating evidence suggests that astrocytes may also actively participate in synaptic plasticity[39-41].

It has been documented that repeated amphetamine treatment results in the increased astrocytic expression of basic fibroblast growth factor, which is necessary for the development of sensitization to amphetamine[91]. It has been also reported that the expression of GFAP-positive astrocytes expression is increased in the VTA and hippocampus following relatively short-term withdrawal subsequent to cocaine exposure[92]. In Chapter 1, I described that the levels of GFAP in the mouse N.Acc. and CG were clearly increased by chronic *in vivo* administration of METH. These data raise the possibility that astrocytes contribute to the synaptic plasticity during the development of rewarding effects induced by psychostimulants. However, little is known about direct action of astrocytes on the development of rewarding effects induced by drugs of abuse.

The present study was then undertaken to clarify the role of astrocytes during the development of rewarding effects induced by METH and MRP.

Materials and Methods

Tissue Processing

Preparation of purified cortical astrocytes was performed following the method described in Chapter 1.

To prepare astrocyte-conditioned medium (ACM), purified cortical astrocytes were grown to confluence. Cells were washed once with DMEM and then covered with an equal volume of serum-free medium for 24 hr at 37 °C and 5 % CO_2 in the presence of the indicated treatments. The supernatant was collected 1 day after changing to serum-free medium culture and centrifuged for 20 min at 1,000 x g. The final supernatant was used as ACM.

Purified cortical microglia were grown as follows; cerebral cortices were obtained from newborn ICR mice (Tokyo Laboratory Animals Co., Ltd.), minced, and treated with trypsin (0.025 %, Invitrogen Co.) dissolved in PBS solution containing 0.02 % L-cysteine (Sigma-Aldrich Co.) monohydrate, 0.5 % glucose (Wako Pure Chemicals Ind., Ltd.) and 0.02 % bovine serum albumin (Wako Pure Chemicals Ind., Ltd.). After enzyme treatment at 37 °C for 15 min, cells were dispersed by gentle agitation through a pipette and plated on a flask with DMEM supplemented with 5 % FBS, 5 % HS, 10 U/mL penicillin and 10 μg/mL streptomycin in a humidified atmosphere of 95 % air and 5 % CO_2 at 37 °C. The cultured medium was exchanged to new medium every 3 days. About 9 days after seeding, the flask was shaken for 2 min to remove microglia. A cell suspension were collected and centrifuged (20 min, 3,000 x g). The cells were seeded

at a density of 1 x 10^5 cells/cm^3. The cells were maintained for 3 days in DMEM supplemented with 5 % FBS, 5 % HS, 10 U/mL penicillin and 10 μg/mL streptomycin in a humidified atmosphere of 95 % air and 5 % CO_2 at 37 °C.

To prepare microglia-conditioned medium (MCM), purified cortical microglia were grown to confluence. Cells were washed once with DMEM and then covered with an equal volume of serum-free medium for 24 hr at 37 °C and 5 % CO_2 in the presence of the indicated treatments. The supernatant was collected 1 day after changing to the serum-free medium culture and centrifuged (20 min, 3,000 x g). The final supernatant was used as MCM.

Preparation of cortical neuron/glia co-cultures was performed following the method described in Chapter 1.

Drug treatment and immunohistochemistry

Mouse cortical neuron/glia co-cultures were treated with either normal medium, METH (10 μM), METH + a glial modulator 3-methyl-1-(5-oxohexyl)-7-propylxanthine (propentofylline: PPF, 1-3 μM, Sigma-Aldrich Co.), MRP (10 μM) or MRP (10 μM) + PPF (1-3 μM) for 3 days. To explore the effect of astrocyte-released soluble factors, mouse purified cortical astrocytes were treated with either DMEM, ACM, ACM collected from METH (10, 100 μM, 3 days)-treated astrocytes (METH 10 μM-ACM, METH 100 μM-ACM) or ACM collected from MRP (10, 100 μM, 3 days)-treated astrocytes (MRP 10 μM-ACM, MRP 100 μM-ACM) for 1 day. Mouse purified cortical microglia were treated with either normal medium, METH (1-100 μM) or MRP

(1-100 μM) for 3 days. The cells were then identified by immunofluorescence using a mouse antibody to GFAP (1:1000) or a rat antibody to OX42 (1:250, Serotec Ltd., Oxford, UK) followed by incubation with Alexa 488-conjugated goat anti-mouse IgG (1:4000 for GFAP) or with Alexa 488-conjugated goat anti-rat IgG (1:4000 for OX42). Images were collected using a Radiance 2000 laser-scanning microscope. The experiments were repeatedly performed by, at least, 3 independent culture preparations.

The measurement of GFAP-like immunoreacivity was conducted as previously described in Chapter 1.

Surgery and microinjection

Male ICR mice weighing 25-30 g were obtained from Tokyo Laboratory Animals Science Co. Animals were housed in a room maintained at 23 ± 1 °C with a 12 hr light-dark cycle. Food and water were available *ad libitum*.

After 3 days of habituation to the main animal colony, all mice were anesthetized with sodium pentobarbital (70 mg/kg, i.p.). The anesthetized animals were placed in a stereotaxic apparatus (Kopf Ins., Tujanga, CA, USA). The skull was exposed and a small hole was made using a dental drill. An infusion cannula (D-1-6-02, Eicom Co., Kyoto, Japan) was positioned into the N.Acc. (from bregma: anterior +1.5 mm, lateral -0.9 mm, ventral -4.6 mm), CG (from bregma: anterior +1.0 mm, lateral -0.3 mm, ventral -1.4 mm) or corpus striatum (CPu: from bregma: +1.5 mm, lateral -1.3 mm, ventral -3.5 mm) according to the atlas of Paxinos and Franklin[93]. The animals were injected with either DMEM, ACM, ACM + a Janus tyrosine kinase/signal transducers of activated

transcription (Jak/STAT) inhibitor α-cyano-(3,4-dihydroxy)-N-benzylcinnamide (AG490, 0.1 nmol, Calbiochem-Novabiochem, La Jolla, CA, USA), DMEM-AG490 (0.1 nmol), METH 10 μM-ACM or MCM in a volume of 100 nL/mouse into the N.Acc. via the infusion cannula using a Hamilton syringe at an infusion rate of 10 nL/min. Other groups of animals were injected with DMEM or ACM in a volume of 100 nL/mouse into the CG or CPu via the infusion cannula using a Hamilton syringe at an infusion rate of 10 nL/min. These mice were returned to their home cages after microinjection. One day after microinjection, mice were used for the behavioral study.

Place conditioning

Place conditioning study was conducted as previously described in Chapter 2. To examine the effect of microinjection with ACM and MCM in the rewarding effects induced by METH and MRP, microinjection of either DMEM, ACM, DMEM + AG490 (0.1 nmol), ACM+AG490 (0.1 nmol), METH 10 μM-ACM or MCM was performed 1 day before the pre-conditioning test.

The pre-conditioning test was performed as follows: the partition separating the two compartments was raised to 7 cm above the floor, a neutral platform was inserted along the seam separating the compartments, and mice that had not been treated with either drugs or saline were then placed on the platform. The time spent in each compartment during a 900-sec session was recorded automatically using an infrared beam sensor (KN-80). Conditioning sessions (three for METH or MRP: three for saline) were started next day after pre-conditioning test and conducted once daily for 6 days.

Immediately after injection of either METH (0.0625, 0.125, 0.25, 0.5 or 1mg/kg, s.c.) or MRP (1, 1.7, 3, 5 or 5.6 mg/kg, s.c.); these animals were placed in the compartment opposite that in which they had spent the most time in the pre-conditioning test, for 1 hr. On the day after the final conditioning session, these animals were placed in the test apparatus without any confinements, and then the relative amount of time spent in these compartments was measured (post-conditioning). The preference for drug-paired place was shown as mean difference between time spent during the post-conditioning and pre-conditioning tests. Each preference score represents the mean ± SEM of 7-8 mice.

Differentiation experiments

MEB5 (IFO50472, the Japanese Cancer Research Resources Bank) was used as multipotent neural stem cells (NSCs). MEB5 is a multipotent stem cell line that can differentiate into neurons, astrocytes and oligodendrocytes. The cells were plated in uncoated plastic tissue flasks and maintained at 37 °C and 5 % CO_2. The cells were cultured in serum-free medium: DMEM with 4,500 mg/L glucose, 5 μg/mL insulin, 10 ng/mL erythropoietic growth factor (EGF, 50 μg/mL transferrin, 10 ng/mL biotin and 30 nM Na_2SeO_3. EGF (10 ng/mL) was used to keep the cultures proliferating. For differentiation experiments, approximately 10 neurospheres of the same size were plated onto 10 μg/mL laminin-coated glass slides and 400 μL of serum-free medium with 10 ng/mL EGF was then added to each well. To determine whether ACM or METH could induce astrocytic differentiation from neural stem cells, neural stem cells

were exposed to medium containing, ACM, ACM + AG490 (1 μM) or METH (10 μM) for 5 days. The medium was replaced with fresh medium every 2 days. Ten days after drug treatment, these cells were washed in PBS, and fixed in 4 % paraformaldehyde in phosphate buffer at pH 7.4 and room temperature for 30 min. Thereafter, these cells were stained for GFAP.

Astrocytes with processes longer than their perinuclear diameters were defined as stellate cells according to the criteria used by Kimelberg et al[94] and Shao et al[95]. The experiments were repeatedly performed by, at least, 3 independent astrocyte culture preparations. The percentage of stellate cells in each experimental condition was expressed as a percent increase (mean ± SEM) with respect to that in control cells.

Cytokine array

To assay the components of astrocyte-released solved factors, I used RayBio™ Mouse Cytokine Array (RayBiotech Inc. Norcross, GA, USA). According to the manufacture's protocol, either DMEM, ACM or METH 10 μM-ACM was incubated with RayBio™ Mouse Cytokine Array membranes, which were conjugated with anti-cytokine antibodies. After this incubation, membranes were exposed to x-ray film. Film autoradiograms were analyzed and quantified by computer-assisted densitometry using an NIH Image.

Statistical analysis

The data of GFAP-like immunoreactivity, astrocyte differentiation and cytokine assay

are presented as the mean (percent of control) ± SEM. The statistical significance of differences between the groups was assessed by one-way ANOVA with Student's t-test.

Conditioning scores were obtained by subtracting the cumulative time (sec) spent in the saline-paired side from that in the drug-paired side, were expressed as means ± SEM. A statistical analysis for place conditioning study was performed using one-way ANOVA followed by Bonferroni/Dunnett's test.

Results

The effect of the glial modulator propentofylline (PPF)

In the present study, I used mouse cortical neuron/glia co-cultures to confirm the effect of PPF, which is known to modulate glial activity under pathological conditions[96, 97], in the activation of astrocytes induced by METH and MRP. The activation of astrocytes induced by either METH or MRP was dramatically diminished by treatment with PPF (Figure 3-1A, B).

I next investigated the effect of PPF on the respective rewarding effects of METH and MRP in mice using the conditioned place preference paradigm. Mice conditioned with METH (1 mg/kg, s.c.) or MRP (5 mg/kg, s.c.) exhibited a significant preference for the drug-associated place (23.8 ± 17.9 sec for saline-saline, 163.8 ± 22.0 sec for saline-1 mg/kg METH; $p < 0.001$ vs. saline-saline, 118.9 ± 30.5 sec for saline-5 mg/kg MRP; $p < 0.01$ vs. saline-saline, Figure 3-1C). PPF (3 mg/kg, i.p.) alone did not induce either significant place preference or place aversion in mice (-3.0 ± 22.1 sec). Under these conditions, the significant place preference produced by either METH or MPR was suppressed by treatment with PPF (60.4 ± 15.4 sec for 3 mg/kg PPF-1 mg/kg METH; $p < 0.01$ vs. saline-1 mg/kg METH, 40.1 ± 17.7 sec for 3 mg/kg PPF-5 mg/kg MRP; $p < 0.05$ vs. saline-5 mg/kg MRP, Figure 3-1C). These results indicate that glial cells may be involved in the development of the rewarding effects induced by METH and MRP in mice.

Administration of astrocyte-conditioned medium (ACM) enhances the rewarding effects of METH and MRP

It is well known that the N.Acc. plays an important role in mediating the rewarding effects induced by many drugs of abuse[43, 44]. On the other hand, astrocyte could regulate the neuronal transmission by releasing neurotransmitters[4], neurotrophic factors [98, 99], cytokines[23-25], chemokines[23-25], and extracellular matrix[98]. To examine the role of astrocyte-related soluble factors in the development of the rewarding effects induced by drugs of abuse, ACM was injected into the N.Acc. (Figure 3-2A). In animals in which DMEM was injected into N.Acc., METH (0.0625, 0.125, 0.25 or 0.5 mg/kg, s.c.) and MRP (1, 1.7, 3 or 5.6 mg/kg, s.c.) each produced a dose-dependent preference for the drug-associated place (4 ± 16.9 sec for DMEM-saline, 18.0 ± 19.5 sec for DMEM-0.0625 mg/kg METH, 34.1 ± 14.6 sec for DMEM-0.125 mg/kg METH, 62.3 ± 25.5 sec for 0.25 mg/kg METH; $p < 0.05$ vs. DMEM-saline, 94.4 ± 25.7 sec for DMEM-0.5 mg/kg METH; $p < 0.05$ vs. DMEM-saline, 4.8 ± 20.3 sec for DMEM-1 mg/kg MRP, 26.6 ± 9.9 sec for 1.7 mg/kg MPR, 67.9 ± 18.1 sec for 3 mg/kg MRP; $p < 0.05$ vs. DMEM-saline, 98.9 ± 9.9 sec for 5.6 mg/kg; $p < 0.001$ vs. DMEM-saline, Figure 3-2B, C). Under these conditions, intra-N.Acc. administration of ACM clearly enhanced the rewarding effects of METH (36.6 ± 7.6 sec for ACM-0.0625 mg/kg METH, 54.7 ± 38.0 sec for ACM-0.125 mg/kg METH, 138.5 ± 25.2 sec for ACM-0.25 mg/kg METH: $p < 0.05$ vs. DMEM-0.25 mg/kg METH, 172.0 ± 18.2 sec for ACM-0.5 mg/kg METH; $p < 0.01$ vs. DMEM-0.5 mg/kg METH, Figure 3-2B) and MRP (7.0 ± 8.7 sec for ACM-1 mg/kg MRP, 65.9 ± 21.1 sec for ACM-1.7 mg/kg MRP, 135.7 ± 22.7 sec for ACM-3

mg/kg MRP; $p < 0.01$ vs. DMEM-3 mg/kg MRP, 145.7 ± 23.1 sec for 5.6 mg/kg MRP, Figure 3-2C) in mice.

The implication of Jak/STAT pathway in the enhancement by ACM of METH- and MRP-induced rewarding effects

The Jak/STAT is a pathway that takes signals from the cell membrane to the nucleus in response to extracellular growth factors and cytokines[100]. In addition, the Jak/STAT pathway has been postulated to regulate astrogliosis and astrogliogenesis[101-103]. The place preference produced by MRP (3 mg/kg, s.c.), but not METH (0.5 mg/kg, s.c.), was significantly suppressed by intra-N.Acc. treatment with AG490 (0.1 nmol), which inhibits the Jak/STAT pathway (11.2 ± 16.6 sec for AG490 + DMEM-3mg/kg MRP; $p < 0.05$ vs. DMEM-3 mg/kg MRP, Figure 3-3B, 64.4 ± 24.8 sec for AG490 + DMEM-0.5 mg/kg METH; no significance vs. DMEM-0.5 mg/kg METH, Figure 3-3A). Notably, the enhancement of the rewarding effect of METH by ACM was significantly blocked by intra-N.Acc. treatment with AG490 (0.1 nmol, 70.2 ± 17.7 sec for AG490 + ACM-0.5 mg/kg METH; $p < 0.05$ vs. ACM-0.5 mg/kg METH, Figure 3-3A). These results raise the possibility that astrocyte-related soluble factors could regulate the development of the rewarding effects induced by drugs of abuse via Jak/STAT pathway. Moreover, Jak/STAT-dependent astrogliosis and/or astrogliogenesis may play the important role during the development of the rewarding effects induced by drugs of abuse.

The effects of ACM on the differentiation of multipotent neural stem cells (NSC)

via Jak/STAT pathway

To ascertain whether ACM could induce Jak/STAT-dependent astrogliogenesis, I performed the differentiation experiments using multipotent neural stem cells obtained from the mouse forebrain. ACM clearly induced the differentiation of multipotent NSCs into GFAP-positive astrocytes (Figure 3-4A, C). This effect was reversed by co-treatment with AG490 (1 μM, Figure 3-4A, C). Conversely, treatment of NSCs with METH (10 μM) failed to induce the differentiation to GFAP-positive astrocytes (Figure 3-4B, D), indicating that ACM, but not METH itself, may induce astrogliogenesis via the Jak/STAT pathway in the CNS.

The effect of METH-treated astrocyte-conditioned medium

To examine whether ACM could promote astrogliosis, I next investigated the effect of ACM in the level of GFAP-like immunoreactivity in purified cortical astrocytes. Treatment with DMEM or ACM for 1 day did not produce a significant increase in the level of GFAP-like immunoreactivity in purified cortical astrocytes (Figure 3-5A, B). Treatment with ACM collected from METH (10, 100 μM, 3 days)-treated astrocytes (METH 10 μM-ACM, METH 100 μM-ACM) for 1 day induced a robust activation of astrocyte, as detected by an increase in the level of GFAP-like immunoreactivity, in purified cortical astrocytes ($p < 0.01$, $p < 0.001$ vs. DMEM-treated cells, Figure 3-5A, B). On the other hand, treatment with ACM collected from MRP (10-100 μM, 3 days)-treated astrocytes did not produce any morphological changes in purified cortical astrocytes (Figure 3-5A, B). These results suggest that METH-, but not MRP-, treated

astrocytes could release some soluble factors which could enhance the activation of astrocytes.

As described in Chapter 1, *in vitro* treatment with 100 μM of METH caused neuronal cell death. On the other hand, *in vitro* treatment with 10 μM of METH could cause the activation of astrocytes without neuronal cell death. Therefore, 100 μM of METH might have some neurotoxic effects. In the present study, intra-N.Acc. administration of METH 10 μM-ACM dramatically enhanced the rewarding effects of METH (252.6 ± 47.0 sec for METH 10 μM-ACM-0.5 mg/kg METH; $p < 0.05$ vs. ACM-0.5 mg/kg METH, Figure 3-5C), indicating that astrocyte-related soluble factors released form METH-treated astrocytes potentiate the expression of the rewarding effect induced by METH.

ACM contains some chemokines

As mentioned above, the Jak/STAT pathway could modulate the development of the rewarding effects induced by METH and MRP. The Jak/STAT pathway is coupled to many key cytokine/chemokine receptors and is thus a primary conduit for cytokine/chemokine signal transduction and cellular communication[104]. Therefore, I hypothesized that astrocyte-related cytokines and/or chemokines may contribute to the development of the rewarding effects induced by METH and MRP. Based on this hypothesis, I next performed the cytokine assay. I found that some chemokines, such as monocyte chemoattractant protein-5 (MCP-5) and soluble tumor necrosis factor receptor 1 (sTNFR1), were identified in both ACM and METH 10 μM-ACM (Figure 3-

6A, B).

The effect of intra-N.Acc. administration of microglia-conditioned medium (MCM) on the rewarding effect induced by METH and MRP

Microglial cells are the major immunocompetent cells in the brain and include signaling cascades including cytokines and chemokines[105]. Therefore, I next investigated the effect of microgia-related soluble factors on the development of the rewarding effects induced by METH and MRP.

Treatment with METH (10-100 μM) for 3 days in purified cortical microglia caused a swelling morphology and an increase in the level of immunoreactivity of OX-42, which is a specific marker of microglia (Figure 3-7A). On the other hand, treatment with MRP (1-100 μM, 3 days) failed to induce any morphological changes in purified cortical microglia (Figure 3-7A).

In contrast to ACM, however, intra-N.Acc. administration of MCM failed to enhance the rewarding effects induced by METH (147.0 ± 19.3 sec for MCM-0.5 mg/kg METH; no significance vs. DMEM-0.5 mg/kg METH, Figure 3-7B) and MRP (82.1 ± 16.3 sec for MCM-3 mg/kg MRP; no significance vs. DMEM- 3 mg/kg MRP, Figure 3-7C) in mice.

The effect of intra-CG administration of ACM on the rewarding effect induced by METH and MRP

The CG is responsible for psychostimulant-induced rewarding effects and learning[77].

To compare the effect of intra-N.Acc. administration of ACM, I next investigated the effect of intra-CG administration of ACM on the rewarding effect of METH and MRP. In animals in which DMEM was injected into the CG, METH (0.0625, 0.125, 0.25 or 0.5 mg/kg, s.c.) and MRP (1, 1.7, 3 or 5.6 mg/kg, s.c.) produced a dose-dependent preference for the drug-associated place (-1.8 ± 13.5 sec for DMEM-saline, 20.9 ± 28.8 sec for DMEM-0.0625 mg/kg METH, 36.1 ± 10.6 sec for DMEM-0.125 mg/kg METH, 71.6 ± 14.5 sec for DMEM-0.25 mg/kg METH; $p < 0.05$ vs. DMEM-saline, 94.4 ± 25.8 sec for DMEM-0.5 mg/kg METH; $p < 0.001$ vs. DMEM-saline, 28.9 ± 17.6 sec for DMEM-1 mg/kg MRP, 13.4 ± 21.3 sec for DMEM-1.7 mg/kg MRP, 60.4 ± 24.7 sec for DMEM-3 mg/kg MRP; $p < 0.05$ vs. DMEM-saline, 117.1 ± 20.0 sec for DMEM-5.6 mg/kg MRP: $p < 0.001$ vs. DMEM-saline, Figure 3-8B, C). Under these conditions, intra-CG administration of ACM clearly enhanced the rewarding effect of METH (37.2 ± 22.4 sec for ACM-0.0625 mg/kg METH, 66.0 ± 12.1 sec for ACM-0.125 mg/kg METH, 145.9 ± 26.7 sec for ACM-0.25 mg/kg METH; $p < 0.05$ vs. DMEM-0.25 mg/kg METH, 172.0 ± 29.1 sec for ACM-0.5 mg/kg METH; $p < 0.01$ vs. DMEM-0.5 mg/kg METH, Figure 3-8B) and MRP (11.4 ± 17.1 sec for ACM-1 mg/kg MRP, 70.3 ± 15.1 sec for ACM-1.7 mg/kg MRP; $p < 0.05$ vs. DMEM-1.7 mg/kg MRP, 141. 9 ± 12.5 sec for ACM-3 mg/kg MRP; $p < 0.01$ vs. DMEM-3 mg/kg MRP, 169.1 ± 8.6 sec for ACM-5.6 mg/kg MRP; $p < 0.05$ vs. DMEM-3 mg/kg MRP, Figure 3-8C) in mice.

The effect of intra-corpus striatum (CPu) administration of ACM on the rewarding effect induced by METH and MRP

The CPu is regulated by dopaminergic inputs from the substantia nigra. Intra-CPu administration of ACM failed to enhance the rewarding effects induced by METH (101.1 ± 16.4 sec for DMEM-0.5 mg/kg METH, 99.9 ± 13.7 sec for ACM-0.5 mg/kg METH; no significance vs. DMEM-0.5 mg/kg METH, Figure 3-9B) and MRP (81.9 ± 15.6 sec for DMEM-3 mg/kg MRP, 87.1 ± 21.1 sec for ACM-3 mg/kg MRP; no significance vs. DMEM-3 mg/kg MRP, Figure 3-9C) in mice.

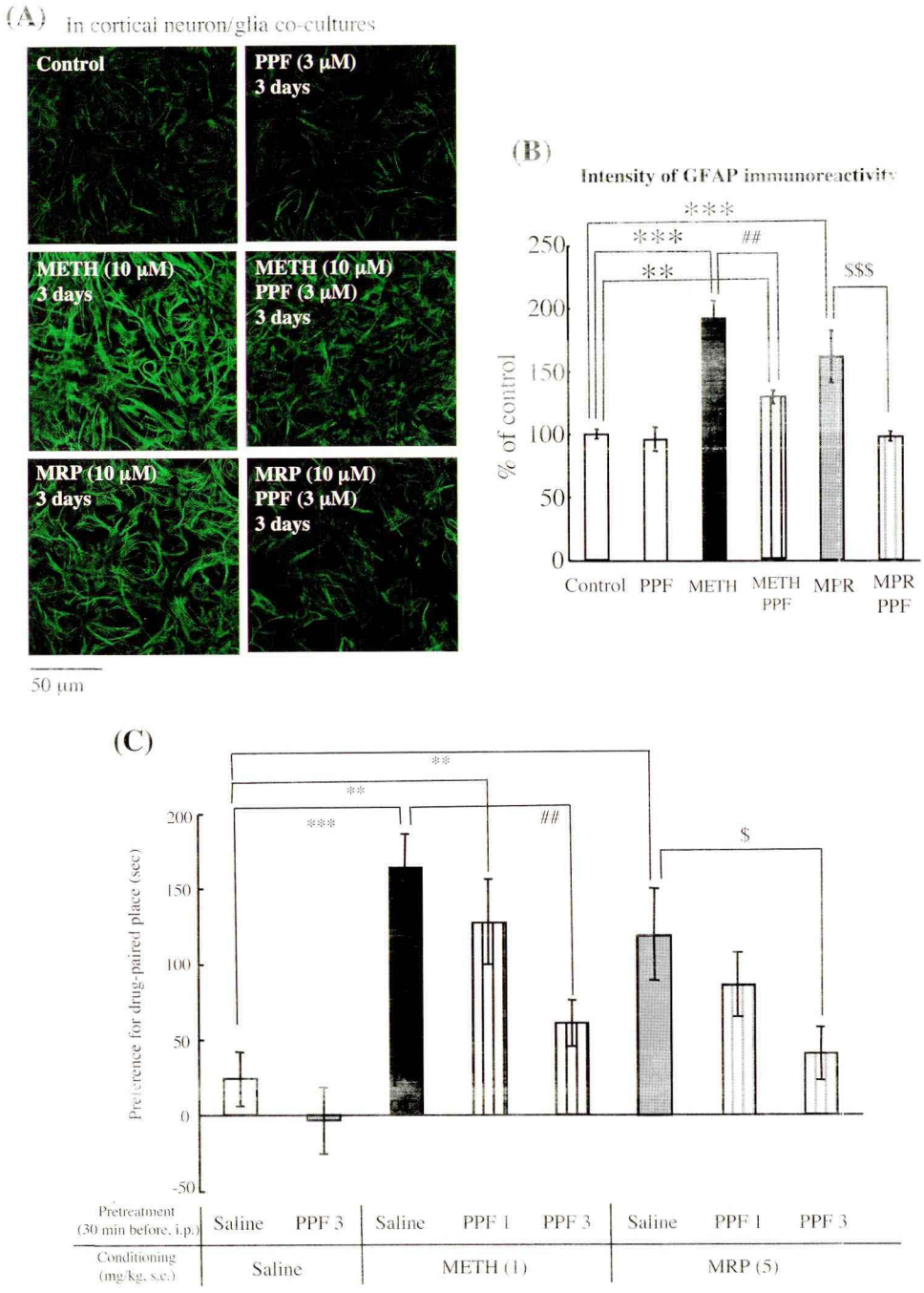

Figure 3-1 The effect of propentofylline (PPF) on the effects of METH and MRP. (A) Cortical neuron/glia co-cultures were treated with METH (10 μM) or MRP (10 μM) with or without PPF (3 μM) for 3 days. The cells were stained with a polyclonal antibody to GFAP. (B) The intensity of GFAP-like immunoreactivity in each image was measured using NIH-image. The level of GFAP-like immunoreactivity is expressed as a percent increase (mean ± SEM) with respect to that in control cells. $^{**}p < 0.01$, $^{***}p < 0.001$ vs. control cells; $^{\#\#}p < 0.01$ vs. METH-treated cells; $^{\$\$\$}p < 0.001$ vs. MRP-treted cells. (C) Chronic s.c. administration of either METH (1 mg/kg) or MRP (5 mg/kg) produced a significant place preference in mice. Each column represents the mean ± SEM of 8-10 mice. Mice were pretreated with PPF (1-3 mg/kg, i.p.) or saline 30 min before s.c. administration of saline, METH or MRP. $^{**}p < 0.01$, $^{***}p < 0.001$ vs. saline-saline group; $^{\#\#}p < 0.01$ vs. saline-METH group; $^{\$}p < 0.05$ vs. saline-MRP group.

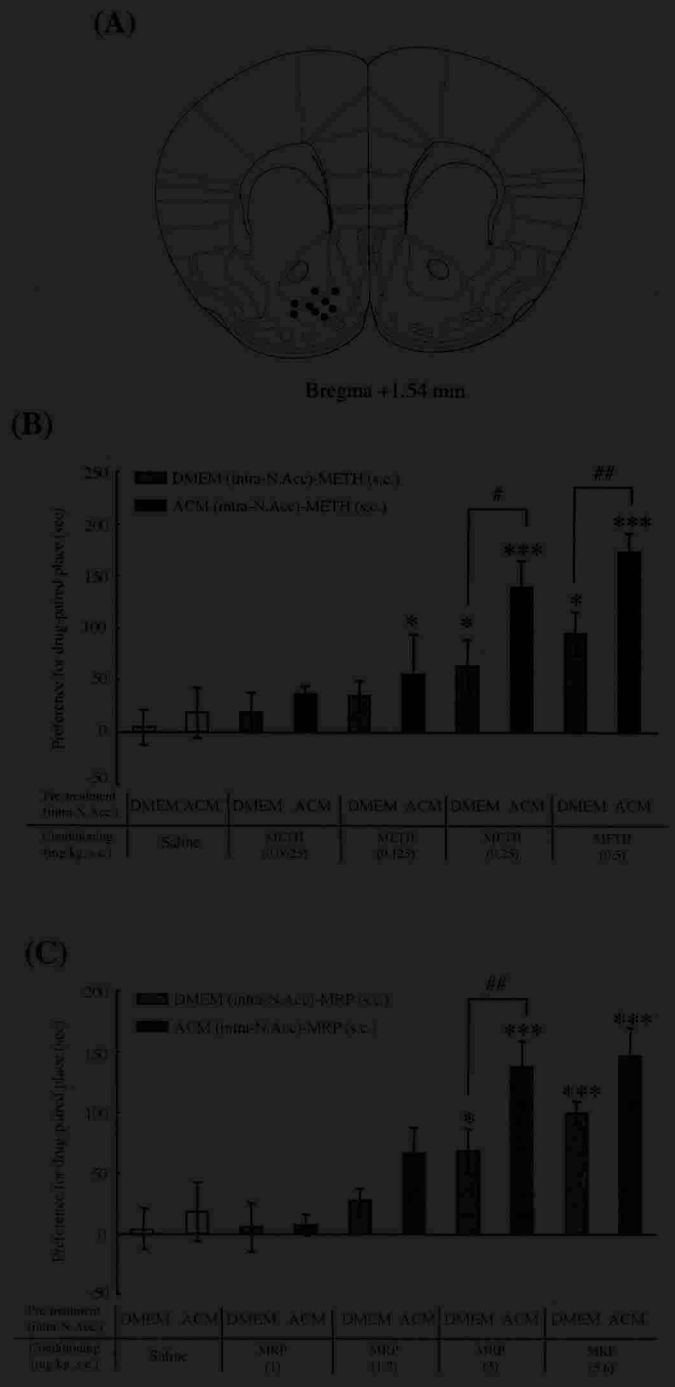

Figure 3-2 The effect of intra-nucleus accumbens (N.Acc.) administration of astrocyte-conditioned medium (ACM) on the place conditioning produced by METH and MRP in mice. (A) Dots represent microinjection regions in mice. The schematic brain sections are from the atlas[93]. (B) Mice were pretreated with DMEM or ACM into the N.Acc. 1 day before pre-conditioning test. In the conditioning session (three days for METH, three days for saline), mice were treated with saline or METH (0.0625, 0.125, 0.25 or 0.5 mg/kg, s.c.). Each point represents the mean ± SEM of 7-8 mice. (C) Mice were pretreated with DMEM or ACM into the N.Acc. 1 day before pre-conditioning test. In the conditioning session (three days for MRP, three days for saline), mice were treated with saline or MRP (1, 1.7, 3 or 5.6 mg/kg, s.c.). Each point represents the mean ± SEM of 7-8 mice. $^{*}p < 0.05$, $^{***}p < 0.001$ vs. saline-treated group; $^{\#}p < 0.05$, $^{\#\#}p < 0.01$ vs. DMEM-pretreated group.

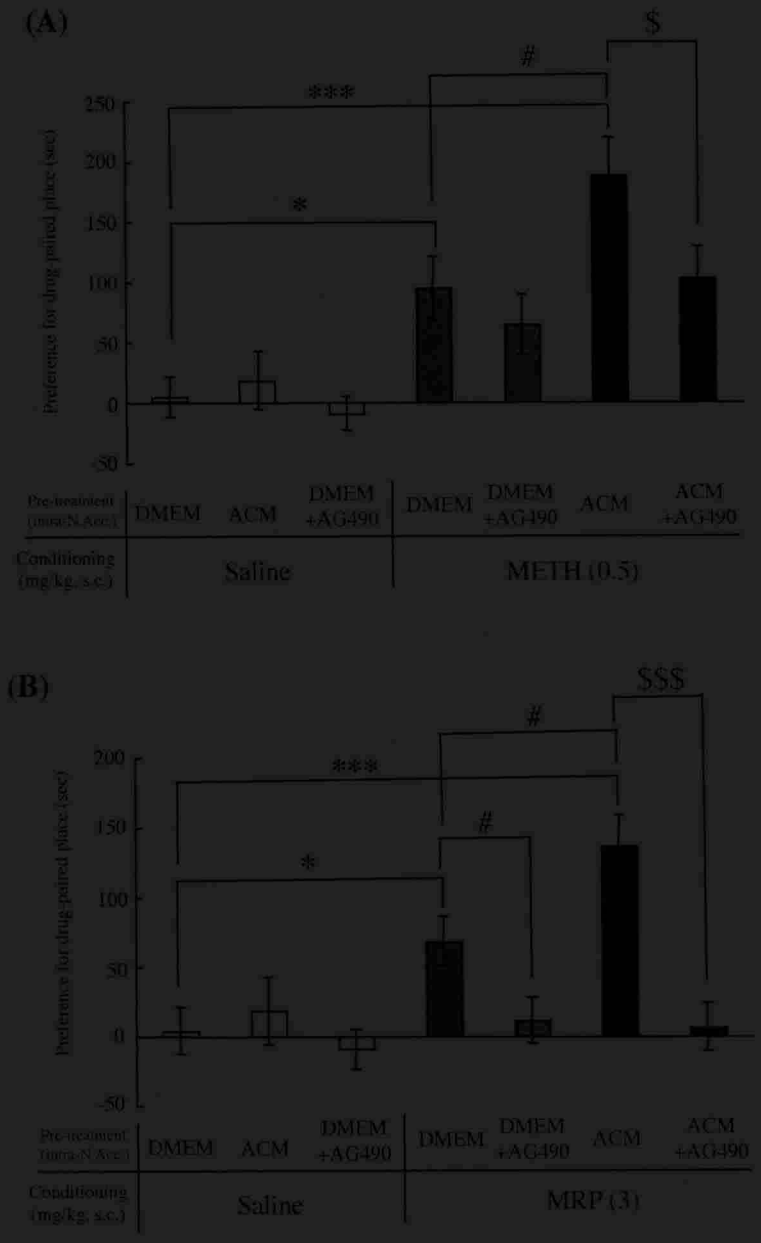

Figure 3-3 The effect of a Jak/STAT inhibitor AG490 on the enhancement by ACM of METH- and MRP-induced place preference in mice. (A) The enhancement by ACM of the METH (0.5 mg/kg, s.c.)-induced place preference was significantly suppressed by the co-injection of AG490 (0.1 nmol/mouse) into the N.Acc.. Each column represents the mean ± SEM of 8-10 mice. $^{*}p < 0.05$, $^{***}p < 0.001$ vs. DMEM-saline group; $^{\#}p < 0.05$ vs. DMEM-0.5 mg/kg METH group; $^{\$}p < 0.05$ vs. ACM-0.5 mg/kg METH group. (B) The enhancement by ACM of the MRP (3 mg/kg, s.c.)-induced place preference was significantly suppressed by the co-injection of AG490 (0.1 nmol/mouse) into the N.Acc.. Each column represents the mean ± SEM of 8-10 mice. $^{*}p < 0.05$, $^{***}p < 0.001$ vs. DMEM-saline group; $^{\#}p < 0.05$ vs. DMEM-3 mg/kg MRP group; $^{\$\$\$}p < 0.001$ vs. ACM-3 mg/kg MRP group.

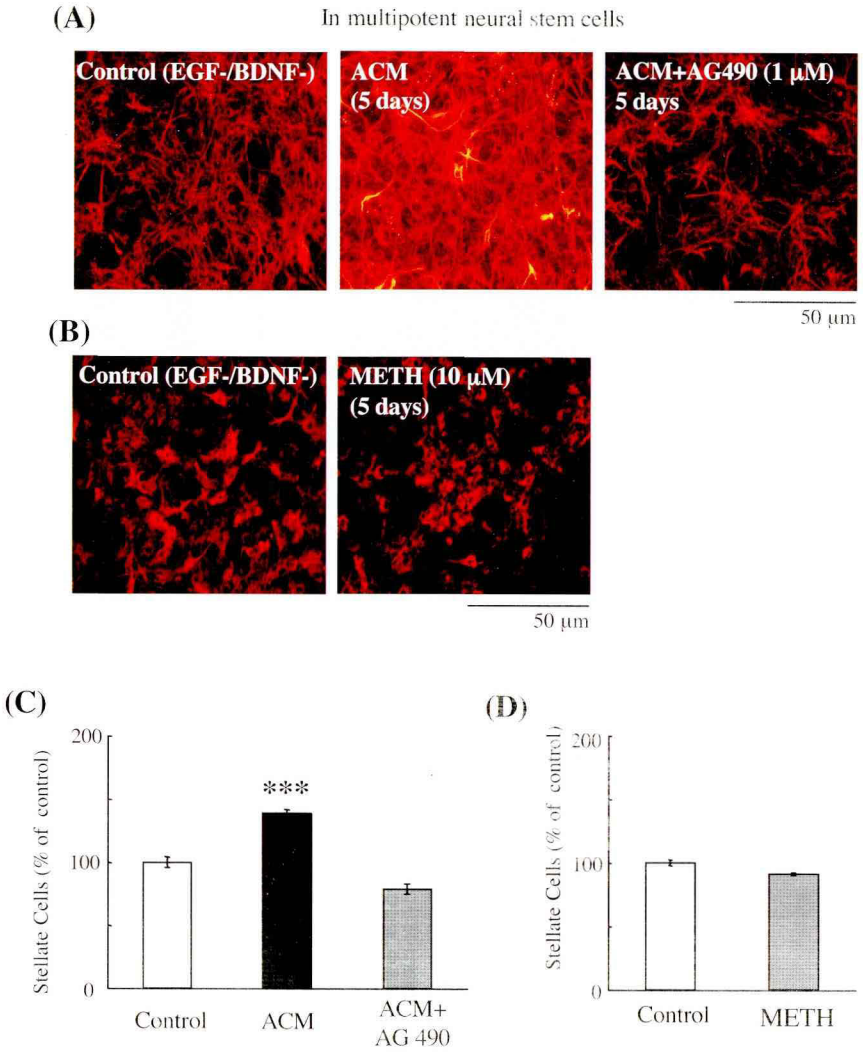

Figure 3-4 The effects of ACM on multipotent neural stem cells (NSCs). (A) NSCs were treated with ACM with or without AG490 (1 μM) for 5 days. The cells were stained with a polyclonal antibody to GFAP. (B) NSCs were treated with METH (10 μM) for 5 days. The cells were stained with a polyclonal antibody to GFAP. (C, D) The differentiation of NSCs into GFAP-positive stellate astrocytes was quantitatively evaluated. Data represent the mean (% of control) ± SEM. ***$p < 0.001$ vs. control cells.

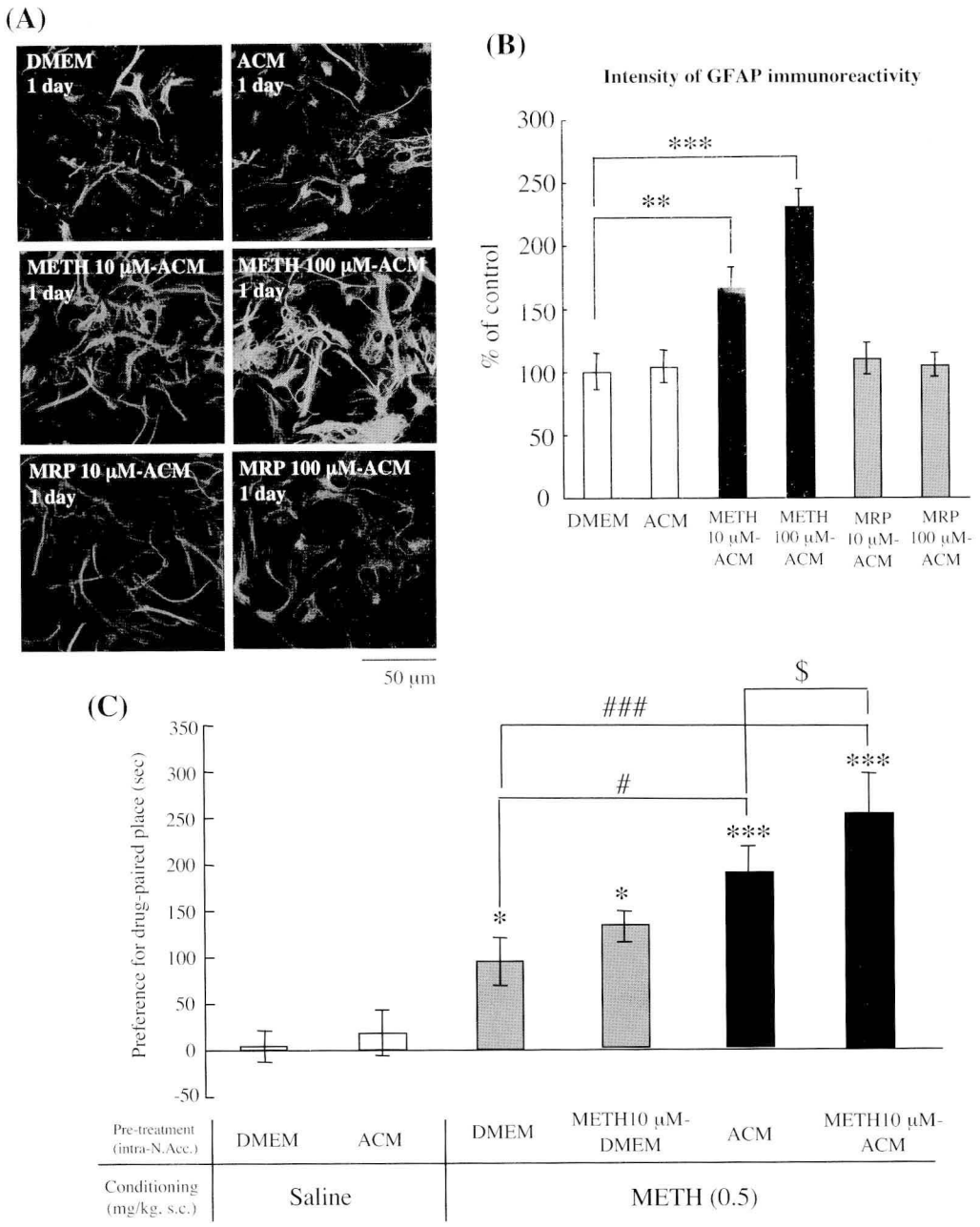

Figure 3-5 The effect of intra-N.Acc. administration of METH (10 μM, 3 days)-treated conditioned medium (METH 10 μM-ACM) on the place conditioning produced by METH in mice. (A) Purified cortical astrocytes were treated with DMEM, ACM, METH (10,100 μM, 3 days)-treated astrocyte-conditioned medium (METH 10 μM-ACM or METH 100 μM-ACM), or MRP (10, 100 μM, 3 days)-treated astrocyte-conditioned medium (MRP 10 μM-ACM or MRP 100 μM-ACM). The cells were stained with a polyclonal antibody to GFAP. (B) The intensity of GFAP-like immunoreactivity in each image was measured using NIH-image. The level of GFAP-like immunoreactivity is expressed as a percent increase (mean ± SEM) with respect to that in control cells. $^{**}p < 0.01$, $^{***}p < 0.001$ vs. control cells. (C) Intra-N.Acc. administration of METH 10 μM-ACM significantly potentiated the rewarding effect of METH (0.5 mg/kg, s.c.) in mice. Each column represents the mean ± SEM of 8 mice. $^{*}p < 0.05$, $^{***}p < 0.001$ vs. DMEM-saline group; $^{\#}p < 0.05$, $^{\#\#\#}p < 0.001$ vs. DMEM-0.5 mg/kg METH group; $^{\$}p < 0.05$ vs. ACM-0.5 mg/kg METH group.

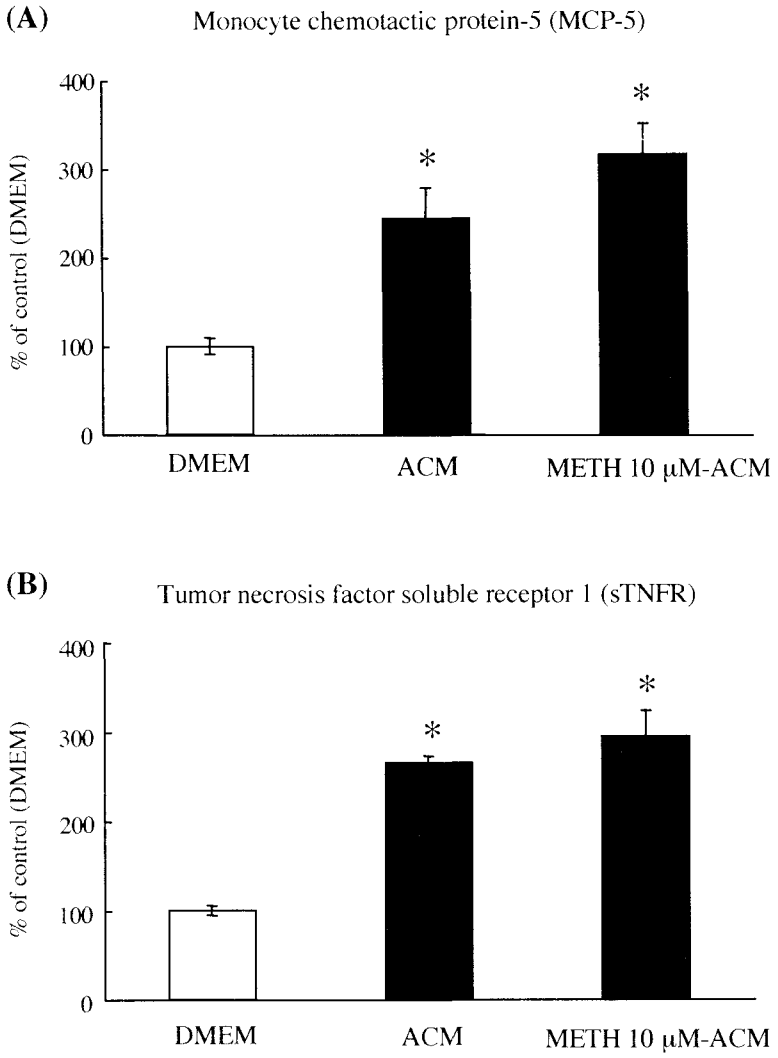

Figure 3-6 Cytokine array of DMEM, ACM and METH 10 μM-ACM. DMEM (control), ACM or METH10-ACM was incubated with cytokine array membranes using anti-cytokine antibodies. The changes in the immunoreactivity of monocyte chemotactic protein-5 (MCP-5, A) and tumor necrosis factor soluble receptor-1 (sTNFR, B) are expressed as a percent increase (mean ± SEM) with respect to that in control (DMEM) cells. *$p < 0.05$ vs. control.

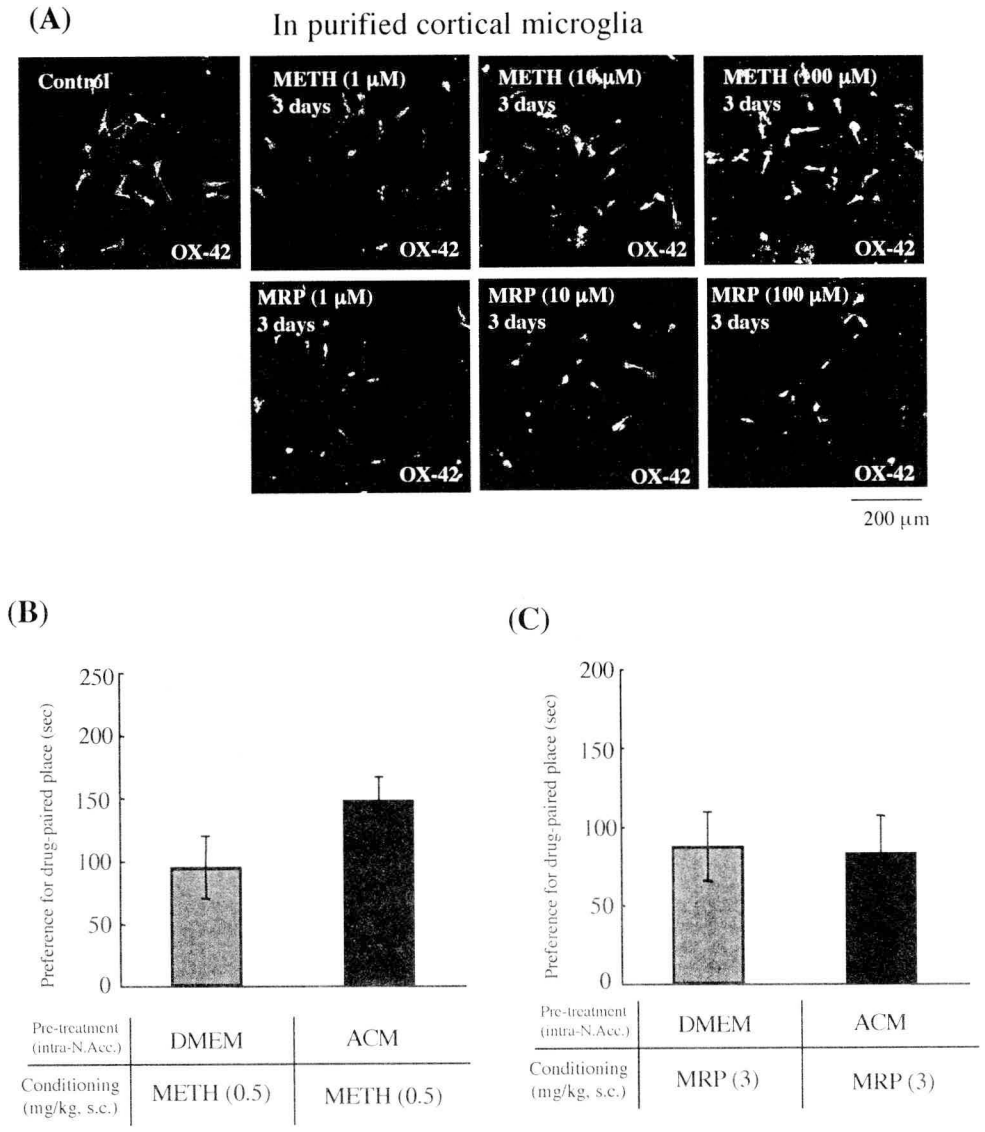

Figure 3-7 The effects of intra-N.Acc. administration of microglia-conditioned medium (MCM) on the place conditioning produced by METH and MRP in mice. (A) Purified cortical microglia were incubated with normal medium, METH (1-100 μM) or MRP (1-100 μM) for 3 days. The cells were stained with a rat antibody to OX-42. (B, C) Intra-N.Acc. administration of MCM failed to induce a significant enhancement in either METH (0.5 mg/kg, s.c., B)- or MRP (3 mg/kg, s.c., C)-induced rewarding effect in mice. Each column represents the mean ± SEM of 7-8 mice.

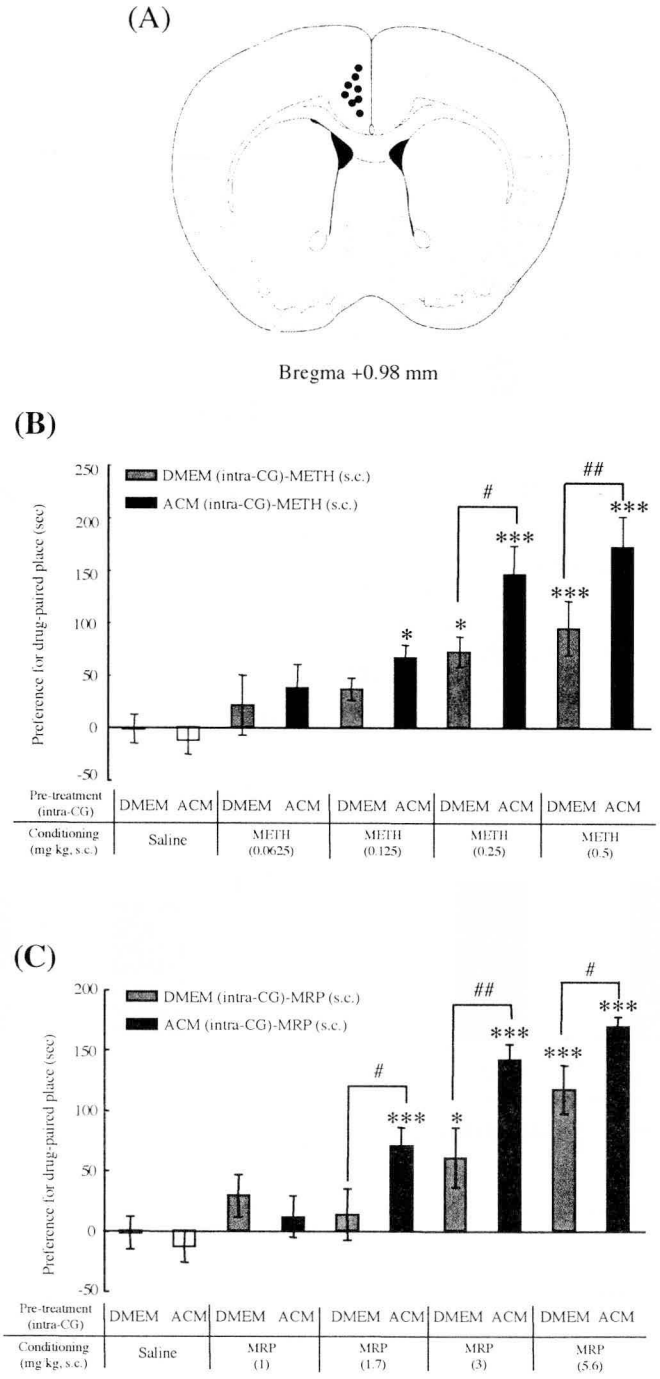

Figure 3-8 The effect of intra-cingulate cortex (CG) administration of astrocyte-conditioned medium (ACM) on the place conditioning produced by METH and MRP in mice. (A) Dots represent microinjection regions in mice. The schematic brain sections are from the atlas[93]. (B) Mice were pretreated with DMEM or ACM into the CG 1 day before pre-conditioning test. In the conditioning session (three days for METH, three days for saline), mice were treated with saline or METH (0.0625, 0.125, 0.25 or 0.5 mg/kg, s.c.). Each point represents the mean ± SEM of 7-8 mice. (C) Mice were pretreated with DMEM or ACM into the CG 1 day before pre-conditioning test. In the conditioning session (three days for MRP, three days for saline), mice were treated with saline or MRP (1, 1.7, 3 or 5.6 mg/kg, s.c.). Each point represents the mean ± SEM of 7-8 mice. $^{*}p < 0.05$, $^{***}p < 0.001$ vs. DMEM-saline group; $^{\#}p < 0.05$, $^{\#\#}p < 0.01$ vs. DMEM pretreated group.

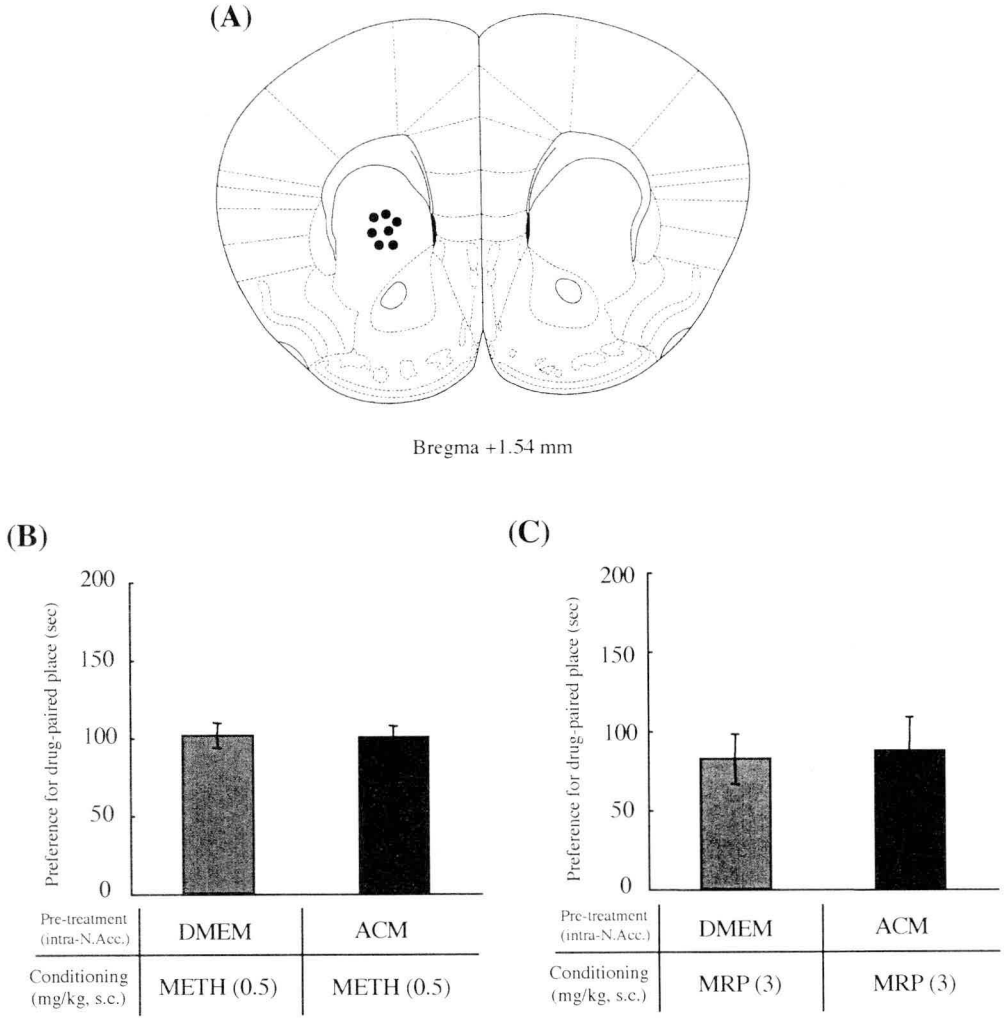

Figure 3-9 The effect of intra-corpus striatum (CPu) administration of astrocyte-conditioned medium (ACM) on the place conditioning produced by METH and MRP in mice. (A) Dots represent microinjection regions in mice. The schematic brain sections are from the atlas[93]. (B, C) Intra-CPu administration of ACM failed to induce a significant enhancement in either METH (0.5 mg/kg, s.c., B)- or MRP (3 mg/kg, s.c., C)-induced rewarding effect in mice. Each column represents the mean ± SEM of 7-8 mice.

Discussion

In the present study, I investigated the direct action of astrocytes on the development of the rewarding effects induced by drugs of abuse. I found here that astrocyte-, but not microglia-, related soluble factors may directly modulate the development of the rewarding effects induced by METH and MRP.

PPF is a xanthine derivative with pharmacological effects different from those of the classical methylxanthines, caffeine, and theophylline. PPF is known to modulate glial activity under pathological condition[96, 97]. The mechanism of glial modulation by PPF under pathological condition could be due to its inhibitory action of phosphodiesterase enzymes and subsequent augmentation of cyclic-AMP signaling[106]. It has been reported that the activity of cyclic-AMP could regulate the morphology of astrocytes[107]. In the present study, I found that the METH- or MRP-induced activation of astrocytes was dramatically diminished by treatment with PPF. Thus, PPF may inhibit the activity of phosphodiesterase in astrocytes, resulting in the inhibition of the activation of astrocytes. I also demonstrated that the place preference produced by repeated *in vivo* treatment of either METH or MRP was significantly suppressed by i.p. treatment with the glial modulator PPF. These findings provide the evidence that the modulation of glial activity may contribute to the development of the rewarding effects induced by METH and MRP.

I next examined whether astrocyte-related soluble factors could regulate the development of psychological modulation on METH and MRP. In the present study,

intra-N.Acc. administration of ACM dramatically enhanced the rewarding effects of METH and MRP. These data suggest that astrocyte-related soluble factors induced by drugs of abuse may directly regulate the development of their rewarding effects.

Chronic administration of cocaine induces the up-regulation of the Jak/STAT pathway in the VTA[108]. It has been reported that treatment with METH at neurotoxic doses induces the robust phosphorylation of STAT3 in the mouse brain[109]. These findings raise the possibility that exposure to the drugs of abuse could produce the synaptic plasticity and/or neuronal toxicity via the Jak/STAT pathway. In the present study, the enhancement of METH-induced rewarding effects by ACM was blocked by intra-N.Acc. administration of the Jak/STAT inhibitor AG490, suggesting that astrocyte-related soluble factors enhance the development of METH-induced rewarding effects via the Jak/STAT pathway.

μ-Opioid receptors, which have been reported to play a role in several of MRP's pharmacological effects, are member of the G protein-coupled-receptor superfamily[110]. Agonist stimulation of many G-protein-coupled receptors has been shown to result in tyrosine phosphorylation and activation of Jak and STAT family members, leading to changes in gene transcription[104]. It has been reported that STAT3 signaling regulates the neuronal growth and differentiation by μ-opioid receptor stimulation in neuroblastoma SH-SY5Y cells[111]. MRP exposed to COS-7 cells, which are transfected with μ-opioid receptors and STAT5A, induces receptor-dependent tyrosine phosphorylation of STAT5A[112]. In the present study, I demonstrated that both the expression of and ACM-induced enhancement of MRP-induced rewarding effects were

blocked by intra-N.Acc. administration of AG490. Thus, it seems likely that chronic treatment with MRP may activate the Jak/STAT pathway via μ-opioid receptors, resulting in the development and expression of rewarding effects in mice.

The Jak/STAT pathway modulates astrogliosis and/or astrogliogenesis[101-103]. It should be mentioned that ACM, but not METH itself, induced the differentiation of NSCs into GFAP-positive astrocytes via Jak/STAT pathway. On the other hand, the treatment with METH-ACM, but not ACM or MRP-ACM, induced the activation of astrocytes in purified cortical astrocytes. Furthermore, intra-N.Acc. administration of METH-ACM significantly and dramatically enhanced the rewarding effect of METH. These findings suggest that astrocyte-related soluble factors could cause astrogliogenesis via the Jak/STAT pathway, promoting the development and expression of rewarding effect induced by METH. Moreover, METH-induced astrocytic secretion might enhance the intensity of astrocytic activation in the CNS. Although the exact binding site for METH in astrocytes or the mechanism underlying METH-induced astrocytic secretion is unclear at this time, METH, which could be taken up by astrocytes across the astrocytic plasma membranes, causes astrocytic secretion, and potentiates the development of the rewarding effect induced by METH.

In the present study, I also observed the difference between METH-ACM and MRP-ACM; while METH-ACM markedly activated astrocytes with morphological changes in astrocytes, MRP-ACM had no such effect. The data suggest that METH, but not MRP, may directly affect astrocytes and lead to the release of astrocyte-related soluble factors, resulting in the robust enhancement of the development of the rewarding effect

induced by METH.

The Jak/STAT pathway transduces signals from cytokines and chemokines. In the present study, some chemokiens, such as MCP-5 and sTNFR1, were identified in ACM and METH-ACM. MCP-5 is a mouse homologue to MPC-1[113]. In addition, treatment with MRP induces the secretion of MCP-1 from astrocytes[113]. On the other hand, the biological functions of the sTNFR1 are not completely understood. TNF-α and other cytokines can bind to this receptor[114]. Some kinds of drugs of abuse, such as MRP[115] and METH[116], could induce the generation of TNF-α, which may in turn stimulate the release of sTNFR1 as astrocyte-related soluble factors. Collectively, these astrocyte-related chemokines may, at least in part, contribute to the positive regulation of neuron-glia communication during the development of the rewarding effects induced by drugs of abuse.

Cytokines, chemokines and their receptors play a major role in the immune responses of the CNS. They are expressed at constitutively low levels in microglia, and induced by inflammatory mediators[105, 117]. Moreover, microglial cells are known to response to drugs of abuse, such as MRP and METH[59, 73, 118]. In the present study, treatment with METH caused a morphological change in purified cortical microglia, whereas MRP had no such effect. In contrast to ACM, intra-N.Acc. administration of MCM failed to enhance the rewarding effects induced by METH and MRP. Thus, it seems likely that METH-induced morphological changes in cortical microglia are not essential for the development of METH-induced rewarding effect. Collectively, these findings indicate that astrocyte-, but not microglia-, related soluble factors could potentially regulate the

development of the rewarding effects induced by drugs of abuse.

It is of interest to note that intra-CG administration of ACM also significantly enhanced the rewarding effects of METH and MRP. The CG projects to the mediodorsal caudate, lateral part of the mediodorsal nucleus of the thalamus, and amygdala[119]. In addition, CG receives major dopaminergic input from the VTA[120]. The CG is, therefore, linked to emotional states and responsible for rewarding and learning[77]. Taken together, these results indicate that astrocyte-related soluble factors directly modify the neuron/glia communication in the CG during the development of the rewarding effects induced by METH and MRP.

Unlike intra-N.Acc. and intra-CG administration of ACM, intra-CPu administration of ACM failed to enhance the rewarding effects induced by METH and MRP. These data suggest that astrocyte-related soluble factors could regulate the development of the rewarding effect induced by drugs of abuse in specific brain regions, such as the N.Acc. and CG.

In conclusion, I demonstrated here that the activation of astrocytes in the N.Acc. and/or CG provides a powerful signal for dopamine-associated behaviors, habits and addiction by drugs of abuse at the synaptic levels. My findings suggest that astrocyte-, but not microglia-, related soluble factors could directly amplify the development of rewarding effect induced by METH and MRP in the N.Acc. and CG. The present findings provide a new insight into the basis of synaptic plasticity during the development of the rewarding effects induced by drugs of abuse.

General Conclusion

The above findings lead to the following conclusions:

In Chapter 1:

In this study, I found that *in vitro* treatment of cortical neuron/glia co-cultures with either METH or MRP caused the activation of astrocytes via PKC. In purified cortical astrocytes, astrocytes were markedly activated by METH, whereas MRP had no such effect. METH, but not MRP, caused a long-lasting astrocytic activation in cortical neuron/glia co-cultures. Furthermore, MRP-induced behavioral sensitization to hyperlocomotion was reversed by 2 months of withdrawal following intermittent MRP administration, whereas behavioral sensitization to METH-induced hyperlocomotion was maintained even after 2 months of withdrawal. *In vivo* treatment with METH, which was associated with behavioral sensitization, caused PKC-dependent astrocytic activation in the mouse CG and N.Acc.. These findings provide direct evidence that METH induces long-lasting astrocytic activation and behavioral sensitization through the stimulation of PKC in the rodent brain. In contrast, MRP produced a reversible activation of astrocytes via neuronal PKC and a reversibility of behavioral sensitization. This information can break through the definition of drugs of abuse and the misleading concept that MRP produces long-lasting neurotoxicity.

In Chapter 2:

I demonstrated that *in vitro* treatment with METH caused the phosphorylation of both neuronal and astrocytic PKC and the activation of astrocytes in cortical neuron/glia co-cultures. Treatment of cortical neuron/glia co-cultures with either the PKC activator PDBu or glutamate also caused the PKC-dependent activation of astrocytes. The PKC inhibitor CHE suppressed the Ca^{2+} responses to glutamate in both cortical neurons and astrocytes. Notably, treatment with METH also enhanced the Ca^{2+} responses to glutamate in cortical neurons. The activation of astrocytes induced by METH was also reversed by co-treatment with glutamate receptor antagonists in cortical neuron/glia co-cultures. In the conditioned place preference paradigm, i.c.v. administration of glutamate receptor antagonists attenuated the METH-induced rewarding effect. These findings provide evidence that the changes in PKC-dependent neuronal and astrocytic glutamatergic transmission induced by METH may, at least in part, contribute to the development of the rewarding effect induced by METH.

In Chapter 3:

I found that the glial modulator PPF dramatically diminished the activation of astrocytes induced by METH and MRP. *In vivo* treatment with PPF also suppressed the rewarding effects induced by both METH and MRP. On the other hand, intra-N.Acc. administration of ACM aggravated the development of rewarding effects induced by METH and MRP via the Jak/STAT pathway. Furthermore, ACM, but not METH itself, clearly induced the differentiation of NSCs into astrocytes. Intra-CG, but not -CPu, administration of ACM also enhanced the rewarding effects induced by

METH and MRP. These findings suggest that astrocyte-related soluble factors could amplify the development of the rewarding effects of METH and MRP in the N.Acc. and CG. The present study provides direct evidence that astrocytes may, at least in part, contribute to the synaptic plasticity induced by drugs of abuse during the development of the rewarding effects induced by METH and MRP. The present findings provide new insight into astrocytic modulation of synaptic plasticity during the development of psychological dependence on drugs of abuse.

List of Publications

This dissertation is based on the following original publications:

1. Minoru Narita, Mayumi Miyatake, Masahiro Shibasaki, Makoto Tsuda, Schuichi Koizumi, Michiko Narita, Yoshinori Yajima, Kazuhide Inoue and Tsutomu Suzuki: Long-lasting change in brain dynamics by methamphetamine: Enhancement of protein kinase C-dependent astrocytic response and behavioral sensitization.
   J Neurochem **93**, 1382-1392 (2005): **Chapter 1**

2. Mayumi Miyatake, Minoru Narita, Masahiro Shibasaki, Atsushi Nakamura and Tsutomu Suzuki: Glutamatergic neurotransmission and protein kinase C play a role in neuron-glia communication during the development of methamphetamine-induced psychological dependence.
   Eur J Neurosci **22**, 1476-1488 (2005): **Chapter 2**

3. Minoru Narita, Mayumi Miyatake, Michiko Narita, Masahiro Shibasaki, Keiko Shindo, Atsushi Nakamura, Naoko Kuzumaki, Yasuyuki Nagumo and Tsutomu Suzuki: Direct evidence of astrocytic modulation in the development of rewarding effects induced by drugs of abuse.
   Neuropsychopharmacology in press: **Chapter 3**

Acknowledgements

This research will never be materialized without the help of the following people and organizations:

First, I would like to express my gratitude and appreciation to Professor Tsutomu Suzuki (Department of Toxicology, Hoshi University School of Pharmacy and Pharmaceutical Sciences) and Associate Professor Minoru Narita (Department of Toxicology, Hoshi University School of Pharmacy and Pharmaceutical Sciences) for their encouragement, helpful guidance in my research work and preparing this dissertation, and for giving a chance of this research work.

I would like to thank Dr. Yoshinori Yajima (Research Assistant, Department of Toxicology) and Ms. Michiko Narita for helpful suggestions and valuable advices.

Further, I wish to thank Professor Kazuhide Inoue (Department of Molecular and System Pharmacology, Graduate School of Pharmaceutical Sciences, Kyushu University), Dr. Schuichi Koizumi (Lab Chief, Section of Neuropharmacology, Division of Pharmacology, National Institute of Health Sciences) and Dr. Makoto Tsuda (Research Assistant, Department of Molecular and System Pharmacology, Graduate School of Pharmaceutical Sciences, Kyushu University) for helpful guidance in my research work.

I wish to thank Mr. Masahiro Shibasaki, Ms. Keiko Shindo, Mr. Atsushi Nakamura, Ms. Naoko Kuzumaki, Mr. Yasuyuki Nagumo and Mr. Keisuke Hashimoto for their excellent technical assistance in my research work. I wish to thank Ms. Tomoko Obama and Ms. Kayoko Fujishita for their expert technical assistance and useful guidance in my work. Further, I wish to thank Ms. Masami Suzuki for her stimulating discussions and kindly guidance in my research work.

Also, I wish to thank all of graduate and undergraduate students of Department of Toxicology, Hoshi University School of Pharmacy and Pharmaceutical Sciences, especially Ms. Tomomi Chikui, Ms. Tomoko Tanaka, Mr. Kazuhiro Kurokawa, Mr. Keisuke Shibata, Ms. Megumi Asado and Ms. Nana Hareyama for their support.

Finally, I would like to express my gratitude to my parents and brother for their assistance in my life.

References

1) Coles J.A. and Deitmer J.W. Extracellular potassium and pH: homeostasis and signaling. In: Kettenmann H. and Ransom B.R. (Eds), Neuroglia, Oxford University press, New York, pp.334-345 (2005).

2) Vesce S., Bezzi P. and Volterra A. Synaptic transmission with the glia. *News Physiol Sci* **16**, 178-184 (2001).

3) Bohn M.C. Motoneurons crave glial cell line-derived neurotrophic factor. *Exp Neurol* **190**, 263-275 (2004).

4) Fellin T. and Carmignoto G. Neuron-to-astrocyte signalling in the brain represents a distinct multifunctional unit. *J Physiol* **559**, 3-15 (2004).

5) Swanson R.A. Astrocyte neurotransmitter uptake. In: Kettenmann H. and Ransom B.R. (Eds), Neuroglia, Oxford University press, New York, pp.346-354 (2005).

6) Glaum S.R., Holzwarth J.A. and Miller R.J. Glutamate receptors activate Ca^{2+} mobilization and Ca^{2+} influx into astrocytes. *Proc Natl Acad Sci USA* **87**, 3454-3458 (1990).

7) Parpura V., Basarsky T.A., Liu F., Jeftinija K., Jeftinija S. and Haydon P.G. Glutamate-mediated astrocyte-neuron signalling. *Nature* **369**, 744-747 (1994).

8) Nedergaard M., Takano T. and Hansen A.J. Beyond the role of glutamate as a neurotransmitter. *Nature Rev Neurosci* **3**, 748-755 (2002).

9) James G. and Butt A.M. P2Y and P2X purinoceptor mediated Ca^{2+} signalling in glial cell pathology in the central nervous system. *Eur J Pharmacol* **447**, 247-260 (2002).

10) Fumagalli M., Brambilla R., D'Ambrosi N., Volonte C., Matteoli M., Verderio C.,

Abbracchio M. P. Nucleotide-mediated calcium signaling in rat cortical astrocytes: Role of P2X and P2Y receptors. *Glia* **43**, 218-203 (2003).

11) Khan Z.U., Koulen P., Rubinstein M., Grandy D.K. and Goldman-Rakic P.S. An astroglia-linked dopamine D2-receptor action in prefrontal cortex. *Proc Natl Acad Sci USA* **98**, 1964-1969 (2001).

12) Reuss B. and Unsicker K. Atypical neuroleptic drugs downregulate dopamine sensitivity in rat cortical and striatal astrocytes. *Mol Cell Neurosci* **18**, 197-209 (2001).

13) Haydon P.G. Glia: listening and talking to the synapse. *Nature Rev Neurosci* **2**, 185-193 (2001).

14) Kang J., Jiang L., Goldman S.A. and Nedergaard M. Astrocyte-mediated potentiation of inhibitory synaptic transmission. *Nat Neurosci* **1**, 683-692 (1998).

15) Newman E.A. New roles for astrocytes: regulation of synaptic transmission. *Trends Neurosci* **26**, 536-542 (2003).

16) Parri H.R., Gould T.M. and Crunelli V. Spontaneous astrocytic Ca^{2+} oscillations in situ drive NMDAR-mediated neuronal excitation. *Nat Neurosci* **4**, 803-812 (2001).

17) Fiacco T.A. and McCarthy K.D. Intracellular astrocyte calcium waves in situ increase the frequency of spontaneous AMPA receptor currents in CA1 pyramidal neurons. *J Neurosci* **24**, 722-732 (2004).

18) Fellin T, Pascual O., Gobbo S., Pozzan T., Haydon P.G. and Carmignoto G. Neuronal synchrony mediated by astrocytic glutamate through activation of extrasynaptic NMDA receptors. *Neuron* **43**, 729-743 (2004).

19) Powell E.M., Mercado M.L., Calle-Patino Y. and Geller H.M. Protein kinase C mediates neurite guidance at an astrocyte boundary. *Glia* **33**, 288-297 (2001).

20) Tom V.J., Doller C.M., Malouf A.T. and Silver J. Astrocyte-associated fibronectin is critical for axonal regeneration in adult white matter. *J Neurosci* **24**, 9282-9290 (2004).

21) Hama H., Hara C., Yamaguchi K. and Miyawaki A. PKC signaling mediates global enhancement of excitatory synaptogenesis in neurons triggered by local contact with astrocytes. *Neuron* **41**, 405-415 (2004).

22) Chotard C. and Salecker I. Neurons and glia: team players in axon guidance. *Trends Neurosci* **27**, 655-661 (2004).

23) Dong Y. and Benveniste E.N. Immune function of astrocytes. *Glia* **36**, 180-190 (2001).

24) Liberto C.M., Albrecht P.J., Herx L.M., Yong V.W. and Levison S.W. Pro-regenerative properties of cytokine-activated astrocytes. *J Neurochem* **89**, 1092-100 (2004).

25) Aloisi F. Cytokine production. In: Kettenmann H. and Ransom B.R. (Eds), Neuroglia, Oxford University press, New York, pp.285-301 (2005).

26) Ridet J.L., Malhotra S.K., Privat A. and Gage F.H. Reactive astrocytes: cellular and molecular cues to biological function. *Trends Neurosci* **20**, 570-577 (1997).

27) Raivich G., Bohatschek M., Kloss C.U., Werner A., Jones L.L. and Kreuzberg G.W. Neuroglial activation repertoire in the injured brain: graded response, molecular mechanisms and cues to physiological function. *Brain Res Rev* **30**. 77-105 (1999).

28) Pekny M. and Nilsson M. Astrocyte activation and reactive gliosis. *Glia* **50**, 427-434 (2005).

29) Ostrow L.W. and Sachs F. Mechanosensation and endothelin in astrocytes-

hypothetical roles in CNS pathophysiology. *Brain Res Rev* **48**. 488-508 (2005).

30) Miller G. The dark side of glia. *Science* **308**, 778-781 (2005).

31) Xu K., Malouf A.T., Messing A. and Silver J. Glial fibrillary acidic protein is necessary for mature astrocytes to react to β-amyloid. *Glia* **25**, 390-403 (1999).

32) Menet V., Gimenez y Ribotta M., Chauvet N., Drian M.J., Lannoy J., Colucci-Guyon E. and Privat A. Inactivation of the glial fibrillary acidic protein gene, but not that of vimentin, improves neuronal survival and neurite growth by modifying adhesion molecule expression. *J Neurosci* **21**, 6147-6158 (2001).

33) Menet V., Prieto M., Privat A. and Gimenezy Ribotta M. Axonal plasticity and functional recovery after spinal cord injury in mice deficient in both glial fibrillary acidic protein and vimentin genes. *Proc Natl Acad Sci USA* **100**, 8999-9004 (2003).

34) Pfrieger F.W. and Barres B.A. Synaptic efficacy enhanced by glial cells in vitro. *Science* **277**, 1684-1687 (1997).

35) Ullian E.M., Sapperstein S.K., Christopherson K.S. and Barres B.A. Control of synapse number by glia. *Science* **291**, 657-661 (2001).

36) Song H., Stevens C.F. and Gage F.H. Astroglia induce neurogenesis from adult neural stem cells. *Nature* **417**, 39-44 (2002).

37) Ullian E.M, Christopherson K.S. and Barres B.A. Role for glia in synaptogenesis. *Glia* **47**, 209-216 (2004).

38) Abrous D.N., Koehl M. and Le Moal M. Adult neurogenesis: from precursors to network and physiology. *Physiol Rev* **85**, 523-569 (2005).

39) Hyman S.E. and Malenka R.C. Addiction and the brain: the neurobiology of compulsion and its persistence. *Nat Rev Neurosci* **2**, 695-703 (2001).

40) Nestler E.J. Molecular basis of long-term plasticity underlying addiction. *Nat Rev Neurosci* **2**, 119-128 (2001).

41) Self D.W. Regulation of drug-taking and -seeking behaviors by neuroadaptations in the mesolimbic dopamine system. *Neuropharmacology* **47**, 242-255 (2004).

42) Shippenberg T.S., Herz A., Spanagel R., Bals-Kubik R. and Stein C. Conditioning of opioid reinforcement: neuroanatomical and neurochemical substrates. *Ann N Y Acad Sci* **654**, 347-356 (1992).

43) Wise R.A. and Hoffman D.C. Localization of drug reward mechanisms by intracranial injections. *Synapse* **10**, 247-263 (1992).

44) De Vries T.J. and Shippenberg T.S. Neural systems underlying opiate addiction. *J Neurosci* **22**, 3321-3325 (2002).

45) Meredith G.E., Pennartz C.M. and Groenewegen, H.J. The cellular framework for chemical signalling in the nucleus accumbens. *Prog Brain Res* **99**, 3-24 (1993).

46) Woolf C.J. and Salter M.W. Neuronal plasticity: increasing the gain in pain. *Science* **288**, 1765-1769 (2000).

47) van Zundert B., Yoshii A. and Constantine-Paton M. Receptor compartmentalization and trafficking at glutamate synapses: a developmental proposal. *Trends Neurosci* **27**, 428-437 (2004).

48) Kim E. and Sheng M. PDZ domain proteins of synapses. *Nat Rev Neurosci* **5**, 771-781 (2004).

49) Nishizuka Y. The molecular heterogeneity of protein kinase C and its implications for cellular regulation. *Nature* **334**, 661-665 (1988).

50) Nishizuka Y. Intracellular signaling by hydrolysis of phospholipids and activation of protein kinase C. *Science* **258**, 607-614 (1992).

51) Rebecchi M.J. and Pentyala S.N. Structure, function, and control of phosphoinositide-specific phospholipase C. *Physiol. Rev* **80**, 1291-1335 (2000).

52) Walsh F.S. and Doherty P. Cell adhesion molecules and neuronal regeneration. *Curr Opin Cell Biol* **8**, 707-713 (1996).

53) Narita M., Akai H., Nagumo Y., Sunagawa N., Hasebe K., Nagase H. Kita, T. Hara. C. and Suzuki T. Implications of protein kinase C in the nucleus accumbens in the development of sensitization to methamphetamine in rats. *Neuroscience* **127**, 941-948 (2004).

54) Steketee J.D., Rowe L.A. and Chandler L.J. The effects of acute and repeated cocaine injections on protein kinase C activity and isoform levels in dopaminergic brain regions. *Neuropharmacology* **37**, 339-347 (1998).

55) Narita M., Mizuo K., Shibasaki M., Narita M. and Suzuki T. Up-regulation of the $G_{q/11\alpha}$ protein and protein kinase C during the development of sensitization to morphine-induced hyperlocomotion. *Neuroscience* **111**, 127-132 (2002).

56) Aujla H. and Beninger R.J. Intra-accumbens protein kinase C inhibitor NPC 15437 blocks amphetamine-produced conditioned place preference in rats. *Behav Brain Res* **147**, 41-48 (2003).

57) Narita M., Aoki T., Ozaki S., Yajima Y. and Suzuki T. Involvement of protein kinase Cγ isoform in morphine-induced reinforcing effects. *Neuroscience* **103**, 309-314 (2001).

58) Pu C. and Vorhees C.V. Protective effects of MK-801 on methamphetamine-induced depletion of dopaminergic and serotonergic terminals and striatal astrocytic response: an immunohistochemical study. *Synapse* **19**, 97-104 (1995).

59) Guilarte T.R., Nihei M.K., McGlothan J.L. and Howard A.S. Methamphetamine-induced deficits of brain monoaminergic neuronal markers: distal axotomy or neuronal plasticity. *Neuroscience* **122**, 499-513 (2003).

60) Fattore L., Puddu M.C., Picciau S., Cappai A., Fratta W., Serra G.P. and Spiga S. Astroglial *in vivo* response to cocaine in mouse dentate gyrus: a quantitative and qualitative analysis by confocal microscopy. *Neuroscience* **110**, 1-6 (2002).

61) Synder S.H. Madness and the Brain. McGraw-Hill, New York (1974).

62) Vanderschuren L.J. and Kalivas P.W. Alterations in dopaminergic and glutamatergic transmission in the induction and expression of behavioral sensitization: a critical review of preclinical studies. *Psychopharmacology* **151**, 99-120 (2000).

63) Robinson T.E. and Kolb B. Alterations in the morphology of dendrites and dendritic spines in the nucleus accumbens and prefrontal cortex following repeated treatment with amphetamine or cocaine. *Eur J Neurosci* **11**, 1598-1604 (1999).

64) Steketee J.D. Neurotransmitter systems of the medial prefrontal cortex: potential role in sensitization to psychostimulants. *Brain Res Rev* **41**, 203-228 (2003).

65) Zhang Y., Loonam T.M., Noailles P.A. and Angulo J.A. Comparison of cocaine- and methamphetamine-evoked dopamine and glutamate overflow in somatodendritic and terminal field regions of the rat brain during acute, chronic, and early withdrawal conditions. *Ann N Y Acad Sci* **937**, 93-120 (2001).

66) Narita M., Suzuki T., Funada M., Misawa M. and Nagase H. Involvement of δ-opioid receptors in the effects of morphine on locomotor activity and the mesolimbic dopaminergic system in mice. *Psychopharmacology* **111**, 423-426 (1993).

67) Kuribara H. Effects of interdose interval on ambulatory sensitization to methamphetamine, cocaine and morphine in mice. *Eur J Pharmacol* **316**, 1-5 (1996).

68) Jiménez A., Jordà E.G., Verdaguer E., Pubill D., Sureda F.X., Canudas A.M., Escubedo E., Camarasa J., Camins A. and Pallàs M. Neurotoxicity of amphetamine derivatives is mediated by caspase pathway activation in rat cerebellar granule cells. *Toxicol Appl Pharmacol* **196**, 223-234 (2004).

69) Wise R.A. Brain reward circuitry: insights from unsensed incentives. *Neuron* **36**, 229-240 (2002).

70) Carlezon W.A. Jr. and Nestler E.J. Elevated levels of GluR1 in the midbrain: a trigger for sensitization to drugs of abuse? *Trends Neurosci* **25**, 610-661 (2002).

71) Verkhratsky A. and Kettenmann H. Calcium signalling in glial cells. *Trends Neurosci* **19**, 346-352 (1996).

72) Stiene-Martin A., Zhou R. and Hauser K.F. Regional, developmental, and cell cycle-dependent differences in μ, δ, and κ-opioid receptor expression among cultured mouse astrocytes. *Glia* **22**, 249-259 (1998).

73) Khurdayan V.K., Buch S., El-Hage N., Lutz S.E., Goebel S.M., Singh I.N., Knapp P.E., Turchan-Cholewo J., Nath A. and Hauser K.F. Preferential vulnerability of astroglia and glial precursors to combined opioid and HIV-1 Tat exposure in vitro. *Eur J Neurosci* **19**, 3171-3182 (2004).

74) Stiene-Martin A., Knapp P.E., Martin K., Gurwell J.A., Ryan S., Thornton S.R., Smith F.L. and Hauser K.F. Opioid system diversity in developing neurons, astroglia, and oligodendroglia in the subventricular zone and striatum: impact on gliogenesis in vivo. *Glia* **36**, 78-88 (2001).

75) Kuhn T.B., Schmidt M.F. and Kater S.B. Laminin and fibronectin guideposts signal sustained but opposite effects to passing growth cones. *Neuron* **14**, 275-285 (1995).

76) Bixby J.L. and Jhabvala P. Inhibition of tyrosine phosphorylation potentiates substrate-induced neurite growth. *J Neurobiol* **23**, 468-480 (1992).

77) Allman J.M., Hakeem A., Erwin J.M., Nimchinsky E. and Hof P. The anterior cingulate cortex. The evolution of an interface between emotion and cognition. *Ann N Y Acad Sci* **935**, 107-117 (2001).

78) Ahlemeyer B., Kolker S., Zhu Y., Hoffmann G.F. and Krieglstein J. Increase in glutamate-induced neurotoxicity by activated astrocytes involves stimulation of protein kinase C. *J Neurochem* **82**, 504-515 (2002).

79) Hu J., Ferreira A. and Van Eldik L.J. S100β induces neuronal cell death through nitric oxide release from astrocytes. *J Neurochem* **69**, 2294-2301 (1997).

80) Suzuki T., Funada M., Narita M., Misawa M. and Nagase H. Pertussis toxin abolishes μ- and δ-opioid agonist-induced place preference. *Eur J Pharmacol* **205**, 85-88 (1991).

81) Mangoura D, Sogos V and Dawson G. Phorbol esters and PKC signaling regulate proliferation, vimentin cytoskeleton assembly and glutamine synthetase activity of chick embryo cerebrum astrocytes in culture. *Dev Brain Res* **87**, 1-11 (1995).

82) Dayton E.T. and Major, E.O. Recombinant human interleukin 1β induces production of prostaglandins in primary human fetal astrocytes and immortalized human fetal astrocyte cultures. *J Neuroimmunol* **71**, 11-18 (1996).

83) Stewart V.C., Sharpe M.A., Clark J.B. and Heales S.J. Astrocyte-derived nitric oxide causes both reversible and irreversible damage to the neuronal mitochondrial respiratory chain. *J Neurochem* **75**, 694-700 (2000).

84) Akama K.T. and van Eldik L.J. β-Amyloid stimulation of inducible nitric-oxide synthase in astrocytes is interleukin-1β- and tumor necrosis factor-α (TNFα)-dependent, and involves a TNFα receptor-associated factor- and NFκB-inducing

kinase-dependent signaling mechanism. *J Biol Chem* **275**, 7918-7924 (2000).

85) Strack S., McNeill R.B. and Colbran R.J. Mechanism and regulation of calcium/calmodulin-dependent protein kinase II targeting to the NR2B subunit of the N-methyl-D-aspartate receptor. *J Biol Chem* **275**, 23798-23806 (2000).

86) Kato H., Narita M., Miyatake M., Yajima Y. and Suzuki T. Role of neuronal NR2B subunit-containing NMDA receptor-mediated Ca^{2+} influx and astrocytic activation in cultured mouse cortical neurons and astrocytes. *Synapse* **59**, 10-17 (2006).

87) Narita M., Matsumura Y., Ozaki S., Ise Y., Yajima Y. and Suzuki T. Role of the calcium/calmodulin-dependent protein kinase II (CaMKII) in the morphine-induced pharmacological effects in the mouse. *Neuroscience* **126**, 415-421 (2004).

88) Tu J.C., Xiao B., Naisbitt S., Yuan J.P., Petralia R.S., Brakeman P., Doan A., Aakalu V.K., Lanahan A.A., Sheng M. and Worley P.F. Coupling of mGluR/Homer and PSD-95 complexes by the Shank family of postsynaptic density proteins. *Neuron* **23**, 583-592 (1999).

89) Conn P.J. and Pin J.P. Pharmacology and functions of metabotropic glutamate receptors. *Annu Rev Pharmacol Toxicol* **37**, 205-237 (1997).

90) Schoepp D.D. Unveiling the functions of presynaptic metabotropic glutamate receptors in the central nervous system. *J Pharmacol Exp Ther* **299**, 12-20 (2001).

91) Flores C., Samaha A.N. and Stewart J. Requirement of endogenous basic fibroblast growth factor for sensitization to amphetamine. *J Neurosci* **20**, RC55 (2000).

92) Bowers M.S. and Kalivas P.W. Forebrain astroglial plasticity is induced following withdrawal from repeated cocaine administration. *Eur J Neurosci* **17**, 1273-1278 (2003).

93) Paxinos G. and Franklin K.B.J. The Mouse Brain in Stereotaxic Coordinates.

Academic Press, San Diego (1997).

94) Kimelberg H.K., Narumi S. and Bourke R.S. Enzymatic and morphological properties of primary rat brain astrocyte cultures, and enzyme development in vivo. *Brain Res* **153**, 55-77 (1978).

95) Shao Y., Enkvist M.O. and McCarthy K.D. Glutamate blocks astroglial stellation: effect of glutamate uptake and volume changes. *Glia* **11**, 1-10 (1994).

96) Sweitzer S.M., Schubert P. and DeLeo J.A. Propentofylline, a glial modulating agent, exhibits antiallodynic properties in a rat model of neuropathic pain. *J Pharmacol Exp Ther* **297**, 1210-1217 (2001).

97) Raghavendra V., Tanga F.Y. and DeLeo J.A. Attenuation of morphine tolerance, withdrawal-induced hyperalgesia, and associated spinal inflammatory immune responses by propentofylline in rats. *Neuropsychopharmacology* **29**, 327-334 (2004).

98) Brightman M.W. The brain's interstitial clefts and their glial walls. *J Neurocytol* **31**, 595-603 (2002).

99) Bohn M.C. Motoneurons crave glial cell line-derived neurotrophic factor. *Exp Neurol* **190**, 263-275 (2004).

100) Justicia C., Gabriel C. and Planas A.M. Activation of the JAK/STAT pathway following transient focal cerebral ischemia: signaling through Jak1 and STAT3 in astrocytes. *Glia* **30**, 253-270 (2000).

101) Bonni A., Sun Y., Nadal-Vicens M., Bhatt A., Frank D.A., Rozovsky I., Stahl N., Yancopoulos G.D. and Greenberg M.E. Regulation of gliogenesis in the central nervous system by the JAK-STAT signaling pathway. *Science* **278**, 477-483 (1997).

102) Sriram K., Benkovic S.A., Herbet M.A., Miller D.B. and O'Callaghan J.P. Induction of gp130-related cytokines and activation of JAK2/STAT3 pathway in

astrocytes precedes up-regulation of glial fibrillary acidic protein in the 1-methyl-4-phenyl-1,2,3,6-tetrahydropyridine model of neurodegeneration: key signaling pathway for astrogliosis *in vivo*? *J Biol Chem* **279**, 19936-19947 (2004).

103) He F., Ge W., Martinowich K., Becker-Catania S., Coskun V., Zhu W., Wu H., Castro D., Guillemot F., Fan G., de Vellis J. and Sun YE. A positive autoregulatory loop of Jak-STAT signaling controls the onset of astrogliogenesis. *Nat Neurosci* **8**, 616-625 (2005).

104) Campbell I.L. Cytokine-mediated inflammation, tumorigenesis, and disease-associated JAK/STAT/SOCS signaling circuits in the CNS. *Brain Res Rev* **48**, 166-177 (2005).

105) Färber K. and Kettenmann H. Physiology of microglial cells. *Brain Res Rev* **48**, 133-143 (2005).

106) Schubert P., Ogata T., Rudolphi K., Marchini C., McRae A. and Ferroni S. Support of homeostatic glial cell signaling: a novel therapeutic approach by propentofylline. *Ann N Y Acad Sci* **826**, 337-347 (1997).

107) Won C.L. and Oh Y.S. cAMP-induced stellation in primary astrocyte cultures with regional heterogeneity. *Brain Res* **887**, 250-258 (2000).

108) Berhow M.T., Hiroi N., Kobierski L.A., Hyman S.E. and Nestler E.J. Influence of cocaine on the JAK-STAT pathway in the mesolimbic dopamine system. *J Neurosci* **16**, 8019-8026 (1996).

109) Hebert M.A. and O'Callaghan J.P. Protein phosphorylation cascades associated with methamphetamine-induced glial activation. *Ann N Y Acad Sci* **914**, 238-262. (2000).

110) Narita M., Funada M. and Suzuki T. Regulations of opioid dependence by opioid receptor types. *Pharmacol Ther* **89**, 1-15 (2001).

111) Yuen J.W., So I.Y., Kam A.Y. and Wong Y.H. Regulation of STAT3 by μ-opioid receptors in human neuroblastoma SH-SY5Y cells. *Neuroreport* **15,** 1431-1435 (2004).

112) Mazarakou G. and Georgoussi Z. STAT5A interacts with and is phosphorylated upon activation of the μ-opioid receptor. *J Neurochem* **93,** 918-931 (2005).

113) El-Hage N., Gurwell J.A., Singh I.N., Knapp P.E., Nath A. and Hauser K.F. Synergistic increases in intracellular Ca^{2+}, and the release of MCP-1, RANTES, and IL-6 by astrocytes treated with opiates and HIV-1 Tat. *Glia* **50**, 91-106 (2005).

114) Ryan A.S. and Nicklas B.J. Reductions in plasma cytokine levels with weight loss improve insulin sensitivity in overweight and obese postmenopausal women. *Diabetes Care* **27**, 1699-1705 (2004).

115) Kapasi A.A., Gibbons N., Mattana J. and Singhal P.C. Morphine stimulates mesangial cell TNF-α and nitrite production. *Inflammation* **24**, 463-476 (2000).

116) Lee Y.W., Hennig B., Yao J. and Toborek M. Methamphetamine induces AP-1 and NF-kappaB binding and transactivation in human brain endothelial cells. *J Neurosci Res* **66**, 583-591 (2001).

117) Mennicken F., Maki R., de Souza E.B. and Quirion R. Chemokines and chemokine receptors in the CNS: a possible role in neuroinflammation and patterning. *Trends Pharmacol Sci* **20**, 73-78 (1999).

118) Thomas D.M., Francescutti-Verbeem D.M., Liu X. and Kuhn D.M. Identification of differentially regulated transcripts in mouse striatum following methamphetamine treatment; An oligonucleotide microarray approach. *J Neurochem* **88**, 380-393 (2004).

119) Bussey T.J., Muir J.L., Everitt B.J. and Robbins T.W. Dissociable effects of

anterior and posterior cingulate cortex lesions on the acquisition of a conditional visual discrimination: facilitation of early learning vs. impairment of late learning. *Behav Brain Res* **82**, 45-56 (1996).

120) Retaux S., Trovero F. and Besson M.J. Role of dopamine in the plasticity of glutamic acid decarboxylase messenger RNA in the rat frontal cortex and the nucleus accumbens. *Eur J Neurosci* **6**, 1782-1791 (1994).